



# **UNIVERSIDAD DE INVESTIGACIÓN DE TECNOLOGÍA EXPERIMENTAL YACHAY**

**Escuela de Ciencias Matemáticas y Computacionales**

**TÍTULO: Explanatory Study of Mathematical Models for  
Realistic Soft Tissue Simulations**

Trabajo de integración curricular presentado como requisito para  
la obtención  
del título de Ingeniero en Tecnologías de la Información

**Autor:**

Bustamante Orellana Carlos

**Tutores:**

Ph.D Guachi Guachi Lorena

Ph.D Antón Castro Francesc

Urcuquí, agosto 2019

Urququí, 20 de agosto de 2019

**SECRETARÍA GENERAL**  
(Vicerrectorado Académico/Cancillería)  
**ESCUELA DE CIENCIAS MATEMÁTICAS Y COMPUTACIONALES**  
**CARRERA DE TECNOLOGÍAS DE LA INFORMACIÓN**  
**ACTA DE DEFENSA No. UITEY-ITE-2019-00002-AD**

En la ciudad de San Miguel de Urququí, Provincia de Imbabura, a los 20 días del mes de agosto de 2019, a las 09:30 horas, en el Aula AI-102 de la Universidad de Investigación de Tecnología Experimental Yachay y ante el Tribunal Calificador, integrado por los docentes:

<b>Presidente Tribunal de Defensa</b>	HIDROBO TORRES, FRANCISCO JAVIER
<b>Miembro No Tutor</b>	THIRUMURUGANANDHAM , SARAVANA PRAKASH
<b>Tutor</b>	GUACHI GUACHI, LORENA DE LOS ANGELES

Se presenta el(la) señor(ita) estudiante **BUSTAMANTE ORELLANA, CARLOS ENRIQUE**, con cédula de identidad No. 0705378933, de la **ESCUELA DE CIENCIAS MATEMÁTICAS Y COMPUTACIONALES**, de la Carrera de **TECNOLOGÍAS DE LA INFORMACIÓN**, aprobada por el Consejo de Educación Superior (CES), mediante Resolución RPC-SO-43-No.496-2014, con el objeto de rendir la sustentación de su trabajo de titulación denominado: **Explanatory Study of Mathematical Models for Realistic Soft Tissue Simulations** , previa a la obtención del título de **INGENIERO/A EN TECNOLOGÍAS DE LA INFORMACIÓN**.

El citado trabajo de titulación, fue debidamente aprobado por el(los) docente(s):

**Tutor** GUACHI GUACHI, LORENA DE LOS ANGELES

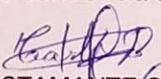
Y recibió las observaciones de los otros miembros del Tribunal Calificador, las mismas que han sido incorporadas por el(la) estudiante.

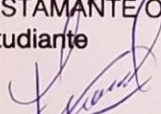
Previamente cumplidos los requisitos legales y reglamentarios, el trabajo de titulación fue sustentado por el(la) estudiante y examinado por los miembros del Tribunal Calificador. Escuchada la sustentación del trabajo de titulación, que integró la exposición de el(la) estudiante sobre el contenido de la misma y las preguntas formuladas por los miembros del Tribunal, se califica la sustentación del trabajo de titulación con las siguientes calificaciones:

Tipo	Docente	Calificación
Tutor	GUACHI GUACHI, LORENA DE LOS ANGELES	10,0
Presidente Tribunal De Defensa	HIDROBO TORRES, FRANCISCO JAVIER	10,0
Miembro Tribunal De Defensa	THIRUMURUGANANDHAM , SARAVANA PRAKASH	10,0

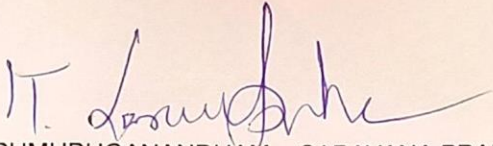
Lo que da un promedio de: **10 (Diez punto Cero)**, sobre 10 (diez), equivalente a: **APROBADO**

Para constancia de lo actuado, firman los miembros del Tribunal Calificador, el/la estudiante y el/la secretario ad-hoc.

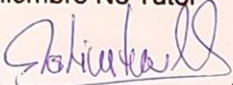
  
**BUSTAMANTE ORELLANA, CARLOS ENRIQUE**  
Estudiante

  
**HIDROBO TORRES, FRANCISCO JAVIER**  
Presidente Tribunal de Defensa

  
**GUACHI GUACHI, LORENA DE LOS ANGELES**  
Tutor



THIRUMURUGANANDHAM , SARAVANA PRAKASH  
Miembro No Tutor



TORRES MONTALVÁN, TATIANA BEATRIZ  
Secretario Ad-hoc

## **AUTORÍA**

Yo, **CARLOS ENRIQUE BUSTAMANTE ORELLANA**, con cédula de identidad 0705378933, declaro que las ideas, juicios, valoraciones, interpretaciones, consultas bibliográficas, definiciones y conceptualizaciones expuestas en el presente trabajo; así cómo, los procedimientos y herramientas utilizadas en la investigación, son de absoluta responsabilidad de el/la autora (a) del trabajo de integración curricular. Así mismo, me acojo a los reglamentos internos de la Universidad de Investigación de Tecnología Experimental Yachay.

Urcuquí, agosto 2019.

---

Carlos Enrique Bustamante Orellana  
CI: 0705378933

## **AUTORIZACIÓN DE PUBLICACIÓN**

Yo, **CARLOS ENRIQUE BUSTAMANTE ORELLANA**, con cédula de identidad 0705378933, cedo a la Universidad de Tecnología Experimental Yachay, los derechos de publicación de la presente obra, sin que deba haber un reconocimiento económico por este concepto. Declaro además que el texto del presente trabajo de titulación no podrá ser cedido a ninguna empresa editorial para su publicación u otros fines, sin contar previamente con la autorización escrita de la Universidad.

Asimismo, autorizo a la Universidad que realice la digitalización y publicación de este trabajo de integración curricular en el repositorio virtual, de conformidad a lo dispuesto en el Art. 144 de la Ley Orgánica de Educación Superior

Urcuquí, agosto 2019.

---

Carlos Enrique Bustamante Orellana  
CI: 0705378933

## **Dedicatoria**

Dedico este trabajo de integración curricular a mi madre, MARÍA ORELLANA, por su apoyo incondicional en todo momento y por ser un ejemplo para mí y mi hermano. A mi hermano, LUIS, por ser parte de mi vida y darme otra razón para seguirme esforzando. A mi tía, DOTILA, por su apoyo palabras de ánimo. A toda mi familia por su apoyo en todos los aspectos de mi vida. A mis profesores por sus enseñanzas sobre ciencia y la vida, y finalmente, a mis compañeros de clase y amigos que han hecho este camino más divertido.

Carlos Enrique Bustamante Orellana

## **Agradecimiento**

Agradezco a todos los maestros que he tenido durante mi carrera en la Universidad Yachay, personas muy sabias que me han dado lecciones tanto profesionales como personales. En especial, me gustaría agradecer a mi tutora, Ph.D. Lorena Guachi, por sus enseñanzas y apoyo durante el desarrollo del presente trabajo, además de varios otros trabajos. También agradezco a Ph.D. Robinson Guachi por su contribución al desarrollo de este trabajo, a pesar de la limitación de la distancia. Agradezco también a mis amigos y compañeros de clase por su dedicación y paciencia durante las largas jornadas que hemos tenido que realizar para completar diferentes proyectos. Finalmente, me gustaría agradecer a la Universidad Yachay, y a todos quienes la conforman, por el apoyo dado a los estudiantes y las oportunidades ofrecidas para crecer académica y personalmente.

Carlos Enrique Bustamante Orellana

## **Resumen**

El modelado matemático adecuado del comportamiento de los tejidos blandos es el mayor desafío para obtener simulaciones más realistas de procedimientos quirúrgicos, entre otras aplicaciones. Durante muchos años, los modelos lineales elásticos se han utilizado para realizar este tipo de simulaciones debido a sus rápidos resultados. Sin embargo, estos modelos no reflejan el comportamiento real de los tejidos blandos cuando se éstos son sometidos a diferentes cargas. Actualmente, los modelos que mejor reproducen este comportamiento son los modelos hiperelásticos, y hay muchos de estos modelos propuestos en la literatura. Este trabajo tiene como objetivo realizar un estudio explicativo de modelos matemáticos adecuados para simulaciones realistas de tejidos blandos mediante el análisis de sus parámetros y características principales. Después de una descripción de un total de 34 modelos matemáticos, se analizaron los aspectos más importantes acerca de ellos y se presentaron clasificaciones según el rango de deformación, la complejidad y la aplicación. Además, se presentó una tabla que resume las características más importantes de los modelos matemáticos.

### **Palabras Clave:**

Modelado matemático, tejidos blandos, simulaciones realistas, modelos lineales elásticos, modelos hiperelásticos, estudio explicativo, rango de deformación, complejidad, aplicación.

## **Abstract**

Adequate mathematical modeling of soft tissues behavior is the biggest challenge to obtain more realistic simulations of surgical procedures, among other applications. For many years, linear elastic models have been used to perform this kind of simulations because of their fast results. However, these models do not reflect the real behavior of soft tissues when they are undergoing to different loads. Currently, the models that better reproduce this behavior are the hyperelastic models, and there are many of these models proposed in the literature. This work aims to perform an explanatory study of mathematical models suitable for realistic soft tissue simulations by analyzing their parameters and main characteristics. After a description of a total of 34 mathematical models, the most important aspects about them were analyzed and classifications according to deformation range, complexity and application were presented. In addition, a table, that summarizes the most important characteristics of the mathematical models, was presented.

### **Key Words:**

Mathematical modeling, soft tissues, realistic simulations, linear elastic models, hyperelastic models, explanatory study, deformation range, complexity, application.

# Contents

<b>1</b>	<b>Introduction</b>	<b>3</b>
1.1	Motivation . . . . .	3
1.2	Scope . . . . .	3
1.3	Dissertation Overview . . . . .	4
<b>2</b>	<b>Theoretical Framework</b>	<b>4</b>
2.1	Concepts . . . . .	4
2.2	Similarities Between Soft Tissues and Rubber Materials . . . . .	9
2.2.1	Mechanical Characteristics . . . . .	10
2.2.2	Composition . . . . .	11
2.2.3	Constitutive Models . . . . .	11
2.3	Continuum Mechanics Foundation . . . . .	11
2.4	Micromechanics Foundation . . . . .	16
2.5	Assumptions . . . . .	17
2.5.1	Homogeneous Materials . . . . .	17
2.5.2	Isotropic Materials . . . . .	18
2.5.3	Incompressible Materials . . . . .	18
2.6	Stress-Strain Curve . . . . .	20
2.6.1	Laboratory Tests . . . . .	20
2.6.2	Engineering Stress and Strain . . . . .	21
2.6.3	True Stress and Strain . . . . .	23
2.6.4	Analysis of Stress-Strain Curve . . . . .	23
2.6.5	Stress-Strain Curve for Mathematical Models . . . . .	26
2.7	Mathematical Models . . . . .	29
2.7.1	Phenomenological Models . . . . .	30
2.7.2	Models Based on Experimental Determination of $\frac{\partial W}{\partial I_1}$ and $\frac{\partial W}{\partial I_2}$ . . . . .	35
2.7.3	Physically-Based Models . . . . .	37
<b>3</b>	<b>Mathematical Models for Realistic Soft Tissue Simulations</b>	<b>46</b>
3.1	Methodology . . . . .	46
3.1.1	State of The Art Review in Mathematical Models . . . . .	46
3.1.2	Models Selection . . . . .	47

---

3.1.3	Analysis and Evaluation of Selected Models . . . . .	48
3.1.4	Establishment of Classification Criteria . . . . .	48
3.1.5	Obtaining Results . . . . .	48
3.2	Models . . . . .	48
3.3	Parameters . . . . .	52
3.3.1	Material Constants Used to Define the SEF of The Model . . . . .	52
3.3.2	Deformation Range . . . . .	53
3.3.3	Accuracy . . . . .	53
3.4	Classifications . . . . .	54
3.4.1	By Deformation Range . . . . .	54
3.4.2	By Complexity . . . . .	54
3.4.3	By Application . . . . .	55
<b>4</b>	<b>Results and Discussion</b>	<b>56</b>
<b>5</b>	<b>Conclusions</b>	<b>70</b>
	<b>References</b>	<b>72</b>
	<b>Appendices</b>	<b>78</b>
<b>A</b>	<b>Appendix 1</b>	<b>78</b>

# 1 Introduction

## 1.1 Motivation

Adequate mathematical modeling of soft tissue behavior is the biggest challenge to obtain more realistic simulations of surgeries. For many years, linear models have been used to perform this kind of simulations because of their fast results. However, they do not reflect the real behavior of soft tissues when they are undergoing to loads. Currently, the models that better reproduce this behavior, in contrast with linear models, are the hyperelastic models. These models are based on different approaches such as observation, physics or biology; and have different results depending on the conditions of the simulation being performed. The hyperelastic models described in this work consider soft tissues as homogenous, isotropic, and incompressible. Several researchers have based their studies on the similarities between soft biological tissues and rubber materials, so, the prediction of soft tissue behavior can be performed using the mathematical models used to determinate rubber behavior. Considering those mathematical models that work on rubber work on soft tissues too, there is a huge amount of models that can be used to simulate the behavior of these materials. These mathematical models can be used for specific applications such as preoperative plans, real-time simulations of surgical procedures, analysis of injury mechanisms in vehicle accidents, airplane ejections, blast-related events, developing and testing surgical implants. So, given the great number of possibilities for mathematical models that can be used for soft tissue simulations and the different applications where they can be used, programmers, engineers, biomedical, etc. do not know which model to choose for their specific needs.

## 1.2 Scope

This project aims to provide a point-of-view to choose between mathematical models for simulations of soft tissue deformations considering their material constants, range of deformation, and accuracy for their computation and representation. The existent mathematical models that can be used for these purposes will be categorized by deformation range, complexity, and application. These classifications will be performed in such a way that allows people in need of mathematical models for soft tissue simulations to choose the most adequate model for their particular application. An extensive literature review must be done to achieve such a goal. The literature review is necessary to understand the theory behind the different mathematical models and their results in simulations.

### 1.3 Dissertation Overview

This work presents an explanatory study of mathematical models that are suitable for realistic soft tissue simulations. In order to achieve such a task, chapter 2 presents the theoretical framework of the project where the most important concepts, used during the work, are described. Then, some similarities, shared between soft tissues and rubber materials, are addressed. After that, reviews, about continuum mechanics and micromechanics, are performed. In addition, the simplification of formulas, for incompressible materials, is shown; followed by an explanation of the stress-strain curve for materials. Finally, the mathematical models, found in the literature, are explained. In chapter 3, the methodology of the work is presented together with the selection of the models to be analyzed and classified, the parameter chosen to evaluate the models, and the type of classifications to be performed. Chapter 4 presents the results and discussion and finally, chapter 5 presents the principal conclusions obtained in this work.

## 2 Theoretical Framework

In the last years, many experiments introduced in the literature have demonstrated that soft tissues correspond highly to nonlinear viscoelastic materials. The difficulties present in the laboratory tests to find the material constants that define a non-linear viscoelastic model have placed the hyperelastic models among the most used to describe the behavior of soft tissues, these hyperelastic models are similar to rubber in properties. In this sense, several approaches to model soft tissue mechanical behavior have been adopted looking for a realistic simulation with a trade-off between deformation range and accuracy. The hyperelastic models are mostly based on continuum mechanics and micromechanics.

In this chapter, essential concepts, used in this work, are presented, then the mathematical models found in literature are described, and a classification of several models is presented taking into account the taxonomy proposed in [1], mainly based on the approach that the authors have followed to develop the structure of the models.

### 2.1 Concepts

For a better comprehension of the different terminology, used in this work, a set of important concepts and its definitions are presented, before starting the description of it.

- Anisotropic Material

It is a material that has properties that change with the direction.

- Coaxial  
Having the same axis as another body.
- Compression Force  
Application of power, pressure, or exertion against an object which causes it to become squeezed, squashed, or compacted.
- Constitutive Modeling  
Mathematical description of the response of materials to different loads.
- Continuum Mechanics  
Branch of mechanics dealing with the mechanical behavior of materials which are modeled as a continuous mass instead of discrete particles.
- Coordinate  
Each of a group of numbers used to indicate the position of a point, line, or plane.
- Creep Effect  
The tendency of a solid material to move slowly or deform permanently under the influence of persistent mechanical stresses.
- Deformation  
Changing in shape or distorting, especially through the application of pressure.
- Eigenvector  
A non-zero vector that changes by only a scalar factor when a linear transformation is applied to it.
- Eigenvalue  
Characteristic root associated with an eigenvector.
- Elasticity  
The ability of a material to resist distortion and return to its original state without any alteration. In real-world materials that exhibit perfect elastic behavior do not exist, making this concept of elasticity the characteristic of an ideal material only.
- Elastomer  
A natural or synthetic polymer which has elastic properties. Example: rubber.

- **Engineering Strain**

The response of a system to an applied load. When a material is subjected to a load, it produces stress in the material, which then results in deformation. The amount of deformation divided by the original length of the material gives as result the engineering strain.
- **Engineering Stress**

The force or load applied to a cross-sectional area of the material before any deformation has occurred. In other words, engineering stress is the internal distribution within the material as a reaction to a load being applied.
- **Experimental Data**

Information obtained by measurement, test method, experimental design or quasi-experimental design. This data can be qualitative or quantitative.
- **Heterogeneity**

Quality of being diversified in character or content.
- **Homogeneous Material**

Material of uniform composition throughout that cannot be mechanically separated into different materials.
- **Hook's Law**

Law of physics that states that the force needed to extend or compress a spring by some distance scales linearly with respect to that distance.
- **Hyperelasticity**

A term used on materials that exhibit highly nonlinear elastic stress-strain behavior such as rubber. These materials can remain elastic up to large strain values (often 100 % and more).
- **Hysteresis**

A phenomenon in which the value of a physical property lags behind changes in the effect causing it.
- **Incompressible Material**

Material that changes its volume in an inappreciable way when it is subjected to pressure.
- **Isotropic Material**

Material that has identical values for a property in all directions.

- **Linearity**  
Property of a mathematical relationship or function meaning that it can be graphically represented as a straight line.
- **Macromolecule**  
Molecule That contains a very large number of atoms, such as a protein, nucleic acid, or synthetic polymer.
- **Material Parameters**  
Unique constants for each material that must be determined through laboratory tests.
- **Mathematical Model**  
The description of a phenomenon using math concepts. It can be used to represent, analyze and make predictions about such phenomena in real life.
- **Mechanical Behavior**  
The response of a material to a stimulus, which is described by its mechanical properties.
- **Mechanical Property**  
Part of the specifications of a material, which are obtained using laboratory tests. Some examples of mechanical properties of materials are elasticity module, yield, ultimate tensile strength, ductility, stress-strain relationship, etc.
- **Micromechanics**  
Branch of mechanics dealing with the analysis of composite or heterogeneous materials on the level of the individual constituents that constitute these materials.
- **Monomer**  
A molecule that can be bonded to other identical molecules in order to form a polymer.
- **Nonlinearity**  
Property of a mathematical relationship or function of not being able to be represented as a straight line.
- **Plasticity**  
Property describing an irreversible change of shape that a material suffers after applying certain forces or loads.

- **Polymer Chains**  
Group of substances with a molecular structure consisting mainly or entirely of a large number of similar units bonded together.
- **Reference System**  
A system that uses coordinates to establish a position.
- **Rubber Material**  
Material that presents characteristics, which are similar to rubber's characteristics, especially the exhibition of very large strains, with strongly non-linear stress-strain relation. These materials consist of chain-like macromolecules that are more or less closely connected to each other via entanglements or cross-links.
- **Soft Tissue**  
The substance making up the organs, which connects, supports or surrounds other structures and organs of the body. This term refers to tendons, ligaments, fascia, skin, fibrous tissues, fat, synovial membranes, muscles, nerves, and blood vessels.
- **Soft Tissues Simulation**  
Reproduction of the behavior of soft tissues when subjected to different loads and stretches, usually performed through mathematical models.
- **Spectral Decomposition Theorem**  
Result about when a linear operator or matrix can be diagonalized, i.e. represented as a diagonal matrix on some basis. This theorem also provides an eigenvalue decomposition of the underlying vector space on which the operator acts.
- **Strain Hardening Phenomenon**  
Incident observed as a strengthening of material during large strain deformation, which is caused by large scale orientation of chain molecules and lamellar crystals.
- **Stress-Strain Diagram**  
A graphic that shows the relationship between the stress that suffers an object and the strain that the object has been subjected to. It is unique for each material and helps to determine the properties of such material. This diagram is usually determined by laboratory tests by recording the amount of deformation at distinct intervals of tensile or compressive loading (stress), and in the case of a simulation, it must be obtained through a mathematical model.

- **Stretch Ratios**

Deformation suffered by a determined material in a specific direction, which is computed as the final length over the initial length of the material in a direction.

- **Tension Force**

A force which is transmitted through a rope, string or wire when pulled by forces acting from opposite sides.

- **Tensor**

A geometric object that maps in a multi-linear manner geometric vectors, scalars, and other tensors to a resulting tensor.

- **True Strain**

Deformation obtained with the instantaneous length instead of the original length that is used in the case of engineering strain.

- **True Stress**

The measurement obtained with the instantaneous area instead of the non-deformed area that is used in the case of engineering stress.

- **Viscoelasticity**

Property of a substance of exhibiting both elastic and viscous behavior.

- **Viscosity**

The ability of a material to resist flow, where the flow is the gradual deformation by shear or tensile stress.

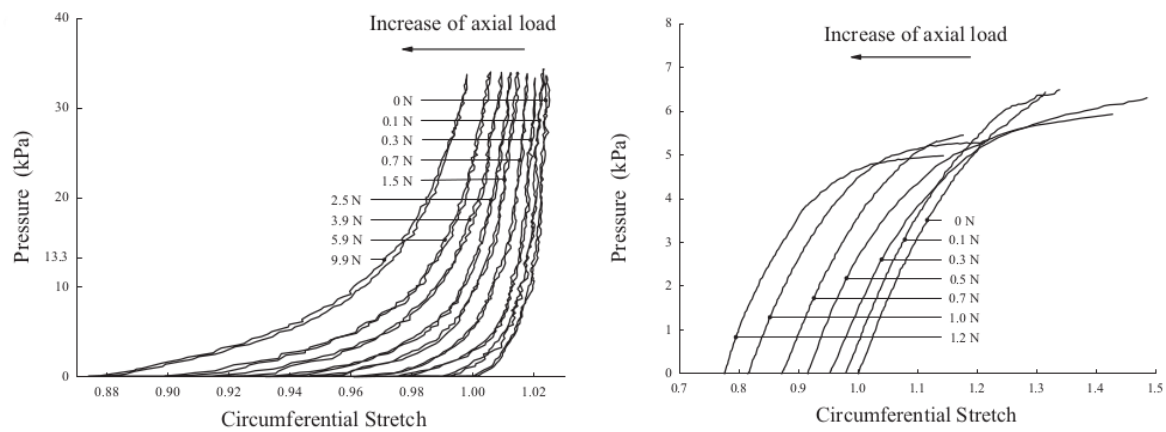
## **2.2 Similarities Between Soft Tissues and Rubber Materials**

The focus of this work is to perform an explanatory study of the mathematical models suitable for realistic soft tissue simulations, although little research has been done regarding the application of mathematical models for such purpose. However, there is plenty of research about mathematical models to simulate the mechanical behavior of rubber, which is due to the high demand for this material in the industry. According to Holzapfel [2], soft tissues and rubber materials have similarities in structure, mechanical characteristics, and constitutive modeling. The findings of this work are described next.

### 2.2.1 Mechanical Characteristics

The mechanical characteristics that soft tissues and rubber materials share are nonlinearity, anisotropy, heterogeneity, inelasticity, pre-conditioning, thermoelasticity, age dependency, among others.

Both soft tissues and rubber materials can be characterized as highly nonlinear materials that are subjected to finite strains. Such characteristics can be appreciated in Figure 1 which shows pressure/stretch plots about experimental data of arterial and rubber tubes during inflation and various axial loads.



(a) Inflation tests performed with a human iliac artery in its non-active state of smooth muscle cells

(b) Inflation tests performed with a Latex tube

Figure 1: Response of soft tissues and rubber to inflation tests [2]

Regarding anisotropy, it is caused by the stiffening effect on soft tissues. Such an effect is based on the recruitment of the embedded wavy collagen fibers. Biopolymers are oriented along the loading direction for some tissues, which is similar for rubber materials at high stretches when the polymer chains align along the loading direction. Soft tissues and rubber materials also respond in a homogeneous way to macroscopic problems, and heterogeneity is not taken into account except for specific cases.

Soft tissues and rubber materials usually exhibit viscoelasticity, which is identified through hysteresis, relaxation and creep effects. This behavior reveals inelasticity on behalf of both materials. Regarding pre-conditioning, the biological material is referred as pre-conditioned when the number of load cycles until the material exhibits a nearly repeatable cyclic behavior is diminished due to the pronounced stress softening displayed by the cyclic loading and unloading. The same term is not applicable for rubber materials, for which the name of this behavior is the Mullins effect.

Thermoelastic properties of soft-tissues and rubber materials are similar too. A piece of vulcanized rubber subjected to a weight generates a slight cooling effect in the very low strain range and changes to a heating effect when increasing the weight, while rubber will contract its length under tension when its temperature

is raised. Finally, the mechanical properties of these two materials also depend on age. Physical-mechanical properties of rubber compounds are influenced by the effect of thermal aging; and regarding soft tissues, tests on aortic strips have proved that the distensibility of the human aorta decreases as a function of age.

### 2.2.2 Composition

Both soft tissues and rubber materials are composite structures that present nonlinear properties derived from specific distributions of their internal constituents. Soft tissues are formed by structural proteins and cells, besides having elastin and collagen as determinants of their nonlinear mechanical properties (studies have been done in arterial walls). Natural rubber, on the other hand, is formed by 95% of cis 1,4-polyisoprene, 2.5% of protein and 2.5% of lipids, phenols, sugars, and fatty acids. Then, vulcanized rubber is obtained after the vulcanization of natural rubber with sulfur. In addition, several rubber materials are obtained by reaction chemistry, which means chemical cross-linking of the molecules either by sulfur or other chemical substances.

### 2.2.3 Constitutive Models

The composition and mechanical characteristics of materials are determinant in the design of constitutive models on the basis of comprehensive experimental data. So, as soft tissues and rubber materials share many of these characteristics, the models designed for one type of these materials will be also applicable to the other type. Therefore, the prediction of soft tissue behavior can be obtained from a precise prediction of rubber behavior.

## 2.3 Continuum Mechanics Foundation

Given that many mathematical models that will be covered in this work have their basis on continuum mechanics, especially in stretch ratios and invariants, a brief review of this topic is needed in order to state some important definitions and formulations that will be used later when the models are presented. The explanation of continuum mechanics reviewed in this subsection is based on [3, 4, 5].

Let us start by the deformation gradient  $\mathbf{F}$ , which is defined as the change of a material from an initial configuration to a deformed configuration. Figure 2 shows the process of material deformation and Figure 3 shows the form of  $\mathbf{F}$  for a stretching. So, assuming that at its initial configuration, a material occupies a region  $R_0$ , and that a point  $P_0$  inside that region has position vector  $\mathbf{X}$ ; as well as in the deformed configuration, the material occupies a region  $R$ , and a point  $P$  inside that region has position vector  $\mathbf{x}$ . Then,  $\mathbf{F}$  can be expressed

as:

$$F_{ij} = \frac{\partial x_i}{\partial X_j} \text{ or } \mathbf{F} = \frac{\partial \mathbf{x}}{\partial \mathbf{X}} \tag{1}$$

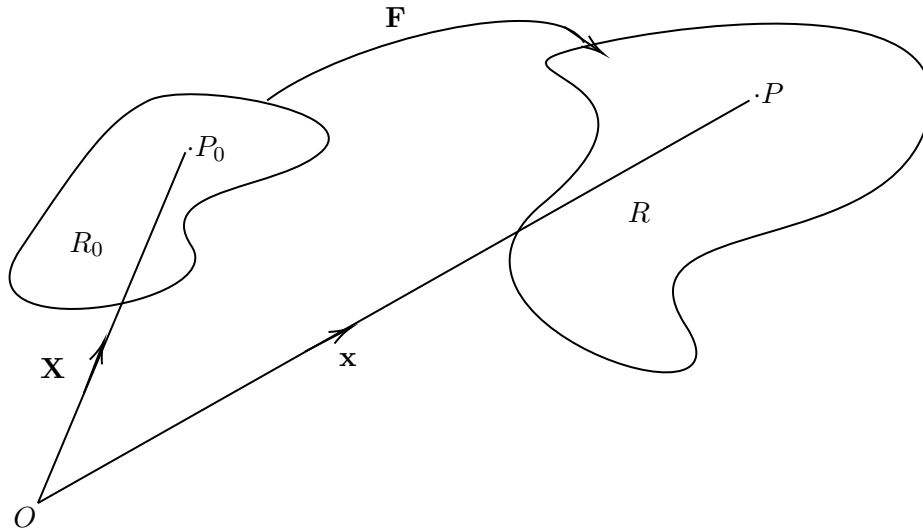


Figure 2: Change of a material from a initial configuration to a deformed configuration

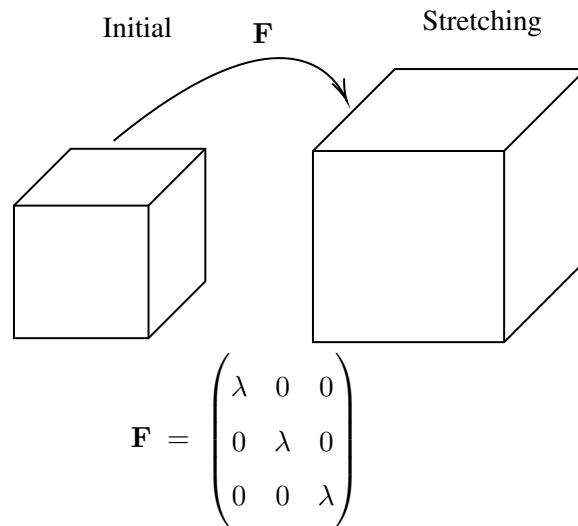


Figure 3: Form of deformation gradient for the stretching of a material

So,  $\mathbf{F}$  is a mixture of rotation and pure stretch. In order to define  $\mathbf{P}$ , either  $\mathbf{X}$  or  $\mathbf{x}$  coordinates can be used, and the same case happens with any other quantity associated with  $\mathbf{P}$ . Using  $\mathbf{X}$  coordinates is known as material or Lagrangian point of view, whereas using the  $\mathbf{x}$  coordinates takes the name of spacial or Eulerian point of view. In the Lagrangian approach, each particle is identified by the coordinates of the point it occupies

initially (also called material coordinates) that are taken as independent variables. In the second approach, called Eulerian, the attention is focused on a fixed point in space with some coordinates (also called spatial coordinates) that can be occupied by different particles at different times. In this case, the coordinates also play the role of independent variables. Both approaches are equivalent because, since the functions that define the transformation are invertible, given the initial coordinates of a particle it is possible to determine its position at any time and given the position of a particle at a given instant it is possible to determine its initial position.

Using the spectral decomposition theorem, the matrix  $\mathbf{F}$  can be decomposed into two forms: the first is a rotation  $\mathbf{R}$  followed by left stretch  $\mathbf{V}$ , and the second is a right stretch  $\mathbf{U}$  followed by a rotation  $\mathbf{R}$ . The matrix  $\mathbf{R}$  is orthogonal, i.e.  $\mathbf{R}^T = \mathbf{R}^{-1}$ , and the matrices  $\mathbf{V}$  and  $\mathbf{U}$  are symmetric with positive eigenvalues. Then,  $\mathbf{F}$  can be decomposed as:

$$\mathbf{F} = \mathbf{V}\mathbf{R} = \mathbf{R}\mathbf{U} \quad (2)$$

Isolating  $\mathbf{V}$  and  $\mathbf{U}$  respectively:

$$\mathbf{V} = \mathbf{R}\mathbf{U}\mathbf{R}^T \quad (3)$$

$$\mathbf{U} = \mathbf{R}^T\mathbf{V}\mathbf{R} \quad (4)$$

The equation 4 can be interpreted by considering that the components of  $\mathbf{V}$  expressed in a coordinate system whose axes are rotated by  $\mathbf{R}$  relative to the reference system are identical to those of  $\mathbf{U}$ . Then, taking the Lagrangian principal directions  $L$  (eigenvectors of  $\mathbf{U}$ ) as the reference system, and the Eulerian principal directions  $E$  (the eigenvectors of  $\mathbf{V}$ ) as the new system, the result will be:

$$[\mathbf{V}]_E = [\mathbf{U}]_L = \begin{pmatrix} \lambda_1 & 0 & 0 \\ 0 & \lambda_2 & 0 \\ 0 & 0 & \lambda_3 \end{pmatrix} \quad (5)$$

where  $\lambda_1, \lambda_2, \lambda_3$  are the principal stretch ratios (ratios of extended to initial length of line segments in the principal directions). Equation 5 shows that even though matrices  $\mathbf{V}$  and  $\mathbf{U}$  are different, their expressions as matrices of components are the same when different but appropriate coordinates are chosen. In addition, if pure strain occurs, i.e. there is no rotation, equation 2 can be simplified as  $\mathbf{F} = \mathbf{V} = \mathbf{U}$ .

Regarding strains, strain tensors are usually defined to be coaxial to either  $\mathbf{V}$  or  $\mathbf{U}$  and to have principal values reducing to  $e = \lambda - 1$  at small strains. Two forms would meet such requirement:  $(\lambda^n - 1)/n$  with  $n \neq 0$  and  $\log(\lambda)$ . Then, one possible family of strain tensors is  $(\mathbf{V}^n - \mathbf{I})/n$  and choosing  $n = 2$  for convenience

because  $\mathbf{V}^2$  can be expressed in terms of  $\mathbf{F}$ , we have:

$$\mathbf{U}^2 = \mathbf{F}^T \mathbf{F}, \text{ and} \quad (6)$$

$$\mathbf{V}^2 = \mathbf{F} \mathbf{F}^T \quad (7)$$

The left Cauchy Green deformation tensor is defined as  $\mathbf{B} = \mathbf{V}^2 = \mathbf{F} \mathbf{F}^T$ , and the right Cauchy Green deformation tensor as  $\mathbf{C} = \mathbf{U}^2 = \mathbf{F}^T \mathbf{F}$ . The matrix  $\mathbf{E} = (\mathbf{F}^T \mathbf{F} - \mathbf{I})/2$  is known as the Green Lagrange strain tensor. The described family of strain tensors will be the only one covered in this review, because it leads to the formulations and concepts needed for the mathematical models to be analyzed later.

For various purposes, three principal stretches would be enough to describe the deformation of a material. So, given a deformation  $\mathbf{F}$ , the tensors  $\mathbf{U}$  and  $\mathbf{V}$  can be found in some steps:

1. Find the eigenvectors of  $\mathbf{C}$  by solving the characteristic equation:

$$\det(\mathbf{C} - \lambda^2 \mathbf{I}) = 0 \quad (8)$$

$$\Rightarrow \lambda^6 - \mathbf{I}_1(\mathbf{C})\lambda^4 + \mathbf{I}_2(\mathbf{C})\lambda^2 - \mathbf{I}_3(\mathbf{C}) = 0 \quad (9)$$

Where:

$$I_1(\mathbf{C}) = \text{tr}(\mathbf{C}) = \lambda_1^2 + \lambda_2^2 + \lambda_3^2 \quad (10)$$

$$I_2(\mathbf{C}) = \frac{1}{2}(\text{tr}(\mathbf{C}))^2 - \text{tr}(\mathbf{C}^2) = \lambda_1^2 \lambda_2^2 + \lambda_2^2 \lambda_3^2 + \lambda_3^2 \lambda_1^2 \quad (11)$$

$$I_3(\mathbf{C}) = \frac{1}{6}(\text{tr}(\mathbf{C}))^3 - 3\text{tr}(\mathbf{C})\text{tr}(\mathbf{C}^2) + 2\text{tr}(\mathbf{C}^3) = \lambda_1^2 \lambda_2^2 \lambda_3^2 \quad (12)$$

In this formulations,  $\det(\cdot)$  is the determinant, and  $I_1$ ,  $I_2$ , and  $I_3$  are the principal invariants of  $\mathbf{C}$  (the ones to be used to build the hyperelastic models later). The rest of the invariants can be obtained from these three principals. An important remark is that the principal invariants are not unique in this feature because the eigenvalues  $\lambda_1^2$ ,  $\lambda_2^2$  and  $\lambda_3^2$  form another set of three independent variables.

2. After solving the equation 9 for  $\lambda_1^2$ ,  $\lambda_2^2$  and  $\lambda_3^2$ , we can substitute these eigenvalues in:

$$\mathbf{C} \mathbf{u} = \lambda^2 \mathbf{u} \quad (13)$$

And solve for each case the three simultaneous equations in order to give the three components of the corresponding eigenvectors  $\mathbf{u}_1$ ,  $\mathbf{u}_2$ , and  $\mathbf{u}_3$ . Given a symmetric tensor, the eigenvectors are orthogonal, i.e.  $\mathbf{u}_i^T \mathbf{u}_j = \delta_{ij}$  (unit length eigenvectors), or can be chosen to be so if the eigenvalues are equal. Therefore, the matrix  $\mathbf{C}$  is expressed as follows:

$$\mathbf{C} = \lambda_1^2 \mathbf{u}_1 \mathbf{u}_1^T + \lambda_2^2 \mathbf{u}_2 \mathbf{u}_2^T + \lambda_3^2 \mathbf{u}_3 \mathbf{u}_3^T \quad (14)$$

3. Following that  $\mathbf{U}$  is coaxial with  $\mathbf{U}^2$ , and  $\mathbf{C} = \mathbf{U}^2$ , we have:

$$\mathbf{U} = \lambda_1^2 \mathbf{u}_1 \mathbf{u}_1^T + \lambda_2^2 \mathbf{u}_2 \mathbf{u}_2^T + \lambda_3^2 \mathbf{u}_3 \mathbf{u}_3^T \quad (15)$$

In that way  $\mathbf{u}_i$  form the Lagrangian triad.

4.  $\mathbf{U}^{-1}$  can be built from  $\mathbf{U}$  as follows:

$$\mathbf{U}^{-1} = \frac{1}{\lambda_1} \mathbf{u}_1 \mathbf{u}_1^T + \frac{1}{\lambda_2} \mathbf{u}_2 \mathbf{u}_2^T + \frac{1}{\lambda_3} \mathbf{u}_3 \mathbf{u}_3^T \quad (16)$$

5. Once  $\mathbf{U}^{-1}$  has been determined,  $\mathbf{R}$  can be obtained as:

$$\mathbf{R} = \mathbf{F} \mathbf{U}^{-1} \quad (17)$$

6. Finally,  $\mathbf{V}$  can be obtained as:

$$\mathbf{V} = \mathbf{F} \mathbf{R}^T \quad (18)$$

From now on, the only pure strain will be considered because it is the common deformation applied in laboratory tests from where the mathematical models are derived. Models that are built using continuum mechanics theory can take into account either the principal stretch ratios or the principal invariants of the right Cauchy Green deformation tensor. Wherever the case is, it is necessary to define a strain energy function (SEF) for the model in question. Such SEF is denoted  $W = W(\mathbf{C})$  and can be divided into volumetric (shape-preserving) and isochoric (volume preserving but shape changing) parts because rubber materials commonly present a decoupled response to volumetric and deviatoric deformations. So, the SEF for models based on continuum mechanics is expressed as:

$$W(\mathbf{C}) = W_{vol}(J) + W_{iso}(\bar{\mathbf{C}}) \quad (19)$$

where  $J = \det(\mathbf{F})$  and  $\bar{\mathbf{C}} = J^{-\frac{2}{3}} \mathbf{C}$ . As this work focuses on soft tissues, which are incompressible materials like rubber; the previous equations can be simplified. So, in case of incompressible materials  $\det(\mathbf{F}) = 1$ , and therefore,  $J = 1$  and  $\bar{\mathbf{C}} = \mathbf{C}$ . An explanation about rubber being an incompressible material and the deduction of  $\det(\mathbf{F}) = 1$  will be given in Section 2.5.3 on this work.

Models that are built considering the principal stretch ratios have the following general form of strain energy function:

$$W = \sum_{n=1}^N \frac{\mu_n}{\alpha_n} [\bar{\lambda}_1^{\alpha_n} + \bar{\lambda}_2^{\alpha_n} + \bar{\lambda}_3^{\alpha_n} - 3] \quad (20)$$

where  $\mu_n$  is the shear modulus,  $\alpha_n$  is a dimensionless exponent and  $\bar{\lambda}_i$  are the modified principal stretches ( $\bar{\lambda}_i = J^{-\frac{1}{3}} \lambda_i$ );  $\mu_n$  and  $\alpha_n$  must satisfy that  $\mu_n \alpha_n > 0$ . For incompressible materials  $\bar{\lambda}_i = \lambda_i$ .

On the other hand, models that are designed using the principal invariants of the right Cauchy Green deformation tensor usually have the following general form:

$$W = W(I_1, I_2, I_3) = \sum_{i,j,k=0}^{\infty} C_{ijk} (I_1 - 3)^i (I_2 - 3)^j (I_3 - 3)^k \quad (21)$$

where  $C_{ijk}$  are material parameters. For incompressible materials, equation 21 can be simplified as follows:

$$W = W_{iso}(I_1(\mathbf{C}), I_2(\mathbf{C})) = W_{iso}(\bar{I}_1(\bar{\mathbf{C}}), \bar{I}_2(\bar{\mathbf{C}})) \sum_{i,j=0}^{\infty} C_{ij} (I_1 - 3)^i (I_2 - 3)^j \quad (22)$$

Such simplification is done because  $I_3 = 1$  in case of incompressible materials, so equation 21 is reduced to the isochoric strain energy function where the invariants of  $\bar{\mathbf{C}}$  coincide with the invariants of  $\mathbf{C}$ .

## 2.4 Micromechanics Foundation

Even though most of the mathematical models able to reproduce the mechanical behavior of soft tissues found in the literature are based on continuum mechanics, there are some models that have their basis on micromechanics. So, a brief review of this topic is provided in order to specify some important concepts and formulations that will be used when the methods based on this theory are presented. The explanation of micromechanics reviewed in this subsection is based on the analysis of [5] and all deductions will be done assuming incompressibility.

The micromechanical approaches for rubber elasticity commonly start by the definition of the deformation behavior of a single polymer chain, which is constituted by a macromolecule built from monomers. Such structure is modeled as a chain of  $N$  rigid beams of length  $l$ , which can be oriented with respect to each other. The maximum distance between two chain ends, denoted  $r_{max}$  is equal to its contour length, i.e.  $r_{max} = Nl$ ; and the end-to-end distance of a stress-free undeformed chain is obtained as  $r_0 = \sqrt{N}l$ . So, a chain stretch is introduced based on such considerations, as follows:

$$\Lambda = \frac{r}{r_0} = \frac{r}{\sqrt{N}l} \in [0, \sqrt{N}] \quad (23)$$

The elastic behavior of a single chain is described using a free energy function  $W = W(\Lambda)$ . Gauss and Langevin chains are the most used, and have the following energy functions:

$$W^{Gauss}(\Lambda) = \frac{3}{2} k_B \Theta \Lambda^2 + W_0 \quad (24)$$

$$W^{Langevin}(\Lambda) = k_B \Theta N \left[ \frac{\Lambda}{\sqrt{N}} \mathcal{L}^{-1}(\Lambda \sqrt{N-1}) + \ln \left( \frac{\mathcal{L}^{-1}(\Lambda \sqrt{N-1})}{\sinh(\mathcal{L}^{-1}(\Lambda \sqrt{N-1}))} \right) \right] + W_0 \quad (25)$$

where  $k_B$  is the Boltzmann's constant,  $\Theta$  is absolute temperature and  $\mathcal{L}^{-1}$  is the inverse of Langevin function obtained as  $\mathcal{L}(\cdot) = \coth(\cdot) - (\cdot)^{-1}$ . It is important to mention that the Gaussian chain is valid only for stretches from low to moderate, i.e.  $\Lambda \ll \sqrt{N}$ , because the corresponding chain force denoted as:

$$f^{Gauss}(\Lambda) = \frac{\partial W^{Gauss}}{\partial \Lambda} = 3k_B\Theta\Lambda \quad (26)$$

is a linear function, and therefore, it does not reflect finite chain extensibility in an adequate way. In addition, the inverse of Langevin function is commonly substituted by the Padé approximation for numerical applications:

$$\mathcal{L}^{-1}(\Lambda\sqrt{N^{-1}}) \approx \Lambda\sqrt{N^{-1}}\frac{3N - \Lambda^2}{N - \Lambda^2} \quad (27)$$

Taking as reference the previous description of a chain, models based on this theory are derived by averaging the energies of a certain ensemble of chains. This number of chains is chosen such that they reflect the mechanical behavior of the true polymer network in a realistic way. So, the general form of defining a model based on micromechanics theory is:

$$W = W(\mathbf{C}) := n(W) \approx \frac{n}{K} \sum_{k=1}^K W(\Lambda_k) \quad (28)$$

where  $n$  is the chain density and  $K$  is the number of chains.

## 2.5 Assumptions

In order to simplify the work, some assumptions have to be done regarding the characteristics of rubber materials, and therefore, soft tissues. These assumptions consider that rubber materials, as well as soft tissues, are homogeneous, isotropic and incompressible.

### 2.5.1 Homogeneous Materials

A homogeneous material has a uniform composition which cannot be separated into different materials. According to [2], it is reasonable to consider that soft tissues and rubber materials have a homogeneous response although they are composites. This consideration is more valid for macroscopic problems. However, there may be occasions where the heterogeneity has to be considered, but it happens in special cases only as in the modeling of the structure of arterial walls because they are composed of three layers [2]. So, as the homogeneity of rubber and soft tissues is a valid assumption, especially in macroscopic problems, this work will assume that these materials are homogeneous in its development.

### 2.5.2 Isotropic Materials

Isotropic materials are simply materials that are uniform in all directions, so their properties are the same in all directions. Chagnon et al. [6] have performed a literature review where it is mentioned that many authors have considered isotropic approaches to model soft tissues such as liver, kidney, bladder and rectum, pelvic floor, breast, cartilage, meniscus, ligaments, eardrum, arteries, brain, lungs, uterus, and skin. Besides, many authors have assumed rubber materials to be isotropic [1, 5, 7, 8, 9, 10, 11] too. So, this work will consider rubber materials and soft tissues as isotropic in order to simplify the equations, given that the consideration of anisotropy leads to very complex forms that involve much more strain invariants than it would be assuming isotropy. The forms for this type of mathematical model can be reviewed in [6].

### 2.5.3 Incompressible Materials

An incompressible material does not change significantly its volume when it is subjected to any deformation, so that, such change can be despised. This is the case of rubber materials, which have a Poisson ratio of approximately  $\frac{1}{2}$ . The relationship between Poisson's ratio and the incompressibility of material will be explained in the next lines based on the information provided in [12].

#### Poisson's Ratio

The Poisson's ratio  $\nu$  compares the strains in the transverse  $e_t$  and longitudinal  $e_l$  directions under uniaxial stress in the following way:

$$\nu = -\frac{e_t}{e_l} = \frac{\Delta D/D}{\Delta L/L} \quad (29)$$

In addition,  $\nu$  can be expressed in terms of the bulk and shear modulus for isotropic materials:

$$\nu = \frac{3(B/G - 2)}{6(B/G + 2)} \quad (30)$$

where  $B$  and  $G$  are the bulk (related to the change in size of a material) and shear (related to the change in shape of a material) modulus respectively. So, the Poisson's ratio is numerically limited by  $-1$  and  $\frac{1}{2}$ :  $-1 \leq \nu \leq \frac{1}{2}$ , for  $0 \leq \frac{B}{G} < \infty$ . Therefore, when  $\frac{B}{G} \ll 1$ , materials are extremely compressible; and when  $\frac{B}{G} \gg 1$ , materials are extremely incompressible. Figure 4 shows this relationship, and identifies the rubber materials as incompressible, with  $\nu = \frac{1}{2}$  approximately.

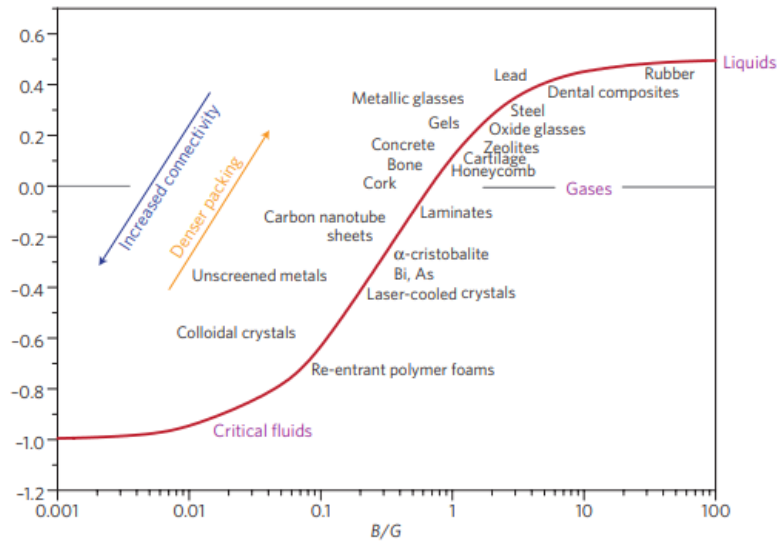


Figure 4: Relationship between bulk/shear modulus and Poisson’s ratio [12]

**Invariants for Incompressible Materials**

As previously stated, principal stretches  $\lambda_1$ ,  $\lambda_2$  and  $\lambda_3$  are the ratios of extended to initial length in the principal directions, that is:

$$\lambda_1 = \frac{l_x}{l_{x0}}, \quad \lambda_2 = \frac{l_y}{l_{y0}} \text{ and } \lambda_3 = \frac{l_z}{l_{z0}} \tag{31}$$

where  $l_{x0}$ ,  $l_{y0}$  and  $l_{z0}$  are the initial length in the directions  $x$ ,  $y$  and  $z$  respectively; while  $l_x$ ,  $l_y$  and  $l_z$  are the final length in the directions  $x$ ,  $y$  and  $z$  respectively. The rest of the deductions will be done assuming that the material of the study has the shape of a cube for simplicity, the calculus for other shapes are analogous.

For materials with cubic shape, its volume can be obtained in the following way:

$$Volume = l_{x0} * l_{y0} * l_{z0} = c \tag{32}$$

where  $c$  is any number. As the volume of an incompressible material does not change when subjected to deformations, the volume of this material after it has been deformed is:

$$Volume = \lambda_1 l_{x0} * \lambda_2 l_{y0} * \lambda_3 l_{z0} = c \tag{33}$$

Grouping stretches and longitudes, we obtain:

$$(\lambda_1 \lambda_2 \lambda_3) * (l_{x0} l_{y0} l_{z0}) = c \tag{34}$$

From equations 33 and 34, we deduce:

$$\lambda_1 \lambda_2 \lambda_3 = 1 \tag{35}$$

In addition, the third invariant  $I_3$  is defined as the determinant of  $\mathbf{C}$ , that is:

$$I_3 = \det(\mathbf{C}) = \lambda_1^2 \lambda_2^2 \lambda_3^2 \quad (36)$$

From equations 35 and 36, we finally obtain that for incompressible materials  $I_3 = 1$ .

Given the previous explanations, from now on rubber materials and, therefore, soft tissues will be assumed to be homogeneous, isotropic and incompressible.

## 2.6 Stress-Strain Curve

Some laboratory tests are needed to obtain the stress-strain curve of material, and this curve is usually built with engineering stresses and strains. Then, this part explains in detail the process to obtain the stress-strain curve for materials starting from the different laboratory tests commonly performed on materials to determine their characteristics, the way of computing engineering and true stresses and strains, a description of the curve and its main components, and finishing with an explanation of the procedure to obtain the curve for the mathematical models to be studied in this work.

### 2.6.1 Laboratory Tests

In order to find the stress-strain curve of a material, laboratory tests must be done where the material is subjected to tension or compression forces. The common types of tests performed to determine the characteristics of a material are six, which can be seen in Figure 5.

Now, considering hyperelastic materials as incompressible, which is the case of rubber and soft tissues, the number of tests needed to determine its characteristics is reduced to three uniquely because hydrostatic stresses can be superimposed on other stresses without altering the material deformation as Figure 6 shows. These three tests that can be used to characterize a hyperelastic material are uniaxial tension, uniaxial compression, and planar tension; however, compression can be replaced by an equal biaxial tension test for experimental reasons [14]. This leads to the conclusion that the mechanical tests commonly performed in hyperelastic materials are those shown in Figure 7.

The uniaxial tension test is performed using a uniaxial tension machine with dumbbells up and down and placing the material in the middle, subjected by the dumbbells. Then, the material is pulled from both sides using the same load, and the displacement is measured using an extensometer.

A planar tension test is similar to a uniaxial tension test, but the specimen is designed such that the gauge width is much larger than the gauge height or specimen thickness. The importance of using this design of

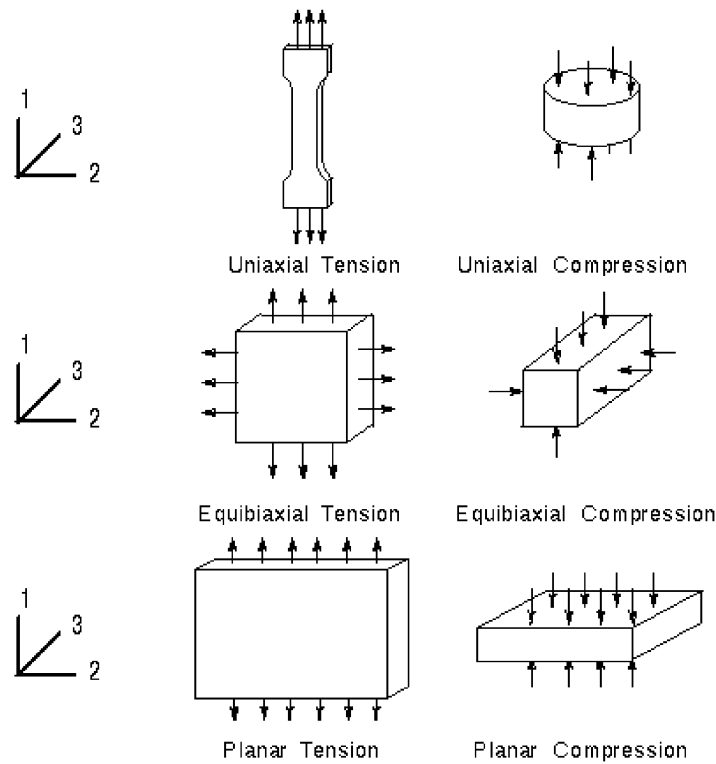


Figure 5: Test methods used to determine material properties [13]

the test is that the large aspect ratio constrains the specimen and prevents “thinning” in the width direction, resulting in a plane strain state of stress.

Equal biaxial tension of a specimen creates a state of strain which is equivalent to pure compression for incompressible or nearly incompressible materials. Even though the actual experiment is more complex than the simple compression experiment, a pure state of strain can be achieved which will result in a more accurate material model. The equal biaxial strain state can be achieved by radial stretching a circular disc.

The uniaxial compression can be performed simply by using forces from both (up and down) sides to compress the material and use a machine to measure the deformation that the material suffers.

### 2.6.2 Engineering Stress and Strain

Measurements for engineering stress and strain are obtained using the original specimen [15] (without deformations). Engineering stress, also called nominal stress or first Piola-Kirchhoff stress, is given by the formula:

$$\sigma_e = \frac{F}{A_0} \quad (37)$$

where:

- $\sigma_e$  is the engineering stress

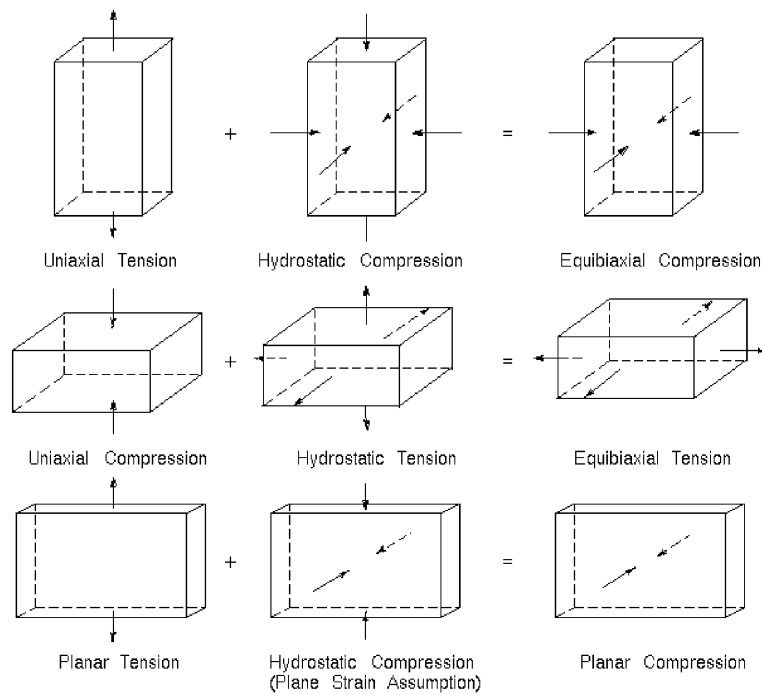


Figure 6: Test methods used to determine hyperelastic material properties because of superposition of hydrostatic stresses [13]

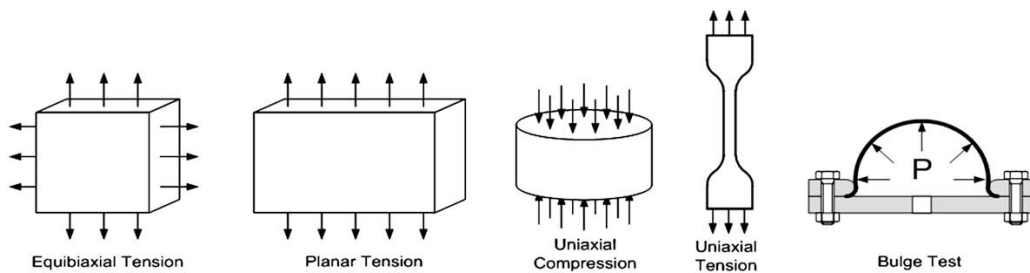


Figure 7: Mechanical tests performed on rubber [8]

- $F$  is the force, and
- $A_0$  is the undeformed or initial area

The engineering strain is given by:

$$\epsilon_e = \frac{l - l_0}{l_0} \tag{38}$$

where:

- $\epsilon_e$  is the engineering strain
- $l_0$  is the initial length of the material, and
- $l$  is the length at the time the strain is measured.

### 2.6.3 True Stress and Strain

Measurements for true stress and strain are obtained using the specimen in question at a time  $t$ . True stress, also called Cauchy stress, is given by:

$$\sigma_{true}(t) = \frac{F}{A(t)} \quad (39)$$

where:

- $\sigma(t)$  is the true stress at a time  $t$
- $F$  is the force, and
- $A(t)$  is the area of the specimen at a time  $t$

On the other hand, the true strain is given by:

$$\epsilon_{true} = \int_{l_0}^l \frac{dl}{l} = \ln \left( \frac{l}{l_0} \right) \quad (40)$$

where:

- $\epsilon_{true}$  is the true strain
- $l_0$  is the initial length of the material, and
- $l$  is the instantaneous length.

### 2.6.4 Analysis of Stress-Strain Curve

Typically, the laboratory measurements are expressed in engineering stresses and strains, so, the result of plotting the engineering stress  $\sigma_e$  against the engineering strain  $\epsilon_e$  gives as result an engineering stress-strain curve such as that shown in Fig 8. In the x-axis goes the engineering strain and in the y-axis goes the engineering stress. The stress is usually expressed in Pascals [15, 14, 8, 16, 17] ( $1Pa = 1 \frac{N}{m^2}$ ) and the strain in percentage of deformation.

Many materials obey Hooke's law of elasticity in the initial part of the curve [15], which can be seen in the gray part of Figure 8. In this portion of the curve, the stress is approximately proportional to the strain with a constant of proportionality  $E$ , known as modulus of elasticity or Young's modulus.

$$\sigma_e = E\epsilon_e \quad (41)$$

As the strain is increased, a wide range of materials usually reach a point where they deviate from the linear proportionality of Hooke's law, such a point is called the **proportional limit** [15]. After passing this limit,

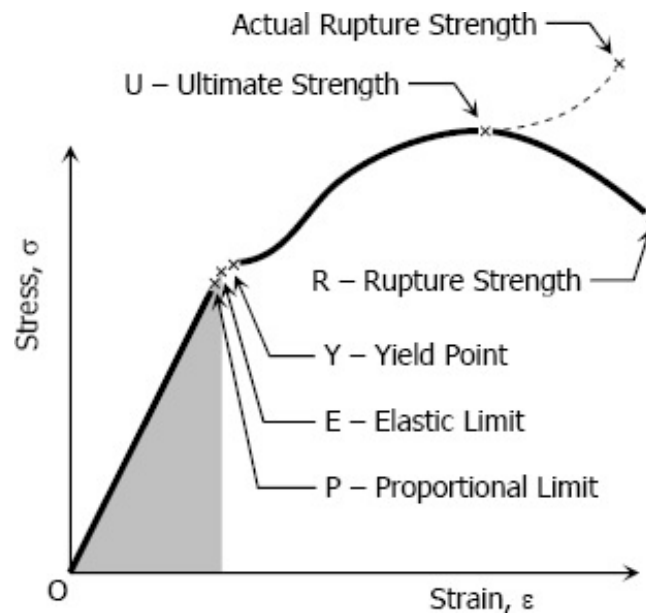


Figure 8: Stress-strain curve of a medium-carbon structural steel [18]

materials reach a point called the **elastic limit**; from this point on, materials will no longer recover their original shape, i.e. the deformation is permanent. The **yield point** is the point at which the material will suffer an elongation or yielding without increasing the load. The **ultimate strength** is the maximum stress that a material can resist before breaking and the **rupture strength** is the point where the material does not resist more load and finally breaks.

Two principal regions can be distinguished in most stress-strain curves: elastic and plastic regions. In Figure 8 the elastic region goes from O to P, and the region from P to R is known as plastic region. While the applied load produces a strain that is within the elastic region, the material will be able to return to its initial shape, but, if the produced strain surpasses the elastic region and falls into the plastic region, the deformation will be irreversible.

Each material has its own characteristics, so the stress-strain curve is unique for each material. It is possible to find materials that do not present all the characteristics previously mentioned, which is the case of the brittle materials that do not have plastic region [19]. According to Kaufman [19], materials can be classified into ductile, brittle, and polymeric; each type of material presents differentiating characteristics and stress-strain curves as shown in Figure 9.

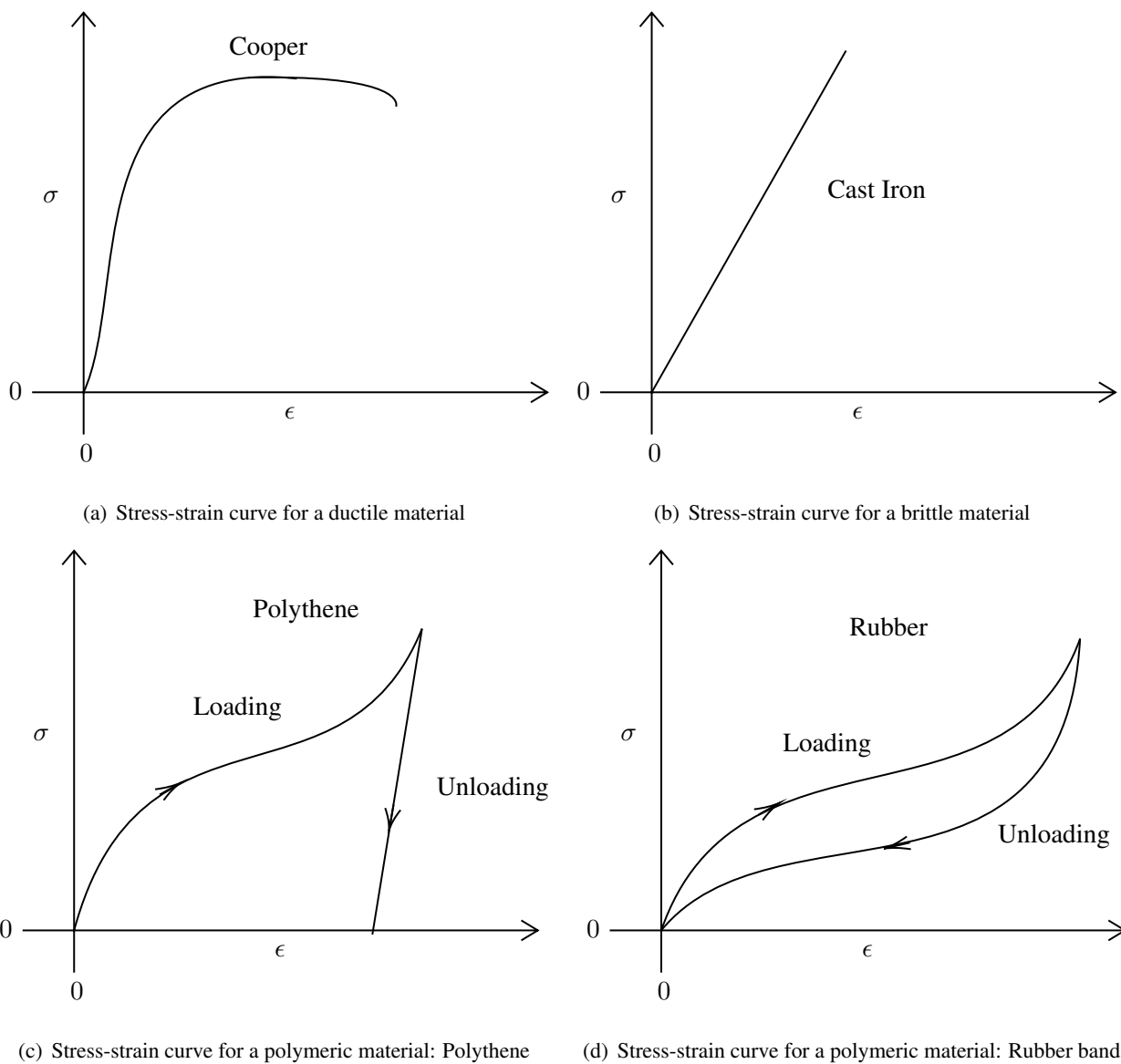


Figure 9: Stress-strain curves for different types of materials

Ductile materials such as the copper deform elastically at the beginning and stretch with little load increases after passing the yield point 9(a). This type of material presents an elastic limit that marks the point from which the deformation is irreversible, and shows necking before reaching the breaking point or rupture strength.

Brittle materials do not have plastic region as Figure 9(b) shows. Instead, this type of material obeys Hooke’s law in all strain range and breaks without advice.

Polymeric materials can be divided into two types based on how they behave after the load is removed in a tensile test, these subdivisions are the polythene and rubber materials. Both types of materials behave in a similar way when a load is applied, but when the load is removed after passing the elastic limit, polythene

adopts a new shape in a linear way 9(c), whereas rubber materials return their initial shape in a particular way 9(d).

### 2.6.5 Stress-Strain Curve for Mathematical Models

The way of obtaining the stress-strain curve for a mathematical model differs a little from the way it is done with experimental data. Although the computation of strain is the same, stresses must be obtained from the own definition of the model. Stresses are internal forces that neighboring particles of a continuous material exert on each other. For the matter of large strain problems, as mentioned before, there are two major classifications of stress tensors: the Cauchy or true stress tensor, denoted  $\sigma_{true}$ , and the first Piola-Kirchhoff or nominal stress tensor, denoted  $\sigma_e$ . In order to be in concordance with the literature,  $\sigma$  will denote the Cauchy stress tensor and  $\mathbf{P}$  will denote the first Piola-Kirchhoff stress tensor. These two types of stress tensors are related as follows:

$$\mathbf{P} = \det(\mathbf{F})\sigma\mathbf{F}^{-T} \quad (42)$$

where  $-T$  represents the transpose of the inverse. In this formula,  $\mathbf{P}$  and  $\sigma$  are matrices that have the stresses of each direction in the diagonal.

In laboratory tests, the stresses are computed using the simple formula stated in 37; however, for the mathematical models, they must be obtained from the SEF corresponding to the model, which is denoted  $W$ . So, the Cauchy stress tensor, which depends on both strain and an arbitrary scalar parameter  $p$ , can be obtained with equilibrium equations as follows:

$$\sigma = 2\mathbf{B}\frac{\partial W}{\partial \mathbf{B}} - p\mathbf{I} \quad (43)$$

where  $\mathbf{I}$  is the identity tensor. From equations 42 and 43 we obtain the formula for the first Piola-Kirchhoff stress tensor:

$$\mathbf{P} = \frac{\partial W}{\partial \mathbf{F}} - p\mathbf{F}^{-T} \quad (44)$$

Assuming the material as isotropic and incompressible, the SEF depends only on the first and second invariants of Green-Cauchy deformation tensor. Then:

$$\sigma = 2\left(\frac{\partial W}{\partial I_1} + I_1\frac{\partial W}{\partial I_2}\right)\mathbf{B} - 2\frac{\partial W}{\partial I_2}\mathbf{B}^2 - p\mathbf{I} \quad (45)$$

and

$$\mathbf{P} = 2\mathbf{F}\left[\left(\frac{\partial W}{\partial I_1} + I_1\frac{\partial W}{\partial I_2}\right)\mathbf{I} - \frac{\partial W}{\partial I_2}\mathbf{C}\right] - p\mathbf{F}^{-T} \quad (46)$$

Expressing the stress tensors in terms of principal stretch ratios, we obtain:

$$\sigma_i = 2 \left( \lambda_i^2 \frac{\partial W}{\partial I_1} - \frac{1}{\lambda_i^2} \frac{\partial W}{\partial I_2} \right) - p \quad i = 1, 2, 3 \quad (47)$$

and

$$P_i = 2 \left( \lambda_i \frac{\partial W}{\partial I_1} - \frac{1}{\lambda_i^3} \frac{\partial W}{\partial I_2} \right) - p \frac{1}{\lambda_i} \quad i = 1, 2, 3 \quad (48)$$

Given the general form of obtaining stress tensors, it must be adapted to the different types of experiments that are performed on rubber or soft tissues: uniaxial tension, equibiaxial tension, and pure shear. As experimental data is usually given in engineering strains and stresses, only the first Piola-Kirchhoff stress tensor will be considered for the deduction of stresses in the different experiments.

- **Uniaxial Tension (UT)**

In a uniaxial tension experiment, the material is elongated in one direction uniquely, that is, for instance,  $\lambda_1 = \lambda$ . Assuming the material in question is isotropic and incompressible, the other principal stretches have the form  $\lambda_2 = \lambda_3 = \lambda^{-1/2}$ . Therefore, the corresponding deformation gradient  $\mathbf{F}$  and the invariants  $I_1$  and  $I_2$  has the form:

$$\mathbf{F}^{UT} = \begin{pmatrix} \lambda & 0 & 0 \\ 0 & \lambda^{-1/2} & 0 \\ 0 & 0 & \lambda^{-1/2} \end{pmatrix}, \quad I_1^{UT} = 2\lambda^{-1} + \lambda^2, \quad I_2^{UT} = \lambda^{-2} + 2\lambda \quad (49)$$

In this type of experiment, the contraction is unhindered in the traversal directions, so, the stresses  $P_{2,3}^{UT}$  are zero and the only stress to be determined is  $P_1^{UT}$ . This stress is obtained by making equation 48 equal to zero for either  $i = 1$  or  $i = 2$  and determining the value of  $p$  as follows:

$$p = \frac{2}{\lambda} \left( \frac{\partial W}{\partial I_1} - \lambda^2 \frac{\partial W}{\partial I_2} \right) \quad (50)$$

Then, the first principal stress is obtained by inserting the value of  $p$  into the equation 48 for  $i = 1$ :

$$P_1^{UT} = 2 \left( \lambda - \frac{1}{\lambda^2} \right) \left( \frac{\partial W}{\partial I_1} + \frac{1}{\lambda} \frac{\partial W}{\partial I_2} \right) \quad (51)$$

- **Equibiaxial Tension (ET)**

In equibiaxial tension experiments, the material is equally stretched in two orthogonal directions, i.e.  $\lambda_1 = \lambda_2 = \lambda$ . As previously, by assuming isotropy and incompressibility on behalf of the material in question, the remaining stretch has the form  $\lambda_3 = \lambda^{-2}$ , and the corresponding deformation gradient and

invariants have the form:

$$\mathbf{F}^{ET} = \begin{pmatrix} \lambda & 0 & 0 \\ 0 & \lambda & 0 \\ 0 & 0 & \lambda^{-2} \end{pmatrix}, \quad I_1^{ET} = \lambda^{-4} + 2\lambda^2, \quad I_2^{ET} = 2\lambda^{-2} + \lambda^4 \quad (52)$$

In this type of experiment the stresses are equal in the load directions, i.e.  $P_1^{ET} = P_2^{ET}$  and the unhindered contraction in third direction causes it to be stress free,  $P_3^{ET} = 0$ . So, the stresses  $P_{1,2}^{ET}$  are obtained by making equation 48 equal to zero for  $i = 3$  and determining the value of  $p$  as follows:

$$p = \frac{2}{\lambda^4} \left( \frac{\partial W}{\partial I_1} - \lambda^8 \frac{\partial W}{\partial I_2} \right) \quad (53)$$

Then, the first and second principal stresses are obtained by inserting the value of  $p$  into the equation 48 for  $i = 1$  or  $i = 2$ :

$$P_1^{ET} = P_2^{ET} = 2 \left( \lambda - \frac{1}{\lambda^5} \right) \left( \frac{\partial W}{\partial I_1} + \lambda^2 \frac{\partial W}{\partial I_2} \right) \quad (54)$$

#### • Pure Shear (PS)

This type of experiment uses rectangular sheets, which have a much larger width than length to realize a zero deformation perpendicular to the loading direction  $\lambda_1 = \lambda$ , so  $\lambda_2 = 1$  holds almost everywhere except for the vicinity of the free edges. Again, by assuming isotropy and incompressibility in the material, the deformation gradient and invariants are:

$$\mathbf{F}^{PS} = \begin{pmatrix} \lambda & 0 & 0 \\ 0 & 1 & 0 \\ 0 & 0 & \lambda^{-1} \end{pmatrix}, \quad I_1^{PS} = I_2^{PS} = \lambda^2 + \lambda^{-2} + 1 \quad (55)$$

As contraction is unhindered in the third direction,  $p$  can be obtained, in a similar way than before, by setting the equation 48 equal to zero for  $i = 3$ . Then:

$$p = \frac{2}{\lambda^2} \left( \frac{\partial W}{\partial I_1} - \lambda^4 \frac{\partial W}{\partial I_2} \right) \quad (56)$$

Inserting  $p$  into the equation 48 for  $i = 1, 2$  will finally give the two stresses for this type of experiment:

$$P_1^{PS} = 2 \left( \lambda - \frac{1}{\lambda^3} \right) \left( \frac{\partial W}{\partial I_1} + \frac{\partial W}{\partial I_2} \right) \quad (57)$$

$$P_2^{PS} = 2 \left( 1 - \frac{1}{\lambda^2} \right) \left( \frac{\partial W}{\partial I_1} + \lambda^2 \frac{\partial W}{\partial I_2} \right) \quad (58)$$

#### Material Parameters Determination

As the stresses for a mathematical model are derived from its strain energy function, obtaining such stresses

will require to compute the material parameters corresponding to the model in question. According to [20], the material constants determined for a specific type of load may not be valid for other types of loads, so it is necessary to compute these constants for each type of load, which are: uniaxial tension, equibiaxial tension, and pure shear. The material parameters are obtained through the least squares procedure to make the deviations of the experimental data and the fitted data least [21]. So the function to be minimized is:

$$\phi = w \sum_{i=1}^n [Y_i - \hat{Y}_i]^2 \quad (59)$$

where  $w$  is a weighting factor that depends on the type of load being modeled,  $n$  is the number of experimental data for each type of load,  $Y_i$  are the values of stresses provided by the experimental data, and  $\hat{Y}_i$  are the theoretical values calculated from equations 51, 54 and 58 depending on the type of load.

### Data Sets Used to Fit The Mathematical Models

In the wide range of literature, the most used data set used to fit the different mathematical models and compute the material parameters is the Treloar's data set [22], which contains engineering stress-strain data for vulcanized rubber under various types of deformation. This data set has been widely used by many authors [1, 3, 5, 9, 8, 23, 24, 25, 26]. The rubber used in this data set exhibits a highly reversible elastic response and no stretch-induced crystallization up to 400% [1]. Another data set that can be used for fitting the mathematical models is that provided by [27] which contains data about isoprene rubber vulcanizate. This data set has been obtained using an experimental apparatus for general biaxial tension testing [1]. This work will use information from papers that perform studies of mathematical models using the data set of Treloar, because such data set is used in most of the researches found in literature and because it will allow comparing the models with equality of conditions.

Once the strains and stresses have been obtained for the mathematical model, the stress-strain curve can finally be plotted using the results provided by each model.

## 2.7 Mathematical Models

Many models found in the literature for the characterization of elastomers, such as the rubber and soft tissues, can be classified according to the addressed stress-strain relationship. This main classification would be hyperelastic for those models able to reproduce the highly non-linear mechanical behavior of elastomers; and linear for those models that are based in the Hooke's law of elasticity, which establish a linear relationship between stress and strain. This work will focus on hyperelastic mathematical models because they are the ones that produce an adequate prediction of soft tissue behavior with reasonable complexity.

Many hyperelastic models express the strain energy function depending on the three strain invariants  $I_1$ ,  $I_2$  and  $I_3$  stated before, as follows:

$$W = f(I_1, I_2, I_3) \quad (60)$$

These three parameters are invariants of Green deformation tensor, which are expressed in terms of principal stretch ratios  $\lambda_1$ ,  $\lambda_2$  and  $\lambda_3$  as equations 10, 11, and 12 state. Other mathematical models use the stretch ratios to build their SEF as well. As elastomers are considered incompressible, models that use the three strain invariants can be simplified by using the assumption  $I_3 = 1$ , and therefore,  $W$  can be expressed in function of two invariants only:

$$W = f(I_1 - 3, I_2 - 3) \quad (61)$$

In addition, hyperelastic models use different material constants, which vary depending on the material that is being modeled. Most of these constants will be denoted as  $C_{ij}$  during this work, with some exceptions.

Several mathematical models have been found in the literature which can be classified according to the approach the author follows to develop the strain energy function [1, 5] or the treatments used in the model [25]. According to Marckman and Verron [1], hyperelastic models are classified into three types, depending on the approach that the authors follow to develop the SEF. These three types are phenomenological, based on the experimental determination of  $\frac{\partial W}{\partial I_1}$  and  $\frac{\partial W}{\partial I_2}$ , and physical-based. Other authors [5] suggest a classification in two types: phenomenological and micro-mechanical, this classification is also based on the approach of the authors to define the strain energy function. In addition, Boyce and Aruda [25] have performed a division of mathematical models considering the treatments used in the model, leading to three principal groups of models: statistical mechanics treatments, invariant-based continuum mechanics treatments and stretch-based continuum mechanics treatments.

In the following, a fundamental classification is presented taking into account the taxonomy proposed in [1], mainly focused on the approach followed to the develop the SEF of the models, with the particular difference that herein 14 models are added for the revision and the variants of each model are mentioned within the principal model. In addition, a detailed description has been added for each model and some deductions are explained in detail for a better understanding.

### 2.7.1 Phenomenological Models

Phenomenological Models are simply models that express mathematically the results of observed phenomena without paying detailed attention to their fundamental significance [28]. Material parameters are usually difficult to determine for these models, and they can conduct to errors when used out of the deformation range

in which their parameters were identified [1]. Most of the phenomenological hyperelastic models found in the literature are described next:

- **Money-Rivlin Model**

Initially known as the Money model, it was first proposed by Money [29] in 1940 and then expressed in terms of invariants by Rivlin [30] in 1948. It is known by being one of the first hyperelastic models, which can handle very well strains lower than 100% [24]. However, it cannot capture the upturn (S-curvature) of the force-extension relation in the uniaxial test and the force-shear displacement relation in shear test [23]. The form of the model for a compressible material is:

$$W = C_{10}(\bar{I}_1 - 3) + C_{01}(\bar{I}_2 - 3) + \frac{1}{D_1}(J_{el} - 1)^2 \quad (62)$$

where:

- $C_{10}$  and  $C_{01}$  are material parameters.
- $J_{el}$  is the elastic volume ratio, obtained as  $J_{el} = \det(\mathbf{F}) = \lambda_1 \lambda_2 \lambda_3$ .
- $D_1$  is a constant that defines the compressibility of the material. This constant can be estimated from volumetric test.
- $\bar{I}_1$  and  $\bar{I}_2$  are the first and second invariants of  $\bar{\mathbf{C}}$ , being  $\bar{\mathbf{C}} = J^{-\frac{2}{3}} \mathbf{C}$  the unimodular component of  $\mathbf{C}$  and  $J = \det(\mathbf{C})$ . The form of  $\mathbf{C}$  and the way of obtaining the invariants have already been stated in 2.3.  $\bar{I}_1$  and  $\bar{I}_2$  can be written as:

$$\bar{I}_1 = J^{-\frac{2}{3}} I_1 \quad (63)$$

$$\bar{I}_2 = J^{-\frac{4}{3}} I_2 \quad (64)$$

Considering an incompressible material, such as the rubber, the elastic volume ratio  $J$  becomes 1; and therefore,  $\bar{I}_1 = I_1$  and  $\bar{I}_2 = I_2$ . So, the Money-Rivlin model for an incompressible material has the SEF:

$$W = C_{10}(I_1 - 3) + C_{01}(I_2 - 3) \quad (65)$$

The Money-Rivlin model has some variants which extend the basic model using different approaches. Some of these variants are:

- **Full Polynomial Model**

This variant can be found in the literature with the same name "Money-Rivlin" [1] or as Full Polynomial model [23]. The form of the Full Polynomial model for compressible materials is:

$$W = \sum_{i,j=0}^{\infty} C_{ij}(\bar{I}_1 - 3)^i (\bar{I}_2 - 3)^j + \sum_{i=1}^{\infty} \frac{1}{D_i} (J_{el} - 1)^{2i} \quad (66)$$

This form can be reduced for incompressible materials, in the same way 62 was reduced, as follows:

$$W = \sum_{i,j=0}^{\infty} C_{ij}(I_1 - 3)^i(I_2 - 3)^j \quad (67)$$

This series is often truncated to terms of second and third order [1], such truncations can constitute another model. From now on, all given strain energy functions for the mathematical models will be assuming an incompressible material because this work is focussed on soft tissues and the way of simplifying the equations is similar to the way previously shown.

#### – Biderman Model

This model, is a truncation of 67, but retaining only the terms for which  $i = 0$  or  $j = 0$ . The first three terms for  $I_1$  and one term for  $I_2$  were considered by Biderman [31]:

$$W = C_{10}(I_1 - 3) + C_{01}(I_2 - 3) + C_{20}(I_1 - 3)^2 + C_{30}(I_1 - 3)^3 \quad (68)$$

#### – Hynes-Wilson Model

This model is another truncation of 67, this time choosing to retain only six terms of the series based on the comparison of invariants and principal stretches development of the SEF of Full Polynomial model [32]. The form of  $W$  for this model is:

$$W = C_{10}(I_1 - 3) + C_{01}(I_2 - 3) + C_{11}(I_1 - 3)(I_2 - 3) + C_{02}(I_2 - 3)^2 + C_{20}(I_1 - 3)^2 + C_{30}(I_1 - 3)^3 \quad (69)$$

#### – Yeoh Model

This model, also known as reduced polynomial, is based in the first invariant  $I_1$  only and was proposed by Yeoh [33] in 1993. Like the previous models, it is also the result of selecting specific terms of the series 67. It can capture the upturn of the stress-strain curve of rubber, has good fit over a large strain range and can simulate various modes of deformation with limited data [23]. Specifically, the Yeoh model proposes a SEF for incompressible materials as follows:

$$W = \sum_{i=1}^3 C_{i0}(I_1 - 3)^i \quad (70)$$

#### • Ogden Model

It was proposed in 1972 by Ogden [34], who based his model on principal stretch ratios  $\lambda_1$ ,  $\lambda_2$ , and  $\lambda_3$  instead of invariants as the previous models. This model can capture upturn (stiffening) of the stress-strain curve and model rubber accurately for large ranges of deformation, which can reach up to 700%

[23]. It is not advisable to use this model with limited data, the general form of the model is:

$$W = \sum_{i=1}^n \frac{\mu_i}{\alpha_i} (\lambda_1^{\alpha_i} + \lambda_2^{\alpha_i} + \lambda_3^{\alpha_i} - 3) \quad (71)$$

where  $\mu_n$  and  $\alpha_n$  are material parameters and should fulfill the following stability condition:

$$\mu_i \alpha_i > 0 \quad \forall i = 1, n \quad (72)$$

An excellent convergence between theoretical and experimental results is achieved when  $n = 3$  [1]. This model is one of the most widely used for large strain problems, even if it is hard to determine the material parameters [1].

#### • Shariff Model

In this model, proposed by Shariff [35],  $W$  takes the form of a function series, obeying Valanis-Landel hypothesis form as follows:

$$W = \omega(\lambda_1) + \omega(\lambda_2) + \omega(\lambda_3) \quad (73)$$

where  $\omega$  is a series of regular functions  $\phi_j$  and the parameters  $\alpha_j$  are linear coefficients of these functions. The functions  $\phi_j$  are chosen such that they satisfy the linear theory of incompressible isotropic elasticity for all values of  $\alpha_j$ . Then, the form of  $\omega$  proposed for this model is:

$$\omega(\lambda_i) = E \sum_{j=0}^n \alpha_j \phi_j(\lambda_i) \quad (74)$$

where the functions  $\phi_j$ , until four expansion points, are:

$$\phi_0(\lambda_i) = \frac{[\ln(\lambda_i)]^2}{3} \quad (75)$$

$$\phi_1(\lambda_i) = \int_1^{\lambda_i} \frac{e^{1-s}}{s} ds + \lambda_i - 2\ln(\lambda_i) - 1 \quad (76)$$

$$\phi_2(\lambda_i) = \int_1^{\lambda_i} \frac{e^{s-1}}{s} ds + \lambda_i + 1 \quad (77)$$

$$\phi_3(\lambda_i) = -\frac{1}{0.6\lambda_i^{0.6}} + \frac{3}{1.6\lambda_i^{1.6}} - \frac{3}{2.6\lambda_i^{2.6}} + \frac{1}{5.6\lambda_i^{5.6}} + \frac{107200}{139776} \quad (78)$$

#### • Swanson Model

This model, proposed by Swanson [36], introduces a SEF that contains two sums of weighted noninteger powers of the first two invariants of Green deformation tensor. This form of strain energy function offers the possibility of choosing the complexity of the model by modifying its number of parameters and adjusting its nonlinearity. The material parameters  $A_i$ ,  $\alpha_i$ ,  $B_j$  and  $\beta_j$  of this model do not have a physical

meaning and are difficult to determine. This complication in determining the material parameters is due to their fast-growing, which is the result of being inside a summation. The form of  $W$  for this model is:

$$W = \frac{3}{2} \sum_{i=1}^n \frac{A_i}{1 + \alpha_i} \left[ \frac{I_1}{3} \right]^{1+\alpha_i} + \frac{3}{2} \sum_{j=1}^n \frac{B_j}{1 + \beta_j} \left[ \frac{I_2}{3} \right]^{1+\beta_j} \quad (79)$$

- **Carroll Model**

This model was proposed by Carroll [37], and it is based on a successive extension of the strain energy, using terms that help to reduce the errors that remain from the prediction of the previous terms. First, uniaxial tension data are fitted with the Neo-Hookean function, then the error obtained in that prediction is fitted with a term proportional to  $I_1^4$ . Finally, those terms are used to fit equibiaxial tension data, and the error obtained in that prediction is approximated with the last term, which is proportional to the square root of  $I_2$ . The form of this model is:

$$W = C_1 I_1 + C_2 I_1^4 + C_3 \sqrt{I_2} \quad (80)$$

where  $C_1$ ,  $C_2$  and  $C_3$  are stiffness parameters that must be determined from laboratory tests.

- **Fung-Demiray Model**

In 1967, Fun [38], based on experimental results on the rabbit's mesentery, stated that the stress-strain relation in a one-dimensional case should be exponential in the stretch. Then, Demiray [39], based on the studies performed by Fun, finally proposed a simple SEF for the model as follows:

$$W = \frac{C_1}{2C_2} \left[ e^{C_2(I_1-3)} - 1 \right] \quad (81)$$

where  $C_1$  and  $C_2$  are material parameters to be determined through laboratory tests.

- **Veronda-Westmann Model**

This hyperelastic model [40] is based on uniaxial tests performed on cat skin. It was developed by comparing the experimentally obtained force-extension curves with the analytical stress-strain relations. The form of the model for incompressible materials is:

$$W = C_1 \left[ e^{\beta(I_1-3)} - 1 \right] - C_2(I_2 - 3) \quad (82)$$

where  $C_1$ ,  $C_2$  and  $\beta$  are constants to be determined by curve fitting the plot:

$$\frac{\sigma}{2 \left( \lambda_1 - \frac{\lambda_l}{\lambda_1} \right)} \quad vs \quad \lambda_l \quad (83)$$

Being  $\lambda_l = \sqrt{\lambda_2 \lambda_3}$ .

- **Humphrey Model**

This model was proposed by Humphrey [41] to be used in the study of passive cardiac tissue and proposes a SEF based on limited structural information and multiaxial experimental data. The form of this model, which is the result of experimental observations, is the following:

$$W = C_1 \left[ e^{C_2(I_1-3)} - 1 \right] + C_3 \left[ e^{C_4(\alpha-1)^2} - 1 \right] \quad (84)$$

were  $C_1, C_2, C_3$  and  $C_4$  are material parameters, and  $\alpha = \sqrt{\mathbf{N}^T \mathbf{C} \mathbf{N}}$ .  $\mathbf{C}$  has already been defined in 2.3 and  $\mathbf{N}$  is a unit vector in the direction of an undeformed fiber. This model has a variant called Martins models, which is described next:

- **Martins Model**

This model, proposed by Martins [42], is a generalization of the Humphrey model in order to consider compressible materials, which is the case of skeletal muscles. The model, using the same notation as Humphrey, presents the following form:

$$W = C_1 \left[ e^{C_2(\bar{I}_1-3)} - 1 \right] + C_3 \left[ e^{C_4(\bar{\alpha}-1)^2} - 1 \right] + \frac{1}{D}(J-1)^2 \quad (85)$$

where  $\bar{\alpha} = \sqrt{\mathbf{N}^T \bar{\mathbf{C}} \mathbf{N}}$ ; and  $\bar{\mathbf{C}}, \bar{I}_1, D$  and  $J$  have the same meaning as in the Mooney-Rivlin model. Note that, for an incompressible material, this model is simplified into the Humphrey model.

- **Attard Model**

This model proposes a SEF for isotropic hyperelastic materials which can be considered a generalization of the Mooney-Rivlin model with high order terms in the incompressible part. It has been introduced by Attard and Hunt [43, 44], and the proposed form of  $W$ , in function of principal stretch ratios, is:

$$W = \sum_{i=1}^n \left[ \frac{A_i}{2i} \left( \lambda_1^{2i} + \lambda_2^{2i} + \lambda_3^{2i} - 3 \right) + \frac{B_i}{2i} \left( \lambda_1^{-2i} + \lambda_2^{-2i} + \lambda_3^{-2i} - 3 \right) \right] \quad (86)$$

where  $A_i$  and  $B_i$  are material parameters or shear modules, which must fulfill some stability criteria.

### 2.7.2 Models Based on Experimental Determination of $\frac{\partial W}{\partial I_1}$ and $\frac{\partial W}{\partial I_2}$

This type models directly determines material functions  $\frac{\partial W}{\partial I_1}$  and  $\frac{\partial W}{\partial I_2}$  by using experimental data [1]. The following models correspond to this classification:

- **Rivlin-Saunders Model**

The authors of this model, Rivlin and Saunders [45], used a biaxial tensile tester to obtain experimental conditions for which  $I_1$  and  $I_2$  are set constant. They found out that  $\frac{\partial W}{\partial I_1}$  does not depend on  $I_1$  and  $I_2$

and  $\frac{\partial W}{\partial I_2}$  does not depend on  $I_1$  for carbon black filled natural rubber. In addition, they showed that the ratio  $\frac{\partial W}{\partial I_2} / \frac{\partial W}{\partial I_1}$  decreases with  $I_2$ . So, the proposed form of  $W$  for this model is:

$$W = C(I_1 - 3) + f(I_2 - 3) \quad (87)$$

Experimental data is needed to determine the function  $f$ .

- **Gent-Thomas Model**

Gent and Thomas [46] proposed an empirical SEF which involves only two material parameters, based in the general form of Rivlin-Sanders model 87. However, this model has not proved to be more efficient than the basic Money-Rivlin model 65. The form of this proposed model is:

$$W = C(I_1 - 3) + C_2 \ln \left( \frac{I_2}{3} \right) \quad (88)$$

- **Hart-Smith Model**

This model, proposed by Hart-Smith [47] is an improvement of the model proposed by Rivlin and Sanders [45]. They realized that  $\frac{\partial W}{\partial I_1}$  is constant when the values of  $I_1$  are smaller than 12, and it increases when the values of the first principal invariant are higher. This result was justified by the author of the model by invoking the limit of extensibility of macromolecules which led to the strain-hardening phenomenon observed during mechanical tests. Then, the proposed model has the form:

$$W = C_1 \int \exp \left( C_2 [I_1 - 3]^2 \right) dI_1 + C_3 \ln \left[ \frac{I_2}{3} \right] \quad (89)$$

where  $C_1$ ,  $C_2$  and  $C_3$  are the material parameters of the model.

- **Alexander Model**

This model is an extension of Hart-Smith model, proposed by Alexander [48], which adds more material parameters, leading to a much more complicated SEF:

$$W = C_1 \int \exp \left( C_3 [I_1 - 3]^2 \right) dI_1 + C_2 \ln \left( \frac{I_2 - 3 + C_4}{C_4} \right) + C_3 [I_2 - 3] \quad (90)$$

where  $C_1$ ,  $C_2$ ,  $C_3$  and  $C_4$  are the material constants of the model.

- **Valanis-Landel Assumption**

Valanis and Landel [49] proposed that the form of  $W$  should be in terms of principal stretch ratios  $\lambda_1$ ,  $\lambda_2$  and  $\lambda_3$  because; according to them, the difficulties inherent in the dependence of  $W$  on the strain invariants have caused that no efficient SEF has been found yet. So, they assume the strain separability of the strain energy function as:

$$W = \omega(\lambda_1) + \omega(\lambda_2) + \omega(\lambda_3) \quad (91)$$

So, the determination of  $\omega$  restricts that of  $W$ . The proposed form of  $\omega$  is done through its derivative as follows:

$$\frac{\partial \omega}{\partial \lambda} = 2\mu \ln(\lambda) \quad (92)$$

- **Gent Model**

Gent [50] proposed a SEF by using the concept of limiting chain extensibility to consider that  $I_1$  should admit a maximum value denoted  $I_m$ . The proposed form of  $W$  is:

$$W = -I_m \frac{\mu}{2} \ln \left[ 1 - \frac{I_1 - 3}{I_m} \right] \quad (93)$$

where  $\mu$  and  $I_m$  are material parameters.

- **Pucci-Saccomandi Model**

Pucci and Saccomandi [51] and Ogden found that the Gent model makes very good predictions of uniaxial data for large strains, but it is not so recommendable for small strains. The authors of this model thought that it is worth to consider the dependence on the second invariant in the SEF of the model, so they added a logarithmic term to Gent model as follows:

$$W = -I_m \frac{\mu}{2} \ln \left[ 1 - \frac{I_1 - 3}{I_m} \right] + C_2 \ln \left[ \frac{I_2}{3} \right] \quad (94)$$

where  $\mu$ ,  $I_m$  and  $C_2$  are the material constants of the model.

- **Yeoh-Fleming Model**

This model, proposed by Yeoh and Flemming [52], is a modification of the Gent Model, which has the SEF stated in 93. Yeoh-Fleming Model proposes a new form for  $W$  which involves three new material parameters  $A$ ,  $B$  and  $I_m$ . This proposal is a consequence of the observation that the reduced Mooney stress tends to a constant value that does not depend on  $I_1$  for large strains. So, the form of  $W$  that Yeoh and Flemming proposed is:

$$W = \frac{A}{B} (I_m - 3) (1 - e^{-BR}) - C_{10} (I_m - 3) \ln(1 - R) \quad (95)$$

where  $R = \frac{I_1 - 3}{I_m - 3}$ .

### 2.7.3 Physically-Based Models

These models have been developed from physical motivation, involving the physics of polymer chains network and statistical methods [1]. This type of models tend to have complex formulations, such models are described next:

- **Neo-Hookean Model**

It is the simplest physically based model, being first proposed in 1943. The Neo-Hookean [53] model is very similar to Hooke's law although it is a hyperelastic model, in fact, it is a particular case of Money-Rivlin (cannot capture the upturn of stress-strain curve) when  $C_{01} = 0$ . This model can be used when material data is limited, being able to make good approximations at small strains. The form of  $W$  for this model is:

$$W = C_{10}(I_1 - 3) \quad (96)$$

where  $C_{10}$  can be expressed as  $C_{10} = \frac{1}{2}nk_B\Theta$ , being  $n$  the chain density per unit time,  $k_B$  the Boltzman constant and  $\Theta$  the absolute temperature.

- **Lopez-Pamies Model**

This model was built by Lopez-Pamies [54] with the objective of being as simple as Neo-Hookean and having a minimum number of material parameters with physical interpretation. So, the proposed form of  $W$  for this model is:

$$W = \sum_{i=1}^n \frac{3^{1-\alpha_i}}{2\alpha_i} \mu_i [I_1^{\alpha_i} - 3^{\alpha_i}] \quad (97)$$

where  $\mu_i$  and  $\alpha_i$  are the material parameters of the model.

- **3-Chain**

This model was first proposed in 1943 [55], and it is based in a non-Gaussian theory that takes into account the limiting extensibility of polymer chains. The model is based on the theory of micromechanics described before and substitutes the true polymer network by  $K = 3$  chains besides assuming that each chain is aligned with one of the eigenvectors  $\mathbf{N}_i$  of the isochoric right Cauchy Green tensor. The Figure 10 shows these configurations.

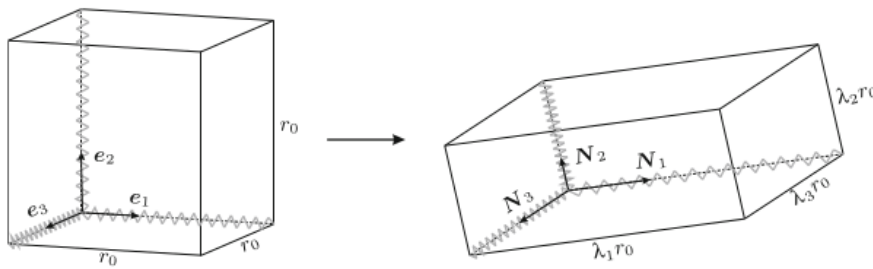


Figure 10: Initial and deformed chain orientations and stretches for 3-Chain model [5]

The chain stretch  $\Lambda$  adopts a particular form due to the choice of orientations:

$$\Lambda_k = \frac{\|\lambda_k r_0 \mathbf{N}_k\|}{r_0 \mathbf{e}_k} = \lambda_k, \quad k = 1, 2, 3 \quad (98)$$

The Langevin chain has proved to provide a rubber model able to simulate large strains, while the Gauss chain produces a model that behaves just like the Neo-Hookean model [5]. So, the SEF for this model, which uses the Langevin chain, is:

$$W = \frac{n}{3} \sum_{k=1}^3 W^{Langevin}(\Lambda_k) = \frac{\mu N}{3} \sum_{k=1}^3 \left[ \sqrt{N^{-1}} \lambda_k \gamma_k + \ln \left( \frac{\gamma_k}{\sinh(\gamma_k)} \right) \right] \quad (99)$$

where  $\mu = nk_B\Theta$  is the shear modulus and  $\gamma_k = \mathcal{L}^{-1}(\sqrt{N^{-1}}\Lambda_k)$  denote the inverse Langevin function of the chain stretches.

- **Isihara Model**

This model, proposed by Isihara [56], uses non-Gaussian theory and linearizes the corresponding equations to obtain a Rivlin series form for  $W$  as follows:

$$W = C_{10}(I_1 - 3) + C_{20}(I_1 - 3)^2 C_{01}(I_2 - 3) \quad (100)$$

- **General Theory of Real Chain Network**

The phantom assumption has been imputed for the deviation in experimental data of the ideal chain models [1]. Then, some researchers have presented the idea of entanglement or topology conservation constraints. This theory proposes the SEF as:

$$W = W_{ph} + W_c \quad (101)$$

where  $W_{ph}$  represents the phantom network and  $W_c$  is the constrained part. This theory has inspired some models, which are described in the next lines:

- **Slip-Link Model**

This model, developed by Ball et.al. [57] considers that chains can slip on a length around a link.

The form of the model is:

$$W = \frac{1}{2} k_B \Theta N_c \sum_{i=1}^3 \lambda_i^2 + \frac{1}{2} k_B \Theta N_s \sum_{i=1}^3 \left[ \frac{(1+\eta)\lambda_i^2}{1+\eta\lambda_i^2} + \ln|1+\eta\lambda_i^2| \right] \quad (102)$$

being  $N_c$ ,  $N_s$ , and  $\eta$  material parameters. The equation 102 corresponds to the Phantom Gaussian model.

### – Van der Waals Model

As its name suggests, this model takes into account the Vander Waals forces by treating the rubber network as a gas where interaction forces are applied between quasi-particles. The model was proposed by Killian [58] and is expressed in terms of strain energy as follows:

$$W = -\mu \left( \lambda_m^2 - 3 \right) \left[ \ln(1 - \Delta) + \Delta \right] - \frac{2}{3} a \mu \left( \frac{\tilde{I} - 3}{2} \right)^{\frac{3}{2}} \quad (103)$$

where  $\Delta = \sqrt{\frac{\tilde{I}-3}{\lambda_m^2-3}}$  and  $\tilde{I} = \beta I_1 + (1 - \beta) I_2$ . In addition,  $\mu$ ,  $a$ ,  $\lambda_m$  and  $\beta (0 \leq \beta \leq 1)$  are the material parameters of the model. Even though this model is based on molecular considerations, its nature is empirical because the material parameter  $\beta$  does not have a physical meaning.

### – Flory-Erman Model

This model, proposed by Flory and Erman [59], is based on equation 100 and considers that junction points between chains are constrained to move in a restricted neighborhood due to other chains. The phantom part is derived from the Neo-Hookean SEF and the cross-linking is obtained from micromechanics of chains:

$$W = C_{10} \sum_{i=1}^3 (\lambda_i^2 - 1) \left[ 1 - \frac{1}{\phi} \right] + C_{10} \sum_{i=1}^3 [B_i + D_i - \ln(B_i + 1) - \ln(D_i + 1)] \quad (104)$$

where  $C_{10} = n k_B \Theta / 2 = \mu / 2$ ,  $B_i = \kappa^2 (\lambda_i^2 - 1) (\lambda_i^2 + \kappa)^{-2}$  and  $D_i = \lambda_i^2 \kappa^{-1} B_i$ . The parameter  $\mu$  represents the shear modulus,  $\phi$  counts the number of chains than join at a junction and  $\kappa$  is a measurement of the constraints strength. The cross-linking part in this model improves the Neo-Hookean model by achieving a better agreement with experimental data, increasing the deformation range that the model is able to emulate correctly up to 300%.

### • Arruda-Boyce (8-Chain)

Also called the 8 Chain Model because of its basis on the representative volume element where 8 chains emanate from the center to the corners of the volume [23]. The Arruda-Boyce [60] model cannot define the transition point between elastic and inelastic response clearly. This model works well with limited data and its SEF, based on strain invariants, for incompressible materials is:

$$W = \mu \sum_{i=1}^5 \frac{C_i}{\lambda_m^{2i-2}} (I_1^i - 3^i) \quad (105)$$

This model has also a form with a basis on micromechanics. It substitutes the true polymer network by  $K = 8$  chains, with each chain oriented along one of the half diagonals of a cuboid as Figure 11 illustrates.

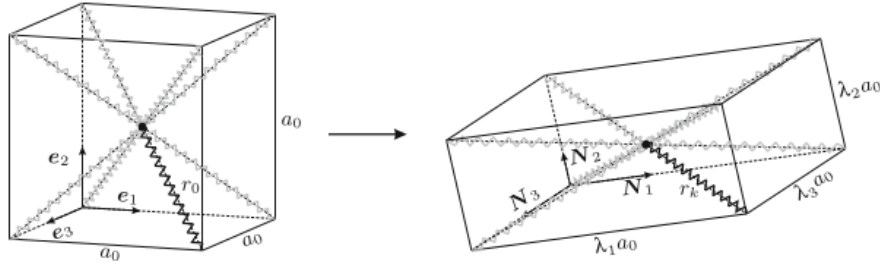


Figure 11: Initial and deformed chain orientations and stretches for 8-Chain model [5]

The chain stretch also changes for this model, due to the choice of orientations. The end-to-end distance between chains adopts the form  $r_k = r_0 \sqrt{3^{-1} \sqrt{\lambda_1^2 + \lambda_2^2 + \lambda_3^2}}$ , and therefore the chain stretch can be expressed as:

$$\Lambda = \Lambda_k = \frac{r}{r_0} = \frac{1}{\sqrt{3}} \sqrt{\lambda_1^2 + \lambda_2^2 + \lambda_3^2} = \sqrt{\frac{I_1}{3}}, \text{ for } k = 1, 2, \dots, 8 \quad (106)$$

which means that one stretch is valid for all chains no matter their orientation within the cuboid. So, the SEF for this model, which uses the Langevin chain, is:

$$W = \frac{n}{8} \sum_{k=1}^8 W^{Langevin}(\Lambda_k) = n W^{Langevin}(\Lambda_k) = \mu N \left[ \sqrt{N^{-1}} \Lambda \gamma + \ln \left( \frac{\gamma}{\sinh(\gamma)} \right) \right] \quad (107)$$

where  $\mu = n k_B \Theta$  is the shear modulus and  $\gamma = \mathcal{L}^{-1}(\sqrt{N^{-1}} \Lambda_k)$  again denotes the inverse Langevin function.

#### • Tube Model

This model, proposed by Heinrich and Kaliske [61], considers that chains are constrained to stay in a tube formed by surrounding chains. The authors have considered such assumption because the rubber network is highly entangled. They propose the use of statistical mechanics to determine the topology restoring potential that rules the confinement of chains. The form of  $W$  for this model is:

$$W = \sum_{i=1}^3 \frac{\mu_c}{2} (\lambda_i^2 - 1) + \frac{2\mu_e}{\beta^2} (\lambda_i^{-\beta} - 1) \quad (108)$$

where  $\mu_c$ ,  $\mu_e$  and  $\beta$  are the material parameters of the model and  $0 < \beta \leq 1$ . The Tube Model has the limitation of moderate deformation and cannot reproduce strain-hardening. This model has a variant, which was developed with the objective of reducing the limitations in the modeling of deformations due to the entanglement constraints. This variant is:

#### – Extended-Tube Model

This model, proposed by the same authors of the previous one [62] two years later, uses a non-

Gaussian distribution instead of the Gaussian one that the Tube model uses. An inextensibility parameter denoted  $\delta$  has been added, so the new form of  $W$  is:

$$W = \frac{\mu_c}{2} \left[ \frac{(1 - \delta^2)(I_1 - 3)}{1 - \delta^2(I_1 - 3)} + \ln \left( 1 - \delta^2(I_1 - 3) \right) \right] + \sum_{i=1}^3 \frac{2\mu_e}{\beta^2} \left( \lambda_i^{-\beta} - 1 \right) \quad (109)$$

- **Unit-Sphere Model**

This model assumes a unit sphere where the chains are oriented along radius vectors from the center to the surface. The model was first proposed by Miehe [11], and then Swanson [5] applied a numerical scheme based on discrete integration over spheres. The resulting SEF for this model is:

$$W = n \sum_{k=1}^{21} w_k W^{Langevin}(\Lambda_k) = \mu N \sum_{k=1}^{21} w_k \left[ \sqrt{N^{-1}} \Lambda_k \gamma_k + \ln \left( \frac{\gamma_k}{\sinh(\gamma_k)} \right) \right] \quad (110)$$

where  $w_k$  are weight factors chosen in such a way that an approximately uniform distribution of the chains across the sphere is performed,  $\mu = nk_B\Theta$  and  $\gamma_k = \mathcal{L}^{-1}(\sqrt{N^{-1}}\Lambda_k)$  denote the inverse Langevin function as in 3-Chain and 8-Chain models.

- **Full-Network Model**

The term full-network is used when the chains are assumed to be randomly oriented in space and the SEF for the corresponding model is derived by integrating the response of all chains over the space. This model proposes a weighted average, instead of computing the integral numerically, by combining the results of individual 3-Chain and 8-Chain models [63]:

$$W = (1 - \rho)W_{3-Chain} + \rho W_{8-Chain} \quad (111)$$

where  $\rho$  is a constant parameter related to some physical quantity (related to the deformation process), and  $W_{3-Chain}$  and  $W_{8-Chain}$  represent the SEF of 3-Chain and 8-Chain models respectively.

Tables 1, 2 and 3 provide a summary of the reviewed classification with the most important aspects of each model in order to facilitate the information handling. The tables show the name of the model, an identifier for the model, and the strain energy function for each respective model.

Table 1: Classification of hyperelastic models: Phenomenological

Phenomenological Models	(I.N.)	Formula
Money-Rivlin	1	$W = C_{10}(I_1 - 3) + C_{01}(I_2 - 3)$
Full Polynomial	1.1	$W = \sum_{i,j=0}^{\infty} C_{ij}(I_1 - 3)^i(I_2 - 3)^j$
Biderman	1.2	$W = C_{10}(I_1 - 3) + C_{01}(I_2 - 3) + C_{20}(I_1 - 3)^2 + C_{30}(I_1 - 3)^3$
Hynes-Wilson	1.3	$W = C_{10}(I_1 - 3) + C_{01}(I_2 - 3) + C_{11}(I_1 - 3)(I_2 - 3) + C_{02}(I_2 - 3)^2 + C_{20}(I_1 - 3)^2 + C_{30}(I_1 - 3)^3$
Yeoh	1.4	$W = \sum_{i=1}^3 C_{i0}(I_1 - 3)^i$
Ogden	2	$W = \sum_{i=1}^n \frac{\mu_i}{\alpha_i} (\lambda_1^{\alpha_i} + \lambda_2^{\alpha_i} + \lambda_3^{\alpha_i} - 3)$
Shariff	3	$W = E \sum_{j=0}^n \alpha_j \phi_j(\lambda_1) + E \sum_{j=0}^n \alpha_j \phi_j(\lambda_2) + E \sum_{j=0}^n \alpha_j \phi_j(\lambda_3)$
Swanson	4	$W = \frac{3}{2} \sum_{i=1}^n \frac{A_i}{1+\alpha_i} \left[ \frac{I_1}{3} \right]^{1+\alpha_i} + \frac{3}{2} \sum_{j=1}^n \frac{B_j}{1+\beta_j} \left[ \frac{I_2}{3} \right]^{1+\beta_j}$
Carroll	5	$W = aI_1 + bI_1^4 + c\sqrt{I_2}$
Fung-Demiray	6	$W = \frac{C_1}{2C_2} \left[ e^{C_2(I_1-3)} - 1 \right]$
Veronda-Westmann	7	$W = C_1 \left[ e^{\beta(I_1-3)} - 1 \right] - C_2(I_2 - 3)$
Humphrey	8	$W = C_1 \left[ e^{C_2(I_1-3)} - 1 \right] + C_3 \left[ e^{C_4(\alpha-1)^2} - 1 \right]$

Phenomenological Models	(I.N.)	Formula
Martins	8.1	$W = C_1 \left[ e^{C_2(\bar{I}_1-3)} - 1 \right] + C_3 \left[ e^{C_4(\bar{\alpha}-1)^2} - 1 \right] + \frac{1}{D}(J-1)^2$
Attard	9	$W = \sum_{i=1}^n \frac{A_i}{2^i} (\lambda_1^{2i} + \lambda_2^{2i} + \lambda_3^{2i} - 3) + \sum_{i=1}^n \frac{B_i}{2^i} (\lambda_1^{-2i} + \lambda_2^{-2i} + \lambda_3^{-2i} - 3)$

Table 2: Classification of hyperelastic models: Based on Experimental Determination of  $\frac{\partial W}{\partial I_1}$  and  $\frac{\partial W}{\partial I_2}$ 

Models Based on Experimental Determination of $\frac{\partial W}{\partial I_1}$ and $\frac{\partial W}{\partial I_2}$	(I.N.)	Formula
Rivlin-Saunders	10	$W = C(I_1 - 3) + f(I_2 - 3)$
Gent-Thomas	11	$W = C_1(I_1 - 3) + C_2 \ln \left( \frac{I_2}{3} \right)$
Hart-Smith	12	$W = C_1 \int \exp \left( C_2 [I_1 - 3]^2 \right) dI_1 + C_3 \ln \left[ \frac{I_2}{3} \right]$
Alexander	12.1	$W = C_1 \int \exp \left( C_3 [I_1 - 3]^2 \right) dI_1 + C_2 \ln \left( \frac{I_2 - 3 + C_4}{C_4} \right) + C_3 [I_2 - 3]$
Valanis-Landel	13	$W = \omega(\lambda_1) + \omega(\lambda_2) + \omega(\lambda_3)$
Gent	14	$W = -I_m \frac{\mu}{2} \ln \left[ 1 - \frac{I_1 - 3}{I_m} \right]$
Pucci-Saccomandi	14.1	$W = -I_m \frac{\mu}{2} \ln \left[ 1 - \frac{I_1 - 3}{I_m} \right] + C_2 \ln \left[ \frac{I_2}{3} \right]$
Yeoh-Fleming	15	$W = \frac{A}{B}(I_m - 3)(1 - e^{-BR}) - C_{10}(I_m - 3) \ln(1 - R)$

Table 3: Classification of hyperelastic models: Physically-Based

Physically-Based Models	(I.N.)	Formula
Neo-Hookean	16	$W = C_{10}(I_1 - 3)$
Lopez-Pamies	17	$W = \sum_{i=1}^n \frac{3^{1-\alpha_i}}{2\alpha_i} \mu_i [I_1^{\alpha_i} - 3^{\alpha_i}]$
3-Chain	18	$W = \frac{\mu N}{3} \sum_{k=1}^3 \left[ \sqrt{N^{-1}} \lambda_k \gamma_k + \ln \left( \frac{\gamma_k}{\sinh(\gamma_k)} \right) \right]$
Isihara	19	$W = C_{10}(I_1 - 3) + C_{20}(I_1 - 3)^2 C_{01}(I_2 - 3)$
Slip-Link	20	$W = \frac{1}{2} k_B \Theta N_c \sum_{i=1}^3 \lambda_i^2 + \frac{1}{2} k_B \Theta N_s \sum_{i=1}^3 \left[ \frac{(1+\eta)\lambda_i^2}{1+\eta\lambda_i^2} + \ln 1 + \eta\lambda_i^2  \right]$
Vander Waals	21	$W = -\mu (\lambda_m^2 - 3) [\ln(1 - \Delta) + \Delta] - \frac{2}{3} a \mu \left( \frac{\tilde{I}-3}{2} \right)^{\frac{3}{2}}$
Flory-Erman	22	$W = C_{10} \sum_{i=1}^3 (\lambda_i^2 - 1) \left[ 1 - \frac{1}{\phi} \right] + C_{10} \sum_{i=1}^3 [B_i + D_i - \ln(B_i + 1) - \ln(D_i + 1)]$
Aruda-Boyce (8-Chain)	23	$W = \mu N \left[ \sqrt{N^{-1}} \Lambda \gamma + \ln \left( \frac{\gamma}{\sinh(\gamma)} \right) \right]$
Tube	24	$W = \sum_{i=1}^3 \frac{\mu_c}{2} (\lambda_i^2 - 1) + \frac{2\mu_e}{\beta^2} (\lambda_i^{-\beta} - 1)$
Extended-Tube	24.1	$W = \frac{\mu_c}{2} \left[ \frac{(1-\delta^2)(I_1-3)}{1-\delta^2(I_1-3)} + \ln(1 - \delta^2(I_1 - 3)) \right] + \sum_{i=1}^3 \frac{2\mu_e}{\beta^2} (\lambda_i^{-\beta} - 1)$
Unit-Sphere	25	$W = \mu N \sum_{k=1}^{21} w_k \left[ \sqrt{N^{-1}} \Lambda_k \gamma_k + \ln \left( \frac{\gamma_k}{\sinh(\gamma_k)} \right) \right]$
Full-Network	26	$W = (1 - \rho)W_{3-Chain} + \rho W_{8-Chain}$

### 3 Mathematical Models for Realistic Soft Tissue Simulations

#### 3.1 Methodology

Currently, there exists a wide range of mathematical models that can be used for soft tissue simulations and no explanatory studies, that analyze all or most of them, have been done to provide the reader with a framework to choose between such amount of models. So, most of the models existing in literature, that can be used for this purpose, have been selected to provide a perspective to choose optimal mathematical models for simulations of soft tissue deformations depending on the context they are needed for. The general framework used for the analysis is organized as depicted in Figure 12.

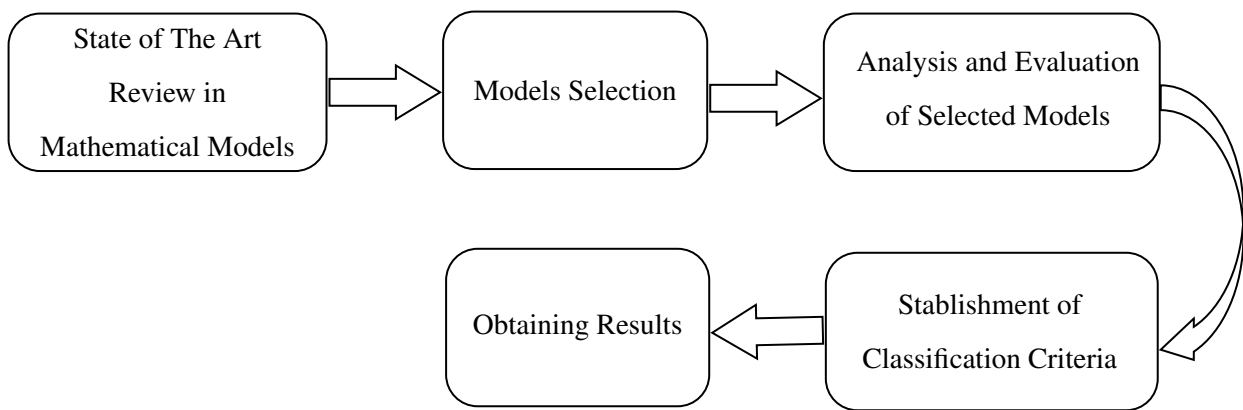


Figure 12: Methodology used to select and classify the mathematical models existing in literature

##### 3.1.1 State of The Art Review in Mathematical Models

The state of the art in mathematical models that can be used for soft tissue simulations is extensive, it practically starts in 1940 when the first hyperelastic model was introduced [29]. The mathematical models, which are studied in this work, have been found in many different papers published across the years [1, 5, 7, 9]. In order to facilitate the finding of the different mathematical models, it was necessary to look for works that perform classifications, comparisons or reviews of such models. After finding such works, the mathematical models were extracted to be analyzed, in case, not enough information was provided in the initial source, it was necessary to appeal to the original source of the model to obtain more details. In addition, in case the original source was not enough, more works, that have performed studies with the model in question, were reviewed (Figure 13 illustrates the described process). So, not only one source was used, but instead, many sources were consulted in order to understand better each model and the way that they have been evolving across the years. As the models use a theory that goes even further back, this theory necessary to understand the models was also reviewed and analyzed.

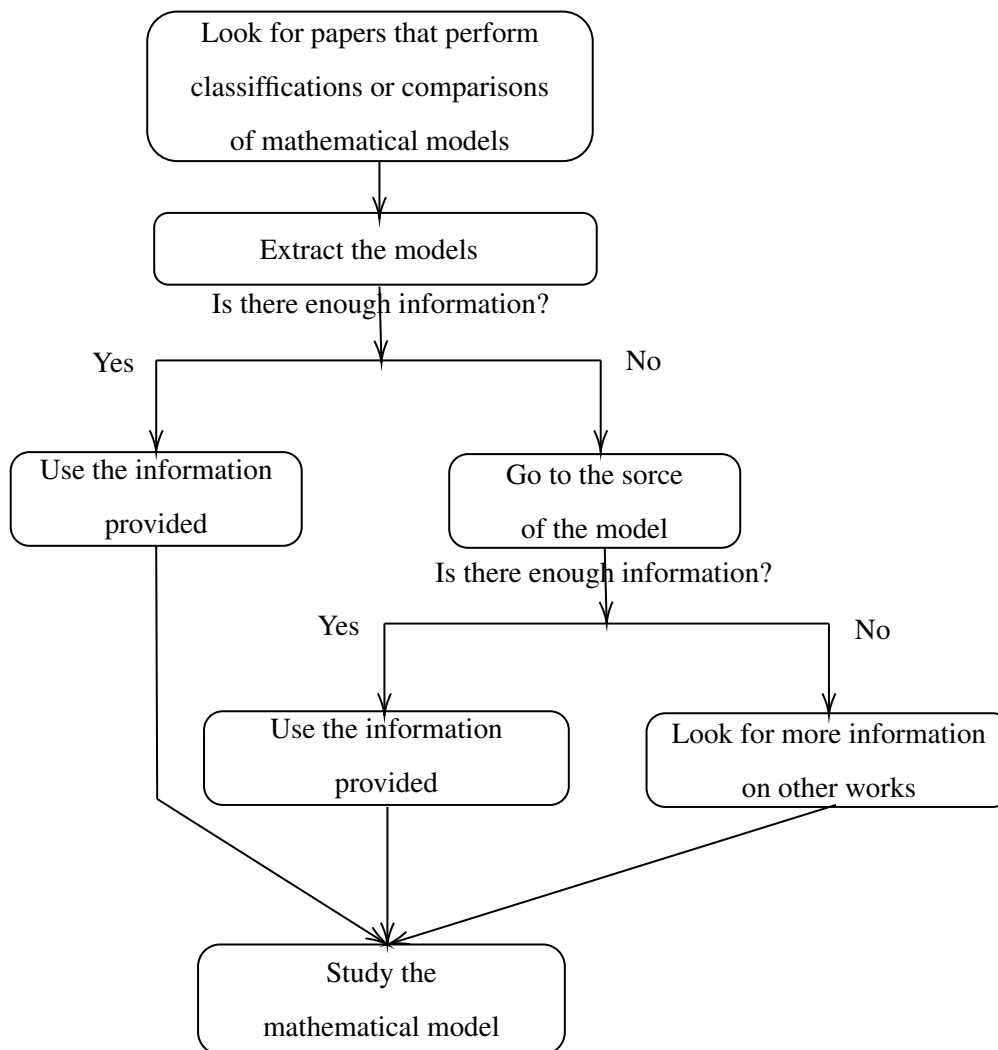


Figure 13: Methododology used to review the state of the art in mathematical models

### 3.1.2 Models Selection

The review of the state of the art in mathematical models led to the finding of 34 models that can be used for soft tissue simulations. Then, the options for this work were whether to use all the models that had been found or select only the most important ones. Such a decision was made based on a literature review of previous works related to this topic in order to determine their successes and flaws. Besides, the necessities that researchers in the field of soft-tissue simulations may have were also considered at the moment of selecting the models found in the literature.

### 3.1.3 Analysis and Evaluation of Selected Models

Once the mathematical models to be used in this work had been selected from the literature, they were analyzed in order to understand their advantages and disadvantages regarding their use to simulate the mechanical behavior of soft tissues. Firstable, their way of defining the strain energy function, and the theory they are based on were studied; and then the most important aspects about the selected models, such as the material constants that they use, the deformation range they are applicable for and the accuracy in the prediction, were analyzed. Such studies and analyses were important in order to establish the conditions for which it is better to apply each model.

### 3.1.4 Establishment of Classification Criteria

After analyzing the different mathematical models, it was determined to classify them into groups according to different criteria in order to provide a perspective of the models to use on different occasions. In order to establish the different criteria for classifications, more literature review was performed to understand the existent necessities regarding soft tissue simulations. In addition, for the different classifications, the mathematical models are ordered according to different aspects for a better appreciation.

### 3.1.5 Obtaining Results

The results of this work are different classifications of mathematical models that can be used for soft tissue simulations. All results are organized in tables and figures to provide a fast way of identifying the adequate model according to the necessities of the researcher in the field of soft tissue simulations. The classifications that will be presented are based on deformation range, complexity, and application. These three types of classifications have been determined, through literature review, to be the most accurate in order to provide a perspective of which model to choose depending on the circumstances.

## 3.2 Models

A total of 34 models have been found in literature among principal and derived models. The most known and studied models are Money-Rivlin, Neo-Hookean, Yeoh, Ogden, and Aruda-Boyce; having an extensive literature about them and their applications to real data [1, 25, 8, 24, 23, 7, 64, 26]. The rest of the models described in the theoretical framework have been studied in a lesser extent, having no much information about their performance in simulations of mechanical behavior of soft tissues or rubber materials. The applications and comparisons performed in literature, which are few, consider only the most known models mentioned before and/or a few of the other models, but there is no work that analyzes all of them. This could be in part due

to the lack of information about some models and the increasing number of models that have been proposed across the years. Then, this work intends to be as complete as possible in the task of providing a framework to choose among all the possible options of mathematical models currently available when performing soft tissue simulations, which makes imperative to consider all of them. So, all 34 models found in the literature are analyzed and classified according to some parameters described later. The models to be analyzed and classified in this work are listed in Table 4, where the classification of the model according to literature, the name of the model with its respective year of proposal, and a brief description of the model, are provided.

Table 4: Summary of hyperelastic models with a description

Classification	Model (year)	Description
Phenomenological	Mooney-Rivlin (1940)	Model that handles very well smoderate strains and cannot reproduce the S-curvature of the force-extension relation in uniaxial test and the force-shear displacement relation in shear test.
	Full Polynomial (1948)	Extension of Mooney-Rivlin, which uses a series of powers of invariants as SEF.
	Biderman (1958)	Truncation of Full Polynomial series but retaining only the terms for which $i = 0$ or $j = 0$ .
	Veronda-Westmann (1970)	Model based on uniaxial tests performed on cat skin and developed by comparing the experimentally obtained force-extension curves with the analytical stress-strain relations.
	Ogden (1972)	Model based on stretch ratios that can capture upturn of stress-strain curve and model rubber accurately for deformations up to 700%.
	Fung-Demiray (1972)	Model based on experimental results on rabbit's mesentery that proposes an exponential stress-strain relation.
	Haines-Wilson (1975)	Truncation of Full Polynomial series that retains only six terms based on the comparison of invariants and principal stretches development.
	Swanson (1985)	Model that proposes a SEF containing two sums of weighted noninteger powers of the first two invariants, which allows to choose the complexity of the model.

Classification	Model (year)	Description
	Humphrey (1987)	Model proposed to be used in the study of passive cardiac tissue and based on limited structural information and multiaxial experimental data.
	Yeoh (1993)	Result of specific terms selection of the Full Polynomial series, which can capture the upturn S-curvature of rubber, has good fit over a large strain range and works well with limited data.
	Martins (1998)	Generalization of Humphrey model to consider compressible materials, which has been applied to skeletal muscles.
	Shariff (2000)	Model where the SEF takes the form of a function series and considers principal stretch ratios.
	Attard (2003)	Generalization of Mooney-Rivlin model with high order terms in the incompressible part.
	Carroll (2011)	Model based on a successive extension of the free energy, using terms that help to reduce the errors that remain from the prediction of the previous terms.
Based on Derivatives	Rivlin-Sanders (1951)	Model deduced from the obtaining of experimental conditions for which $I_1$ and $I_2$ are set constant.
	Gent-Thomas (1958)	Model based on the general form of Rivlin-Sanders model which involves only two material parameters.
	Hart-Smith (1966)	Improvement of Rivlin-Sanders model that uses the limit of extensibility of macromolecules, which leads to a strain-hardening phenomenon observed during mechanical tests.
	Alexander (1968)	Extension of Hart-Smith model which adds more material parameters.
	Valanis-Landel (1967)	Model that defines its SEF in terms of principal stretch ratios instead of invariants in order for this function to be more efficient.
	Gent (1996)	Model that uses the concept of limiting chain extensibility to consider that the first invariant should admit a maximum value.

Classification	Model (year)	Description
	Yeoh-Fleming (1997)	Modification of Gent model which is consequence of the observation that the reduced Mooney stress tends to a constant value that does not depend on the first invariant for large strains.
	Pucci-Saccomandi (2002)	Modification of Gent model that considers dependence on second invariant and adds a logarithmic term.
Physically-Based	Neo-Hookean (1943)	Particular case of Money-Rivlin model that can be used when material data is limited, achieving good approximations at small strains.
	3-Chain (1943)	Model based in a non Gaussian theory that takes into account the limiting extensibility of polymer chains, specifically 3 chains.
	Isihara (1951)	Model that uses a non-Gaussian theory and linearizes the corresponding equations to obtain a Rivlin series form for its SEF.
	Slip-Link (1981)	Model based on the General Theory of Real Chain Network which considers that chains can slip on a length around a link.
	Flory Erman / Constrained Junctions (1982)	Model based on the General Theory of Real Chain Network which considers that junction points between chains are constrained to move in a restricted neighborhood due to other chains.
	Vand der Walls (1986)	Model that model considers Vander Waals forces by treating the rubber network as a gas where interaction forces are applied between quasi-particles.
	Aruda-Boyce / 8-Chain (1993)	Model based on the representative volume element where 8 chains emanate from the center to the corners of the volume.
	Full-Network (1993)	Model that combines the results of individual 3-Chain and 8-Chain models.
	Tube (1997)	Model that considers that chains are constrained to stay in a tube formed by surrounding chains.

Classification	Model (year)	Description
	Extended-Tube (1999)	Improvement to Tube model which uses a non-Gaussian distribution and adds an inextensibility parameter.
	Unit-sphere (2004)	Model that assumes a unit sphere where the chains are oriented along radius vectors from the center to the surface.
	Lopez-Pamies (2010)	Simple model with a minimum number of material parameters with physical interpretation.

### 3.3 Parameters

Some parameters have been established in order to classify and evaluate the models selected for this work. Such parameters, which have been determined from an extensive literature review, are described next:

#### 3.3.1 Material Constants Used to Define the SEF of The Model

Material constants are invariable quantities unique for each material and must be determined through laboratory tests on the material in question. All mathematical models that can be used for soft tissue simulations use material constants in the definition of their strain energy function, so they are an important part in a mathematical model. The more constants a mathematical model has the more difficult it is to implement it because material parameters are generally hard to determine [1]. So, this parameter influences the complexity of a model; in fact, a study performed in [1], established a high number of material constants to be the cause of a model to be ranked lower in contrast with other models that are evaluated in such study. These background information about material constants have led to the inclusion of them as a parameter for the evaluation of mathematical models in this work. The determination of material constants is done often by minimizing the function:

$$\phi = w \sum_{i=1}^n [Y_i - \hat{Y}_i]^2 \quad (112)$$

where:

- $w$  is a weighting factor,
- $Y_i$  are values of experimental data and
- $\hat{Y}_i$  are values approximated by the model.

### 3.3.2 Deformation Range

The deformation range of a mathematical model, in this case, is the area of variation in which the model can make good predictions of the mechanical behavior of a material. Mathematical models are not often valid for the whole range of deformation of a material, some models can predict better small strains while others have better performance in large strains. The wider the validity range of a model the better [1], which makes this parameter a determinant in the scope of a mathematical model. This parameter has been considered in [5] and [1] when evaluating the performance of a model, having to reduce the deformation range in order to obtain better predictions in case large ranges of deformations cause the model to be inaccurate. Therefore, the deformation range has been included as a parameter to evaluate the mathematical models described in this work. As previously mentioned, the stretch that the material has suffered can be obtained as:

$$\lambda = \frac{l_i}{l_{0i}} \quad (113)$$

where  $l_i$  is the final length of the material in question in the direction  $i$  and  $l_{0i}$  is the initial length of the material in the direction  $i$ . So, the range of these stretches that the model is able to predict well will define its validity range.

### 3.3.3 Accuracy

The accuracy of a mathematical model is a measurement of how good the prediction made by the model is in contrast with the real-life data provided by laboratory tests. Different models have different accuracy in the prediction of deformations, and those differences can be huge because there are simple models with few material constants as well as really complex models which are based on micromechanics. The reason of creating a mathematical model is to simulate the real mechanical behavior of a material, and in order to achieve that goal the accuracy of the model must be good, therefore, accuracy is the most important parameter when analyzing a mathematical model. Most of the papers that analyze or propose mathematical models consider the accuracy when evaluating the overall performance of the model [5, 24, 26, 25, 7, 8, 1, 64, 23]. Specifically, the study performed in [1] used the accuracy as the principal parameter to rank a total of 20 hyperelastic models from best to worst in the task of reproducing two sets of experimental data. Another study, took into account the accuracy when analyzing different hyperelastic models by fitting different types of experimental data (Uniaxial Tension, Biaxial Tension, and Pure Shear) [5]. The other mentioned works have also use the accuracy to compare different mathematical models and determine their usefulness in the reproduction of experimental data. So, given the addressed importance of this parameter, it is considered when classifying and evaluating the mathematical models of this work. The common way of measuring the accuracy of any prediction is through

the standard error:

$$E = \frac{\sqrt{\sum_{i=1}^n (Y_i - \hat{Y}_i)^2}}{n - 2} \quad (114)$$

where:

- $n$  is the number of observations,
- $Y_i$  are values of experimental data and
- $\hat{Y}_i$  are values approximated by the model.

### 3.4 Classifications

This work proposes three classifications for the 34 models found in the literature with the objective of providing a framework that researchers in the field of soft tissue simulations can use to choose the optimal mathematical model, depending on their needs, among the huge quantity of models developed for such purpose. As previously mentioned, most of the models presented in the Theoretical Framework section had been tested on rubber materials, but they can be perfectly applied to soft tissues because of their similarities [2]. The three proposed classifications are described next:

#### 3.4.1 By Deformation Range

This classification is proposed because the validity range of a mathematical model is a determinant part in the performance of the model, and therefore, it conditions the circumstances under which a model can be used with optimal results. There are no previous works that perform classifications of mathematical models according to the deformation range, but there are studies that mention the importance of it and evaluate the performance of the models according to it [1, 5, 23]. So, a classification according to the deformation range will be useful to experimentalists, doctors, and computational modelers when it comes to choosing a model to simulate the behavior of soft tissues at a specific deformation range. However, this classification does not consider the inherent difficulties of implementing the models being analyzed, which is also an important detail to consider when making simulations. So, it is necessary to analyze the complexity of the models too.

#### 3.4.2 By Complexity

This classification is considered in this work because the complexity of a mathematical model determines the possibility of using it under different circumstances. Sometimes the high computational cost of implementing a model is not worth for the accuracy it can provide. The complexity of a problem is given by the best algorithm

used to solve it and the way of implementing such an algorithm. In the case of the reviewed mathematical models, their complexity is determined by the way their stress tensors, which are computed from invariants or stretches, are obtained in the context of an algorithm and the number of material constants to be determined previous to the implementation. Assuming that all mathematical models are implemented under the same circumstances and at their prime, the number of material constants that they use is a big influence on their complexity due to the minimization problem that the computation of such constants requires [1, 21, 65]. There are no classifications by complexity in literature, but there is a study that considers that a high number of material constants makes a model not recommendable due to the increase in complexity that the computation of such constants causes [1]. Besides the computation of the material parameters, that is a step previous to the implementation of the model, the form of the SEF of each model also influences their complexity. So, the material constants determine the complexity of the model previous to its implementation, and the form of the SEF influences the complexity at the moment of its implementation. Therefore, both aspects will be considered in this work. Classification according to complexity will provide experimentalists, doctors, and computational modelers with enough information for them to decide whether it is appropriate to use a complex or a simple model depending on their problem.

### 3.4.3 By Application

This classification is actually a combination of the previous two classifications because it uses their information in order to offer the best models to be used in preoperative plans and real-time simulations. Regarding preoperative plans, they refer to the act of prepare all the elements needed for a surgery, so that, everything is planned beforehand. In this case, mathematical models can be used to make simulations of the possible scenarios that may arise in surgery or simulate the steps to be performed during the surgery. In this case, there is plenty of time to prepare the surgery and fast models are not a priority, instead, the priority is accuracy. On the other hand, in case real-time simulations are needed to simulate surgeries so that the inexperienced surgeons can practice how an operation would be, the speed of the model is preferred over the accuracy. Such preference is considered because this kind of simulators must react fast for the trainee to practice with immediate responses. No previous classifications have been done regarding the application the models are going to be used for so this work will be a good contribution to researchers in the sense that it will make it easier for them to choose a model without having to check all of them in different sources.

## 4 Results and Discussion

Table 5: Classification according to deformation range for Uniaxial Tension (UT), Equibiaxial Tension (ET) and Pure Shear (PS) tests

Models	UT			ET			PS		
	SMA	MOD	LAR	SMA	MOD	LAR	SMA	MOD	LAR
Money-Rivlin	x					x			x
Neo-Hookean	x			x			x		
3-Chain			x	x					x
Isihara			x			x			x
Biderman			x			x			x
Gent-Thomas			x	x					x
Hart-Smith			x			x			x
Valanis-Landel		x		x			x		
Alexander			x			x		x	
Veronda-Westmann		x		-	-	-	-	-	-
Ogden			x			x			x
Haines-Wilson			x			x			x
Slip-Link			x	x					x
Flory Erman	x			x					x
Swanson (n=1)	x			x			x		
Vand der Walls			x	x					x
Humphrey		x		-	-	-	-	-	-
Arruda-Boyce / 8-Chain			x			x			x
Yeoh	x			x			x		
Full-Network			x			x			x
Gent			x			x			x
Tube		x			x			x	
Yeoh-Fleming			x			x			x
Martins		x		-	-	-	-	-	-
Extended-Tube			x			x			x
Shariff			x			x			x
Pucci-Saccomandi			x	x					x
Attard			x			x	x		
Unit-sphere			x			x			x
Lopez-Pamies			x			x			x
Carroll			x			x			x

Table 5 shows the classification according to the deformation range of the models being reviewed in this work for different types of loading conditions; which are Uniaxial Tension (UT), Equibiaxial Tension (ET) and Pure Shear (PS). According to the range of validity of a model, it can be useful for small strains (SMA), moderate strains (MOD) or large strains (LAR). Small strains in this work refer to deformations lower than 150%, moderate strains refer to deformations from 151% to 250% and large strains make reference to deformations bigger than 250%. An "X" indicates the corresponding classification for each mathematical model in the different types of loading conditions. In case the symbol "-" appears, it means that there is not enough information in the literature to classify the model adequately. This case occurs for the models Rivlin-Saunders, Full Polynomial and Fung-Demiray; however, the Full Polynomial model does not need a classification because it is actually a series which can be truncated in any way and there are already models that are particular truncations of this series.

From Table 5 it is possible to infer that there is no such thing as the best model for soft tissue simulations, it depends on the range of deformation and the type of loading that must be modeled. In this way; experimentalists, doctors, and computational modelers can easily recur to the presented table when they already know the conditions under which they want to model the behavior of soft tissues.

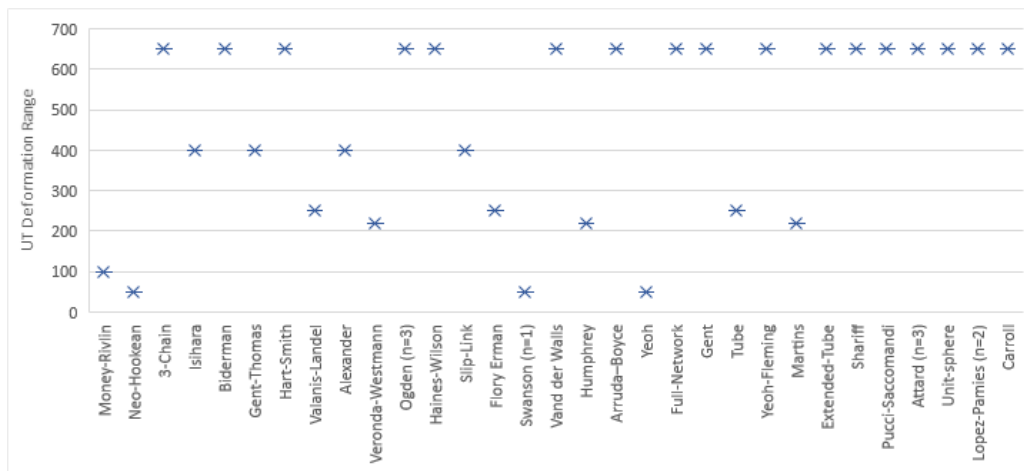


Figure 14: Deformation range for the mathematical models in the Uniaxial Tension (UT) type of load

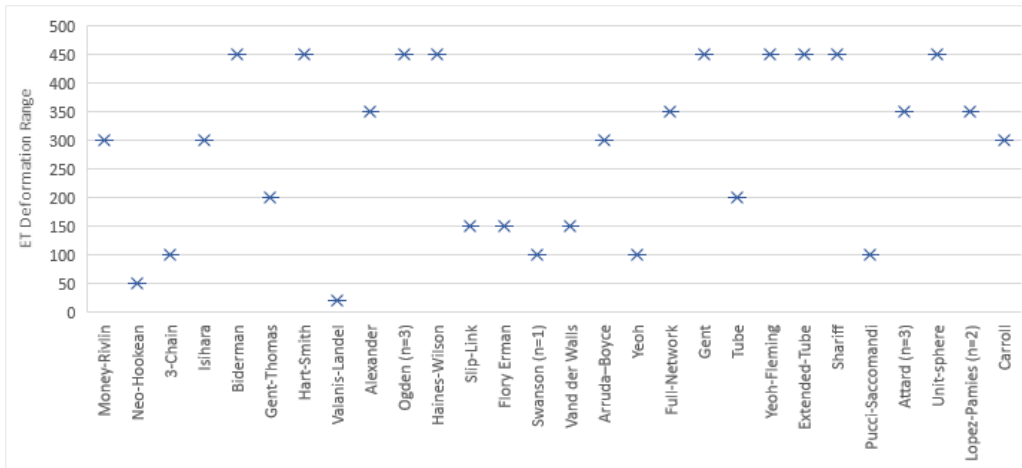


Figure 15: Deformation range for the mathematical models in the Equibiaxial Tension (ET) type of load

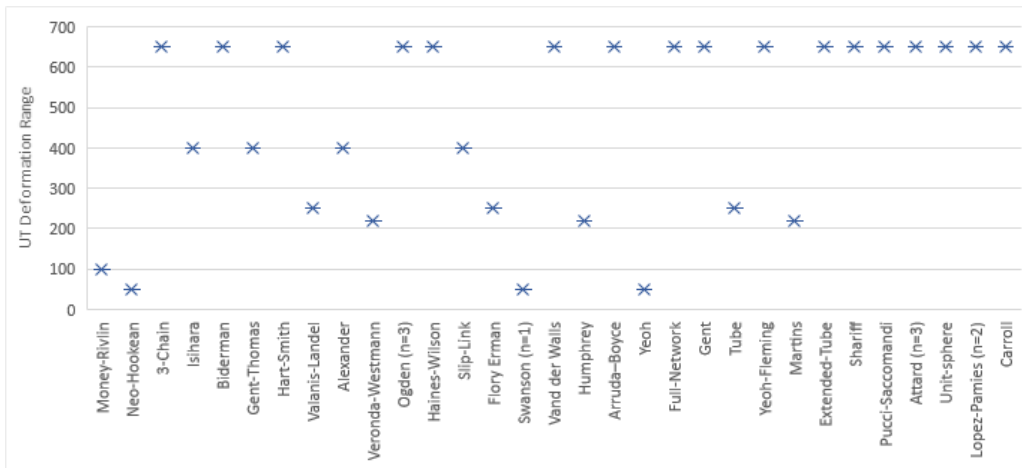


Figure 16: Deformation range for the mathematical models in the Pure Shear (PS) type of load

Figures 14, 15 and 16 illustrate the value of deformation ranges for the mathematical models in the three types of loads that are commonly performed on rubber and soft tissues: Uniaxial Tension (ET), Equibiaxial Tension (ET) and Pure Shear (PS). These figures are a complement to the Table 5 because they provide the value of deformation range for each model in comparison with the others. This can help researchers to have a more precise idea about the deformation range the models are valid for.

Table 6: Classification according to complexity based on number of material constants

Model	Complexity	#M.P	M.P	
Neo-Hookean	Low	1	$C_{10}$	
Rivlin-Saunders			$C$	
Money-Rivlin		2	$C_{10}, C_{01}$	
Valanis-Landel			$\mu$	
3-Chain			$\mu, N$	
Gent-Thomas			$C_1, C_2$	
Fung-Demiray			$C_1, C_2$	
Gent			$\mu, I_m$	
8-Chain			$\mu, N$	
Full-Network			$\mu, N$	
Unit-sphere			$\mu, N$	
Isihara			Medium	3
Hart-Smith	$C_1, C_2, C_3$			
Veronda-Westmann	$C_1, C_2, \beta$			
Slip-Link	$N_c, N_s, \eta$			
Flory Erman	$C_{10}, \phi, \kappa$			
Yeoh	$C_{10}, C_{20}, C_{30}$			
Tube	$\mu_c, \mu_e, \beta$			
Pucci-Saccomandi	$\mu, I_m, C_2$			
Carroll	$C_1, C_2, C_3$			
Biderman	4	$C_{10}, C_{01}, C_{30}, C_{30}$		
Alexander		$C_1, C_2, C_3, C_4$		
Swanson (n=1)		$A, B, \alpha, \beta$		
Humphrey		$C_1, C_2, C_3, C_4$		
Vand der Waals		$\mu, a, \lambda_m, \beta$		
Yeoh-Fleming		$A, B, C_{10}, I_m$		
Martins		$C_1, C_2, C_3, C_4$		
Extended-Tube		$\mu_c, \mu_e, \beta, \delta$		
Lopez-Pamies (n=2)		$\mu_1, \mu_2, \alpha_1, \alpha_2$		
Shariff (n=4)		High		5
Ogden (n=3)	6			$\mu_1, \mu_2, \mu_3, \alpha_1, \alpha_2, \alpha_3$
Haines-Wilson			$C_{10}, C_{01}, C_{11}, C_{02}, C_{20}, C_{30}$	
Attard (n=3)			$A_1, A_2, A_3, B_1, B_2, B_3$	

Table 6 shows the classification according to complexity for the models being analyzed in this work, only for the computation of material constants. The material constants have been considered as the principal determinant of the complexity of a model because there is no data about the time that each model lasts to give a result for a determined data set and because they are hard to determine as previously stated. So, the mathematical models have been grouped into low, medium and high complexity groups according to the number of material constants they use in their SEF. When the models have 1 or 2 materials parameters they are placed in the low complexity group, the models with 3 or 4 parameters belong to the medium complexity group, and the models with 5 or 6 parameters are in the high complexity group. The table also shows the specific parameters that must be computed through experiments on the material in question (rubber or soft tissues). The Full Polynomial model has not been considered in this classification because it is a series that can be truncated at any number and there are other models being analyzed that are truncations of this series.

Table 6 offers the possibility of extracting the most simple, medium and complex models, for the computation of material parameters, depending on the needs of the modeler. However, it is important to consider that a bigger number of parameters does not guarantee the model a better accuracy nor a bigger range of validity as the previous classification, which is based on the deformation range, illustrated. So, it is necessary to consider both classifications in order to get a better perspective of what model should be chosen given their pros and cons.

Although the number of material constants used by the mathematical model in question is a good indicator of its complexity, it is not enough to consider only such constants. It is not enough because the computation of material parameters is only a step previous to the simulation with a mathematical model. Besides, among the models being analyzed, there are models based on micromechanics which require to iterate over a big number of polymer chains, and therefore, the complexity of the model increases because of it. There are also models that use powers of invariants as well as exponential and logarithms. So, it is necessary to perform a classification based on the complexity that goes further and considers more than just the material constants.

Table 7: Complexity of the mathematical models considering material constants and the complexity of their SEF

Model	#M.P.	Complexity of SEF				Total
		REPS	SUMS	MULTS	E.OP.	
Money-Rivlin (1940)	2	1	3(6)	2(12)	0	20
Neo-Hookean (1943)	1	1	1(3)	1(3)	0	9
3-Chain (1943)	2	3	1	8	4	41
Rivlin-Saunders (1951)	1	1	3(6)	1(12)	0	23
Isihara (1951)	3	1	4(6)	5(12)	0	30
Biderman (1958)	4	1	7(6)	7(12)	0	36
Gent-Thomas (1958)	2	1	2(6)	3(12)	1	26
Hart-Smith (1966)	3	1	2(6)	5(12)	3	31
Valanis-Landel (1967)	2	3	1	2	1	14
Alexander (1968)	4	1	6	6	3	19
Veronda-Westmann (1970)	3	1	4(6)	3(12)	1	29
Ogden (1972) n=3	6	3	3	2	0	21
Fung-Demiray (1972)	2	1	2(3)	4(3)	1	15
Haines-Wilson (1975)	6	1	12(6)	11(12)	0	47
Slip-Link (1981)	3	1	6	41	2	52
Flory Erman (1982)	3	4	7	16	2	103
Swanson (1985) n=1	4	1	5(6)	10(12)	2	39
Vand der Walls (1986)	4	1	9(6)	12(12)	3	46
Humphrey (1987)	4	1	5(3)	4(3)	5	24
Arruda-Boyce / 8-Chain (1993)	2	1	1	8	4	15
Yeoh (1993)	3	3	1(3)	1(3)	0	27
Full-Network (1993)	2	1	6	33	16	57
Gent (1996)	2	1	2(3)	4(3)	1	15
Tube (1997)	3	3	3	7	1	36

Model	#M.P.	Complexity of SEF				Total
		REPS	SUMS	MULTS	E.OP.	
Yeoh-Fleming (1997)	4	1	7(3)	6(3)	2	25
Martins (1998)	4	1	7(3)	7(3)	5	29
Extended-Tube (1999)	4	1	12	20	4	40
Shariff (2000) n=4	5	3	12	19	10	128
Pucci-Saccomandi (2002)	3	1	3(6)	6(12)	2	32
Attard (2003) n=3	6	3	7	12	6	81
Unit-sphere (2004)	2	21	2	8	4	296
Lopez-Pamies (2010) n=2	4	2	2	4	3	22
Carroll (2011)	3	1	2(6)	6(12)	1	30

Table 7 shows an overall grade for the complexity of each mathematical model being reviewed in this work, considering the calculus previous to the model implementation, such as the computation of material parameters, and the calculus associated to the model itself. The Full Polynomial model has not been considered, as in the previous classification, due to its generality. The models are presented in chronological order and the parameters used to evaluate their complexity are the number of material parameters (#M.P.), the number of sums to be computed (SUMS), the number of multiplications (MULTS) and the number of special operations (E.OP.). Among the special operations, the models use logarithms, exponentials, decimal or fractional powers, hyperbolic sines and Langevin functions. In addition, there is a number in parenthesis next to the number of sums and multiplications in some models, which means the extra sums and multiplications that involve the computation of strain invariants. In the end, a total grade is shown, which is the result of summing all the parameters considered important in the complexity of the model. As result, the most complex model provided by this approach is the Unit Sphere model, which makes sense because this model involves the iteration over 21 polymer chains and performs complex calculus as the inverse of the Langevin function. This overall evaluation of complexity greatly contrasts with the previous table which grouped the Unit-Sphere model within the models with low complexity. On the other hand, the most simple model is the Neo-Hookean model with an overall grade of 9, which is expected because of the low number of calculations to be performed to implement it and the use of only one material parameter. So, Table 7 is an improvement to Table 6 because it provides an overall

grade to evaluate the complexity of the models instead of only classify them qualitatively into a big group. This approach even offers the possibility to rank the mathematical models from the simplest to the most complex.

As previously mentioned, knowing the complexity of a mathematical model provides an idea about the increase in time that will occur depending on the size of the data set. However, the complexity is not all that matters when performing soft tissue simulations because there may be really complex models that offer poor predictions, being not worthy for the computational time they use. So, it is necessary to also consider the accuracy and range of validity of a model before making a decision on the optimal mathematical model for a specific task.

Table 8: Classification according to application

Application	Model	#M.P	Complexity	Def. Range		
				UT	ET	PS
Real-Time Simulations of Surgical Procedures	Neo-Hookean [66, 67]	1	9	SMA	SMA	SMA
	Valanis-Landel	2	14	MOD	SMA	SMA
	Fung-Demiray	2	15	-	-	-
	Arruda-Boyce / 8-Chain	2	15	LAR	LAR	LAR
	Gent	2	15	LAR	LAR	LAR
	Alexander	4	19	LAR	LAR	MOD
	Money-Rivlin	2	20	SMA	LAR	LAR
	Ogden (n=3)	6	21	LAR	LAR	LAR
	Lopez-Pamies (n=2)	4	22	LAR	LAR	LAR
	Rivlin-Saunders	1	23	-	-	-
	Humphrey [68]	4	24	MOD	-	-
	Yeoh-Fleming	4	25	LAR	LAR	LAR
	Gent-Thomas	2	26	LAR	SMA	LAR
	Yeoh (n=3) [66, 67]	3	27	SMA	SMA	SMA
Preoperative Plans	Veronda-Westmann	3	29	MOD	-	-
	Martins	4	29	MOD	-	-
	Pucci-Saccomandi	3	32	LAR	SMA	LAR
	Tube	3	36	MOD	MOD	MOD
	Swanson (n=1)	4	39	SMA	SMA	SMA
	3-Chain	2	41	LAR	SMA	LAR
	Slip-Link	3	52	LAR	SMA	LAR
	Attard (n=3)	6	81	LAR	LAR	SMA
	Flory Erman	3	103	SMA	SMA	LAR
Surgical Implants Development	Isihara	3	30	LAR	LAR	LAR
	Carroll	3	30			
	Hart-Smith	3	31			
	Biderman	4	36			
	Extended-Tube	4	40			
	Vand der Walls	4	46			
	Full-Network	2	57			
	Shariff (n=4)	5	128			
	Unit-sphere	2	296			

Table 8 shows the classification according to the application, which is a combination of the previous two classifications (by deformation range and by complexity). Three main applications have been determined for soft tissue simulations: real-time simulations of surgical procedures, preoperative plans, and surgical implants development. This table shows each model with its corresponding classification as well as the number of material parameters it uses, its complexity and the range of deformations it is valid for in different loading conditions.

For real-time simulations of surgical procedures, the most important aspect to consider is the complexity of the model because real-time simulations must show results within milliseconds, so, mathematical models with a low complexity have been selected for this application. Neo-Hookean model is the fastest among the other models presented in this application due to its simplicity, but also the less accurate, being able to predict correctly very little strains. On the other hand, Gent and Arruda-Boyce models are the most optimal models to use for this application because they are able to predict large ranges of strains with a low computational cost due to their small number of material parameters (only two). In addition, when selecting a model for this specific application, it is important to address the deformation range to be predicted and the type of loading, so the choice is the most accurate according to the conditions of the problem.

In the case of preoperative plans, the accuracy of the models is more important than their speed, so, more complex models can be used for this specific application. In addition, as surgical procedures often do not require large deformations of the tissue due to the fragility of the human body, models with good accuracy at small and moderate ranges of deformations have been selected. The Tube model presents good predictions of soft tissue behavior at moderate strains while the Swanson model does the same job at small strains.

In surgical implants development, the range of validity of the used model must be large because the tests of such implants involve stretching the material many times its size. So, in this case, models with high accuracy at large strains have been selected. The optimal models to use for this application are the Isihara and Carroll because they present a high accuracy for large strains predictions at a lower computational cost than the other models. On the other hand, Shariff and Unit-Sphere models also present good accuracy in the prediction of soft tissue behavior but the high computational cost of their implementation makes them not feasible due to the existence of models like Isihara that present better accuracy at a lower computational cost.

Table 9: Summary of mathematical models

Model (Year)	Formula	Based On?		S?	#M.P.	M.P.	Deformation Range		
		$I_1$	$I_2$				$\lambda$	UT	ET
Money-Rivlin (1940)	$W = C_{10}(I_1 - 3) + C_{01}(I_2 - 3)$	x	x		2	$C_{10}, C_{01}$	SMA	LAR	LAR
Neo-Hookean (1943)	$W = C_{10}(I_1 - 3)$	x			1	$C_{10}$	SMA	SMA	SMA
3-Chain (1943)	$W = \frac{\mu N}{3} \sum_{k=1}^3 \left[ \sqrt{N^{-1} \lambda_k} \gamma_k + \ln \left( \frac{\gamma_k}{\sinh(\gamma_k)} \right) \right]$			x	2	$\mu, N$	LAR	SMA	LAR
Rivlin-Saunders (1951)	$W = C(I_1 - 3) + f(I_2 - 3)$	x	x		1	$C$	LAR	LAR	LAR
Isihara (1951)	$W = C_{10}(I_1 - 3) + C_{20}(I_1 - 3)^2 C_{01}(I_2 - 3)$	x	x	x	3	$C_{10}, C_{01}, C_{20}$	LAR	LAR	LAR
Biderman (1958)	$W = C_{10}(I_1 - 3) + C_{01}(I_2 - 3) + C_{20}(I_1 - 3)^2 + C_{30}(I_1 - 3)^3$	x	x		4	$C_{10}, C_{01}, C_{30}, C_{20}$	LAR	LAR	LAR
Gent-Thomas (1958)	$W = C(I_1 - 3) + C_2 \ln \left( \frac{I_2}{3} \right)$	x	x		2	$C_1, C_2$	LAR	SMA	LAR
Hart-Smith (1966)	$W = C_1 \int \exp \left( C_2 [I_1 - 3]^2 \right) dI_1 + C_3 \ln \left[ \frac{I_2}{3} \right]$	x	x	x	3	$C_1, C_2, C_3$	LAR	LAR	LAR

Model (Year)	Formula	Based On?			S?	#M.P.	M.P.	Deformation Range		
		I <sub>1</sub>	I <sub>2</sub>	λ				UT	ET	PS
Valanis-Landel (1967)	$W = \omega(\lambda_1) + \omega(\lambda_2) + \omega(\lambda_3)$			x		μ	MOD	SMA	SMA	
Alexander (1968)	$W = C_1 \int \exp(C_3 [I_1 - 3]^2) dI_1 + C_2 \ln\left(\frac{I_2 - 3 + C_4}{C_4}\right) + C_3 [I_2 - 3]$	x	x	x	4	C <sub>1</sub> , C <sub>2</sub> , C <sub>3</sub> , C <sub>4</sub>	LAR	LAR	LAR	MOD
Veronda-Westmann (1970)	$W = C_1 [e^{\beta(I_1-3)} - 1] - C_2(I_2 - 3)$	x	x		3	C <sub>1</sub> , C <sub>2</sub> , β	MOD	-	LAR	
Ogden, n=3 (1972)	$W = \sum_{i=1}^n \frac{\mu_i}{\alpha_i} (\lambda_1^{\alpha_i} + \lambda_2^{\alpha_i} + \lambda_3^{\alpha_i} - 3)$		x	x	6	μ <sub>1</sub> , μ <sub>2</sub> , μ <sub>3</sub> , α <sub>1</sub> , α <sub>2</sub> , α <sub>3</sub>	LAR	LAR	LAR	LAR
Fung-Demiray (1972)	$W = \frac{C_1}{2C_2} [e^{C_2(I_1-3)} - 1]$	x			2	C <sub>1</sub> , C <sub>2</sub>	LAR	LAR	LAR	LAR
Haines-Wilson (1975)	$W = C_{10}(I_1 - 3) + C_{01}(I_2 - 3) + C_{11}(I_1 - 3)(I_2 - 3) + C_{02}(I_2 - 3)^2 + C_{20}(I_1 - 3)^2 + C_{30}(I_1 - 3)^3$	x	x		6	C <sub>10</sub> , C <sub>01</sub> , C <sub>11</sub> , C <sub>02</sub> , C <sub>20</sub> , C <sub>30</sub>	LAR	LAR	LAR	LAR
Slip-Link (1981)	$W = \frac{1}{2} k_B \Theta N_c \sum_{i=1}^3 \lambda_i^2 + \frac{1}{2} k_B \Theta N_s \sum_{i=1}^3 \left[ \frac{(1+\eta)\lambda_i^2}{1+\eta\lambda_i^2} + \ln 1 + \eta\lambda_i^2  \right]$			x	3	N <sub>c</sub> , N <sub>s</sub> , η	LAR	SMA	LAR	LAR
Flory Erman (1982)	$W = C_{10} \sum_{i=1}^3 (\lambda_i^2 - 1) \left[ 1 - \frac{1}{\phi} \right] + C_{10} \sum_{i=1}^3 [B_i + D_i - \ln(B_i + 1) - \ln(D_i + 1)]$			x	3	C <sub>10</sub> , φ, κ	SMA	SMA	SMA	LAR

Model (Year)	Formula	Based On?			S?	#M.P.	M.P.	Deformation Range		
		I <sub>1</sub>	I <sub>2</sub>	λ				UT	ET	PS
Swanson, n=1 (1985)	$W = \frac{3}{2} \sum_{i=1}^n \frac{A_i}{1+\alpha_i} \left[ \frac{I_1}{3} \right]^{1+\alpha_i} + \frac{3}{2} \sum_{j=1}^n \frac{B_j}{1+\beta_j} \left[ \frac{I_2}{3} \right]^{1+\beta_j}$	x	x		4	A, B, α, β	SMA	SMA	SMA	
Vand der Walls (1986)	$W = -\mu (\lambda_m^2 - 3) \left[ \ln(1 - \Delta) + \Delta \right] - \frac{2}{3} a \mu \left( \frac{\tilde{I}-3}{2} \right)^{\frac{3}{2}}$			x	4	μ, a, λ <sub>m</sub> , β	LAR	SMA	LAR	
Humphrey (1987)	$W = C_1 \left[ e^{C_2(I_1-3)} - 1 \right] + C_3 \left[ e^{C_4(\alpha-1)^2} - 1 \right]$	x			4	C <sub>1</sub> , C <sub>2</sub> , C <sub>3</sub> , C <sub>4</sub>	MOD	-	-	
Arruda-Boyce / 8-Chain (1993)	$W = \mu N \left[ \sqrt{N-1} \lambda \gamma + \ln \left( \frac{\lambda \gamma}{\sinh(\lambda \gamma)} \right) \right]$			x	2	μ, N	LAR	LAR	LAR	
Yeoh (1993)	$W = \sum_{i=1}^3 C_{10} (I_1 - 3)^i$	x			3	C <sub>10</sub> , C <sub>20</sub> , C <sub>30</sub>	SMA	SMA	SMA	
Full-Network (1993)	$W = (1 - \rho) W_{3-Chain} + \rho W_{8-Chain}$			x	2	μ, N	LAR	LAR	LAR	
Gent (1996)	$W = -I_m \frac{\mu}{2} \ln \left[ 1 - \frac{I_1-3}{I_m} \right]$	x			2	μ, I <sub>m</sub>	LAR	LAR	LAR	
Tube (1997)	$W = \sum_{i=1}^3 \frac{\mu_c}{2} (\lambda_i^2 - 1) + \frac{2\mu_c}{\beta^2} (\lambda_i^{-\beta} - 1)$			x	3	μ <sub>c</sub> , μ <sub>e</sub> , β	MOD	MOD	MOD	
Yeoh-Fleming (1997)	$W = \frac{A}{B} (I_m - 3) (1 - e^{-BR}) - C_{10} (I_m - 3) \ln(1 - R)$	x			4	A, B, C <sub>10</sub> , I <sub>m</sub>	LAR	LAR	LAR	

Model (Year)	Formula	Based On?			S?	#M.P.	M.P.	Deformation Range		
		I <sub>1</sub>	I <sub>2</sub>	λ				UT	ET	PS
Martins (1998)	$W = C_1 \left[ e^{C_2(I_1-3)} - 1 \right] + C_3 \left[ e^{C_4(\alpha-1)^2} - 1 \right] + \frac{1}{B}(J-1)^2$	x			4	C <sub>1</sub> , C <sub>2</sub> , C <sub>3</sub> , C <sub>4</sub>	MOD	-	-	
Extended-Tube (1999)	$W = \frac{E_c}{2} \left[ \frac{(1-\delta^2)(I_1-3)}{1-\delta^2(I_1-3)} + \ln(1-\delta^2(I_1-3)) \right] + \sum_{i=1}^3 \frac{2\mu_i}{\beta_i^2} \left( \lambda_i^{-\beta} - 1 \right)$		x	x	4	μ <sub>c</sub> , μ <sub>e</sub> , β, δ	LAR	LAR	LAR	
Shariff, n=4 (2000)	$W = E \sum_{j=0}^n \alpha_j \phi_j(\lambda_1) + E \sum_{j=0}^n \alpha_j \phi_j(\lambda_2) + E \sum_{j=0}^n \alpha_j \phi_j(\lambda_3)$		x	x	5	E, α <sub>1</sub> , α <sub>2</sub> , α <sub>3</sub> , α <sub>4</sub>	LAR	LAR	LAR	
Pucci-Saccomandi (2002)	$W = -I_m \frac{\mu}{2} \ln \left[ 1 - \frac{I_1-3}{I_m} \right] + C_2 \ln \left[ \frac{I_2}{3} \right]$	x	x	x	3	μ, I <sub>m</sub> , C <sub>2</sub>	LAR	SMA	LAR	
Attard, n=3 (2003)	$W = \sum_{i=1}^n \frac{A_i}{2^i} (\lambda_1^{2i} + \lambda_2^{2i} + \lambda_3^{2i} - 3) + \sum_{i=1}^n \frac{B_i}{2^i} (\lambda_1^{-2i} + \lambda_2^{-2i} + \lambda_3^{-2i} - 3)$		x	x	6	A <sub>1</sub> , A <sub>2</sub> , A <sub>3</sub> , B <sub>1</sub> , B <sub>2</sub> , B <sub>3</sub>	LAR	LAR	SMA	
Unit-sphere (2004)	$W = \mu N \sum_{k=1}^{2l} w_k \left[ \sqrt{N-1} \Lambda_k \gamma_k + \ln \left( \frac{\gamma_k}{\sinh(\gamma_k)} \right) \right]$		x	x	2	μ, N	LAR	LAR	LAR	
Lopez-Pamies, n=2 (2010)	$W = \sum_{i=1}^n \frac{3^{1-\alpha_i}}{2\alpha_i} \mu_i \left[ I_1^{\alpha_i} - 3^{\alpha_i} \right]$	x		x	4	μ <sub>1</sub> , μ <sub>2</sub> , α <sub>1</sub> , α <sub>2</sub>	LAR	LAR	LAR	
Carroll (2011)	$W = aI_1 + bI_1^4 + c\sqrt{I_2}$	x	x	x	3	C <sub>1</sub> , C <sub>2</sub> , C <sub>3</sub>	LAR	LAR	LAR	

Table 9 shows a summary of the mathematical models analyzed in this work, ordered chronologically, with their principal characteristics, such as: their strain energy function (SEF), whether they are based on strain invariants ( $I_1, I_2$ ) or principal stretches ( $\lambda$ ), whether they are able to reproduce the S-shape (S?) that rubber and soft tissues show in their stress-strain curve, their number of material parameters (#M.P), their material parameters (M.P.) and their deformation range in different types of loads (UT, ET, PS). This table is useful to find out some principal characteristics of the mathematical models, but the other tables must be checked in case more information is needed as the theory in which the model is based, their complexity or the applications they are recommended for.

## 5 Conclusions

There is a wide range of mathematical models suitable for realistic soft tissue simulations, so that, programmers, engineers, biomedical and modelers in general, do not know which of them to use for their specific necessities. Therefore, the aim of the work is to perform an explanatory study of such mathematical models by finding their most important characteristics and parameters. A total of 34 models have been found in literature, which, according to literature, can be classified based on the approach that the author has followed to define their strain energy function. The classification of the literature has placed the mathematical models into the groups: phenomenological models, models based on the experimental determination of  $\frac{\partial W}{\partial I_1}$  and  $\frac{\partial W}{\partial I_2}$ , and physically based models.

It has been determined that the most important aspects of the mathematical models are the material constants that they use, the deformation range they are valid for and their accuracy. The material constants are important because they are hard to determine, and therefore, influence the complexity of the model. The deformation range of the models is imperative to consider in order to establish the conditions under which the model can be used. The accuracy is, perhaps, the most important aspect of a mathematical model because it informs about the usefulness of the model in the prediction of the material's behavior.

After analyzing the most important aspects of a mathematical model, it has been decided to classify the mathematical models being studied by deformation range, by complexity, and by the application. The classification by deformation range divides the mathematical models into those that can make good predictions at small strains ( $< 150\%$ ), at moderate strains ( $151\% - 250\%$ ) and at large strains ( $> 250\%$ ) in different types of loads. The classification by complexity orders the mathematical models by its complexity, which has been determined from their number of material parameters and the operations that must be performed to obtain their strain energy function. Finally, the classification according to the application takes the information of the previous two classifications to recommend the models depending on the application established; the applications analyzed

are real-time simulations of surgical procedures, preoperative plans, and surgical implants development.

In conclusion, there is no best model for all cases, it depends on the conditions of the problem to be modeled. There may be cases when small strains need to be modeled as well as cases where large strains need to be modeled. In other occasions speed may be a priority instead of accuracy, making necessary to choose simple models and sacrifice some precision in the predictions. So, the application where the model is going to be used will determine what model must be chosen.

## References

- [1] G. Marckmann and E. Verron, “Comparison of Hyperelastic Models for Rubber-Like Materials,” *Rubber Chemistry and Technology*, vol. 79, no. 5, pp. 835–858, 2006. [Online]. Available: <http://rubberchemtechnol.org/doi/abs/10.5254/1.3547969>
- [2] G. A. Holzapfel, “Similarities between soft biological tissues and rubberlike materials,” *Leiden*, no. March, pp. 607–617, 2005.
- [3] A. H. Muhr, “Modeling the Stress-Strain Behavior of Rubber,” *Rubber Chemistry and Technology*, vol. 78, no. 3, pp. 391–425, 2011.
- [4] A. Spencer, *Continuum Mechanics*, ser. Dover books on physics. Dover Publications, 2004. [Online]. Available: <https://books.google.com.ec/books?id=AJdfQL0rggC>
- [5] P. Steinmann, M. Hossain, and G. Possart, “Hyperelastic models for rubber-like materials: Consistent tangent operators and suitability for Treloar’s data,” *Archive of Applied Mechanics*, vol. 82, no. 9, pp. 1183–1217, 2012.
- [6] G. Chagnon, M. Rebouah, and D. Favier, “Hyperelastic Energy Densities for Soft Biological Tissues: A Review,” *Journal of Elasticity*, vol. 120, no. 2, pp. 129–160, 2015. [Online]. Available: <http://dx.doi.org/10.1007/s10659-014-9508-z>
- [7] P. A. Martins, R. M. Jorge, and A. J. Ferreira, “A comparative study of several material models for prediction of hyperelastic properties: Application to silicone-rubber and soft tissues,” *Strain*, vol. 42, no. 3, pp. 135–147, 2006.
- [8] M. Sasso, G. Palmieri, G. Chiappini, and D. Amodio, “Characterization of hyperelastic rubber-like materials by biaxial and uniaxial stretching tests based on optical methods,” *Polymer Testing*, vol. 27, no. 8, pp. 995–1004, 2008. [Online]. Available: <http://dx.doi.org/10.1016/j.polymertesting.2008.09.001>
- [9] M. Hossain and P. Steinmann, “More hyperelastic models for rubber-like materials: consistent tangent operators and comparative study,” *Journal of the Mechanical Behavior of Materials*, vol. 22, no. 1-2, pp. 1–24, 2013.
- [10] T. Beda, H. Gacem, Y. Chevalier, and P. Mbarga, “Domain of validity and fit of Gent-Thomas and Flory-Erman rubber models to data,” *Express Polymer Letters*, vol. 2, no. 9, pp. 615–622, 2008.

- [11] C. Miehe, S. Göktepe, and F. Lulei, “A micro-macro approach to rubber-like materials - Part I: The non-affine micro-sphere model of rubber elasticity,” *Journal of the Mechanics and Physics of Solids*, vol. 52, no. 11, pp. 2617–2660, 2004.
- [12] G. N. Greaves, A. L. Greer, R. S. Lakes, and T. Rouxel, “Poisson’s ratio and modern materials,” *Nature Materials*, vol. 10, no. 11, pp. 823–837, 2011.
- [13] I. Pearson and M. Pickering, “The determination of a highly elastic adhesive’s material properties and their representation in finite element analysis,” *Finite Elements in Analysis and Design*, vol. 37, no. 3, pp. 221–232, 2001.
- [14] K. Miller and A. P. Inc, “Testing Elastomers for Finite Element Analysis,” *Studies in Health Technology and Informatics*, 2004.
- [15] D. Roylance, “Stress-Strain Curves,” *Class Note*, pp. 1–14, 2001.
- [16] G. L. Bradley, P. C. Chang, and G. B. McKenna, “Rubber modeling using uniaxial test data,” *Journal of Applied Polymer Science*, vol. 81, no. 4, pp. 837–848, 2001.
- [17] P. Chantereau, M. Brieu, M. Kammal, J. Farthmann, B. Gabriel, and M. Cosson, “Mechanical properties of pelvic soft tissue of young women and impact of aging,” *International Urogynecology Journal*, vol. 25, no. 11, pp. 1547–1553, 2014.
- [18] A. Patole, B. Narkhede, S. Deshmukh, and K. Madulety, “Precincts of Lean Six Sigma : An Academic Perspective,” *Udyog Pragati*, vol. 36, no. 4, 2012.
- [19] M. Kaufman, “Forces and Motion,” *Order and Disorder*, pp. 45–60, 2012.
- [20] D. J. Charlton, J. Yang, and K. K. Teh, “A Review of Methods to Characterize Rubber Elastic Behavior for Use in Finite Element Analysis,” *Rubber Chemistry and Technology*, vol. 67, no. 3, pp. 481–503, jul 1994. [Online]. Available: <http://rubberchemtechnol.org/doi/abs/10.5254/1.3538686>
- [21] Y. Wu, H. Wang, and A. Li, “Parameter Identification Methods for Hyperelastic and Hyper-Viscoelastic Models,” *Applied Sciences*, vol. 6, no. 12, p. 386, 2016.
- [22] L. R. G. Treloar, “Stress-Strain Data for Vulcanized Rubber under Various Types of Deformation,” *Rubber Chemistry and Technology*, vol. 17, no. 4, pp. 813–825, dec 1944. [Online]. Available: <http://rubberchemtechnol.org/doi/abs/10.5254/1.3546701>

- [23] M. Shahzad, A. Kamran, M. Z. Siddiqui, and M. Farhan, “Mechanical Characterization and FE Modelling of a Hyperelastic Material,” *Materials Research*, vol. 18, no. 5, pp. 918–924, 2015. [Online]. Available: [http://www.scielo.br/scielo.php?script=sci\\_arttext&pid=S1516-14392015000500918&lng=en&tlng=en](http://www.scielo.br/scielo.php?script=sci_arttext&pid=S1516-14392015000500918&lng=en&tlng=en)
- [24] M. N. Hamza and H. M. Alwan, “Hyperelastic Constitutive Modeling of Rubber and Rubber- Like Materials under Finite Strain,” vol. 28, no. 13, 2010.
- [25] M. C. Boyce and E. M. Arruda, “Constitutive Models of Rubber Elasticity: A Review,” *Rubber Chemistry and Technology*, vol. 73, no. 3, pp. 504–523, 2011.
- [26] R. W. Ogden, G. Saccomandi, and I. Sgura, “Fitting hyperelastic models to experimental data,” *Computational Mechanics*, vol. 34, no. 6, pp. 484–502, 2004.
- [27] S. Kawabata, M. Matsuda, K. Tei, and H. Kawai, “Experimental survey of the strain energy density function of isoprene rubber vulcanizate,” *Macromolecules*, vol. 14, no. 1, pp. 154–162, jan 1981. [Online]. Available: <http://pubs.acs.org/doi/abs/10.1021/ma50002a032>
- [28] J. Thewlis, “Concise Dictionary of Physics,” *Oxford: Pergamon Press*, p. 248, 1973.
- [29] M. Mooney, “A theory of large elastic deformation,” *Journal of Applied Physics*, no. 11, pp. 582–592, 1940.
- [30] R. Rivlin, “Large elastic deformations of isotropic materials. IV. Further developments of the general theory,” *Philosophical Transactions of the Royal Society of London. Series A*, no. 241, pp. 379–397, 1948.
- [31] V. Biderman, “Calculations of rubber parts (Russian),” *Rascheti na Prochnost*, p. 40, 1958.
- [32] A. James and A. Green, “Strain energy functions of rubber. II. The characterization of filled vulcanizates,” *Journal of Applied Polymer Science*, no. 19, p. 2033, 1975.
- [33] H. Yeoh, “Some forms of the strain energy function for rubber,” *Rubber Chemistry and Technology*, no. 66, pp. 154–771, 1993.
- [34] R. Ogden, “Large Deformation Isotropic Elasticity – On the Correlation of Theory and Experiment for Incompressible Rubberlike Solids,” *Proceedings of the Royal Society of London. Series A, Mathematical and Physical Sciences*, no. 326, pp. 565–584, 1993.

- [35] M. Shariff, “Strain energy function for filled and unfilled rubberlike material,” *Rubber Chemistry and Technology*, no. 73, p. 1, 2000.
- [36] S. R. Swanson, “A Constitutive Model for High Elongation Elastic Materials,” *Journal of Engineering Materials and Technology*, vol. 107, no. 2, p. 110, apr 1985. [Online]. Available: <http://materialstechnology.asmedigitalcollection.asme.org/article.aspx?articleid=1423533>
- [37] M. M. Carroll, “A Strain Energy Function for Vulcanized Rubbers,” *Journal of Elasticity*, vol. 103, no. 2, pp. 173–187, apr 2011. [Online]. Available: <http://link.springer.com/10.1007/s10659-010-9279-0>
- [38] Y. Fung, “Elasticity of soft tissues in simple elongation,” *American Journal of Physiology-Legacy Content*, vol. 213, no. 6, pp. 1532–1544, 2017.
- [39] H. Demiray, “A note on the elasticity of soft biological tissues,” *Journal of Biomechanics*, vol. 5, no. 3, pp. 309–311, 1972.
- [40] D. R. Veronda and R. A. Westmann, “Mechanical characterization of skin-Finite deformations,” *Journal of Biomechanics*, vol. 3, no. 1, 1970.
- [41] J. D. Humphrey and F. C. Yin, “On constitutive relations and finite deformations of passive cardiac tissue: I. A pseudostrain-energy function.” *Journal of biomechanical engineering*, vol. 109, no. 4, pp. 298–304, 1987. [Online]. Available: <http://www.ncbi.nlm.nih.gov/pubmed/3695429>
- [42] J. A. Martins, E. B. Pires, R. Salvado, and P. B. Dinis, “A numerical model of passive and active behavior of skeletal muscles,” *Computer Methods in Applied Mechanics and Engineering*, vol. 151, no. 3-4, pp. 419–433, 1998.
- [43] M. M. Attard, “Finite strain— isotropic hyperelasticity,” *International Journal of Solids and Structures*, vol. 40, no. 17, pp. 4353–4378, aug 2003. [Online]. Available: <https://linkinghub.elsevier.com/retrieve/pii/S0020768303002178>
- [44] M. M. Attard and G. W. Hunt, “Hyperelastic constitutive modeling under finite strain,” *International Journal of Solids and Structures*, vol. 41, no. 18-19, pp. 5327–5350, sep 2004. [Online]. Available: <https://linkinghub.elsevier.com/retrieve/pii/S0020768304001507>
- [45] R. Rivlin and D. Saunders, “Large elastic deformation of isotropic materials, VII. Experiments on the deformations of rubber,” *Philosophical Transactions of the Royal Society of London. Series A*, no. 243, p. 251, 1951.

- [46] A. Gent and A. Thomas, “Forms for the stored (strain) energy function for vulcanized rubber,” *Journal of Polymer Science*, no. 28, pp. 625–628, 1958.
- [47] L. Hart-Smith and Z. Angew, “Elasticity parameters for finite deformations of rubber-like materials,” *Math. Phys.*, no. 17, p. 608, 1966.
- [48] H. Alexander, “A constitutive relation for rubber-like materials,” *International Journal of Engineering Science*, vol. 6, no. 9, pp. 549–563, sep 1968. [Online]. Available: <https://www.sciencedirect.com/science/article/abs/pii/0020722568900062>
- [49] K. Valanis and R. Landel, “The strain-energy function for a hyperelastic material in terms of extension ratios,” *Journal of Applied Physics*, no. 38, pp. 2997–3002, 1967.
- [50] A. Gent, “A new constitutive relation for rubber,” *Rubber Chemistry and Technology*, no. 69, pp. 59–61, 1996.
- [51] E. Pucci and G. Saccomandi, “A Note on the Gent Model for Rubber-Like Materials,” *Rubber Chemistry and Technology*, vol. 75, no. 5, pp. 839–852, nov 2002. [Online]. Available: <http://rubberchemtechnol.org/doi/abs/10.5254/1.3547687>
- [52] O. Yeoh and P. Fleming, “A new attempt to reconcile the statistical and phenomenological theories of rubber elasticity,” *Journal of Polymer Science Part B: Polymer Physics*, no. 35, pp. 1919–1931, 1997.
- [53] L. Treloar, “The statistical length of long-chain molecules,” *Transactions of the Faraday Society*, no. 39, p. 241, 1943.
- [54] O. Lopez-Pamies, “A new I1-based hyperelastic model for rubber elastic materials,” *Comptes Rendus Mécanique*, vol. 338, no. 1, pp. 3–11, jan 2010. [Online]. Available: <https://www.sciencedirect.com/science/article/abs/pii/S1631072109002113>
- [55] H. M. James and E. Guth, “Theory of the Elastic Properties of Rubber,” *The Journal of Chemical Physics*, vol. 11, no. 10, pp. 455–481, oct 1943. [Online]. Available: <http://aip.scitation.org/doi/10.1063/1.1723785>
- [56] A. Isihara, N. Hashitsume, and M. Tatibana, “Statistical theory of rubber-like elasticity-iv (two dimensional stretching),” *Journal of Chemistry and Physics*, no. 19, pp. 1508–1512, 1951.
- [57] R. Ball, M. Doi, S. Edwards, and M. Warner, “Elasticity of entangled networks,” *Polymer*, no. 22, pp. 1010–1018, 1981.
- [58] H. Killian, “Equation of state of real networks,” *Polymer*, no. 22, pp. 209–207, 1981.

- [59] P. J. Flory and B. Erman, "Theory of elasticity of polymer networks. 3," *Macromolecules*, vol. 15, no. 3, pp. 800–806, may 1982. [Online]. Available: <http://pubs.acs.org/doi/abs/10.1021/ma00231a022>
- [60] E. Aruda and M. Boyce, "A three-dimensional model for the large stretch behavior of rubber elastic materials," *Journal of the Mechanics and Physics of Solids*, no. 41, pp. 389–412, 1993.
- [61] G. Heinrich and M. Kaliske, "Theoretical and numerical formulation of a molecular based constitutive tube-model of rubber elasticity," *Computational and Theoretical Polymer Science*, no. 7, pp. 227–241, 1997.
- [62] —, "An Extended Tube-Model for Rubber Elasticity: statistical-mechanical theory and finite element implantation," *Rubber Chemistry and Technology*, no. 72, pp. 602–632, 1997.
- [63] P. Wu and E. Van Der Giessen, "On improved network models for rubber elasticity and their applications to orientation hardening in glassy polymers," *Journal of the Mechanics and Physics of Solids*, vol. 41, no. 3, pp. 427–456, mar 1993. [Online]. Available: <https://www.sciencedirect.com/science/article/pii/S002250969390043F>
- [64] B. Kim, S. B. Lee, J. Lee, S. Cho, H. Park, S. Yeom, and S. H. Park, "A comparison among Neo-Hookean model, Mooney-Rivlin model, and Ogden model for Chloroprene rubber," *International Journal of Precision Engineering and Manufacturing*, vol. 13, no. 5, pp. 759–764, 2012.
- [65] P. A. L. S. Martins, R. M. N. Jorge, A. J. M. Ferreira, and I.-p. Feup, "Determination of Material Parameters for Different Hyperelastic Models," *Optimization*, vol. 1, no. 1, pp. 2–5, 2005.
- [66] R. J. Lapeer, P. D. Gasson, and V. Karri, "Simulating plastic surgery: From human skin tensile tests, through hyperelastic finite element models to real-time haptics," *Progress in Biophysics and Molecular Biology*, vol. 103, no. 2-3, pp. 208–216, 2010. [Online]. Available: <http://dx.doi.org/10.1016/j.pbiomolbio.2010.09.013>
- [67] —, "A hyperelastic finite-element model of human skin for interactive real-time surgical simulation," *IEEE Transactions on Biomedical Engineering*, vol. 58, no. 4, pp. 1013–1022, 2011.
- [68] H. Zhong and T. Peters, "A real time hyperelastic tissue model," *Computer Methods in Biomechanics and Biomedical Engineering*, vol. 10, no. 3, pp. 185–193, 2007.

# Appendices

## A Appendix 1

This appendix presents the stress-strain curves for some mathematical models, which have been obtained from many sources.

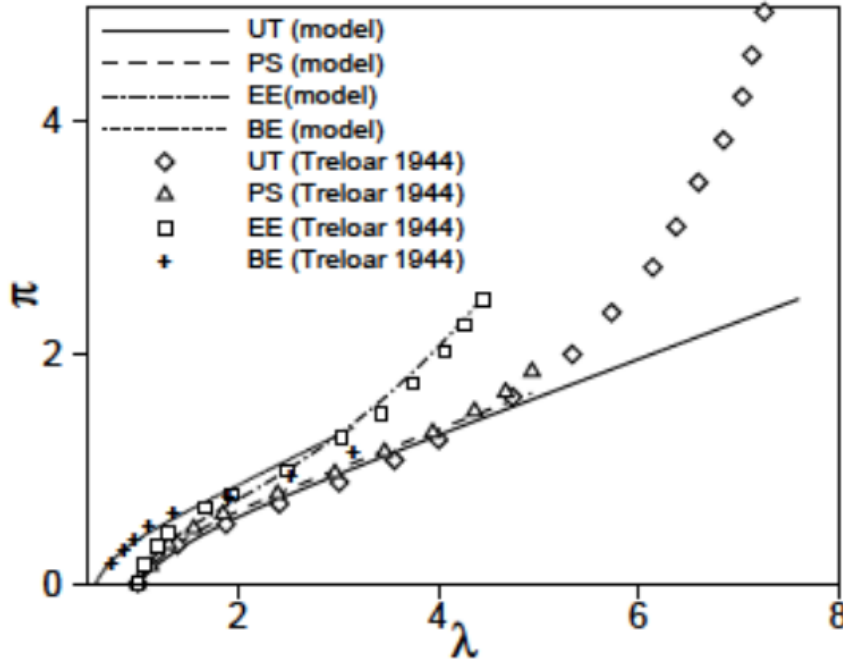


Figure 17: Stress-Strain curve for Money-Rivlin model [1]

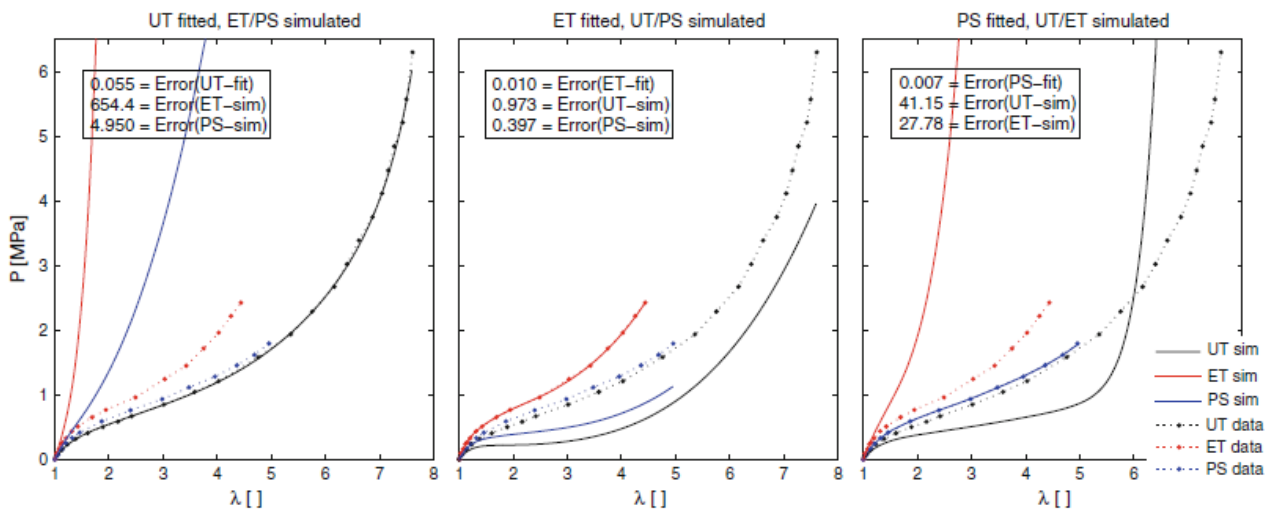


Figure 18: Stress-Strain curve for Yeoh model [5]

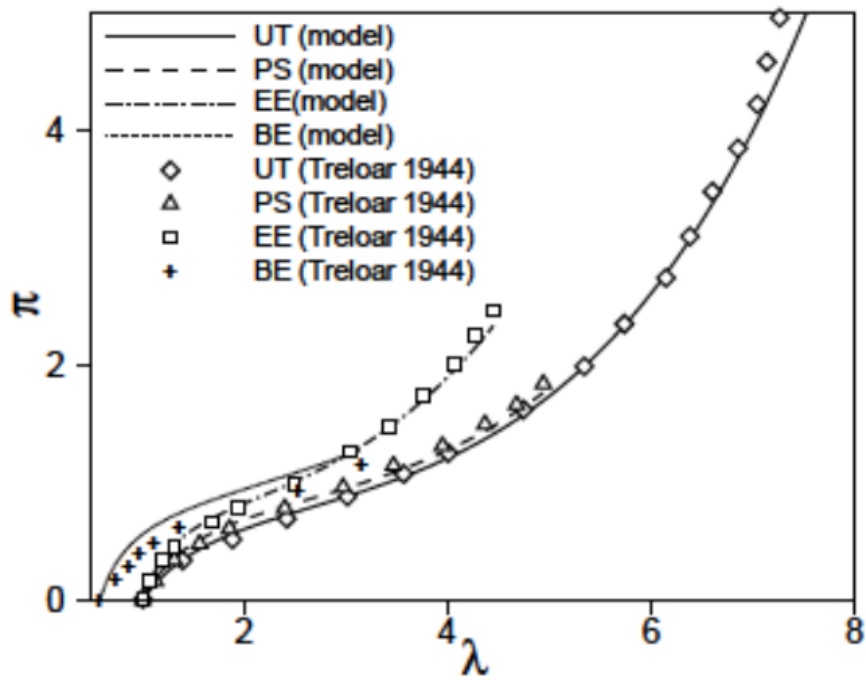


Figure 19: Stress-Strain curve for Ogden model [1]

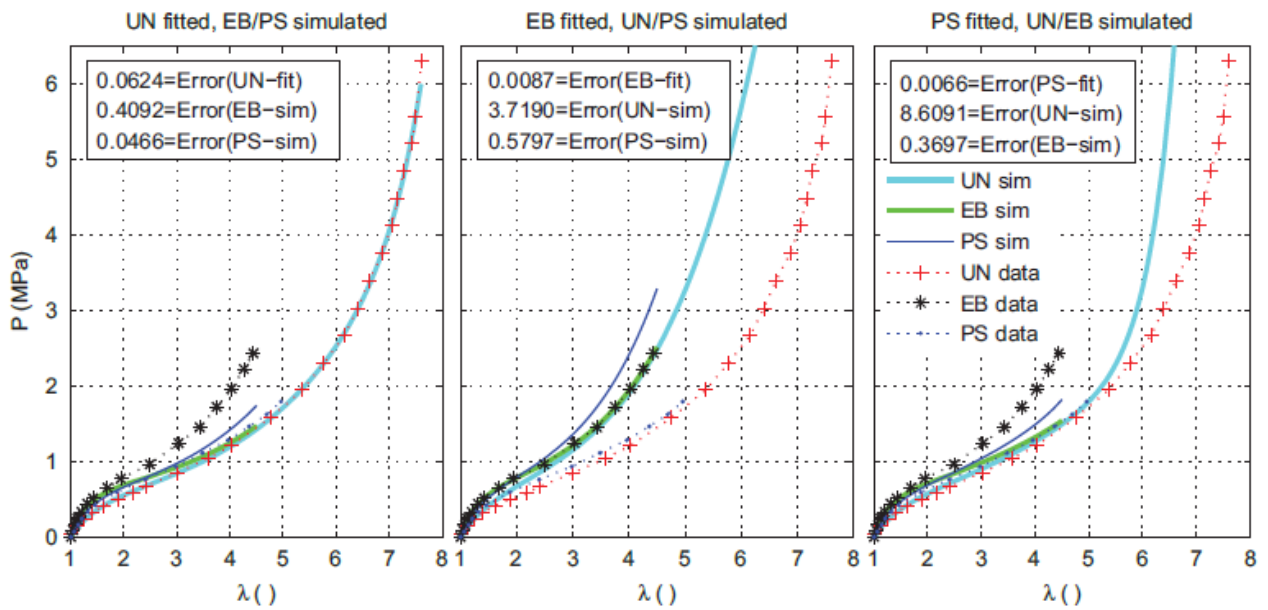


Figure 20: Stress-Strain curve for Ogden model [9]

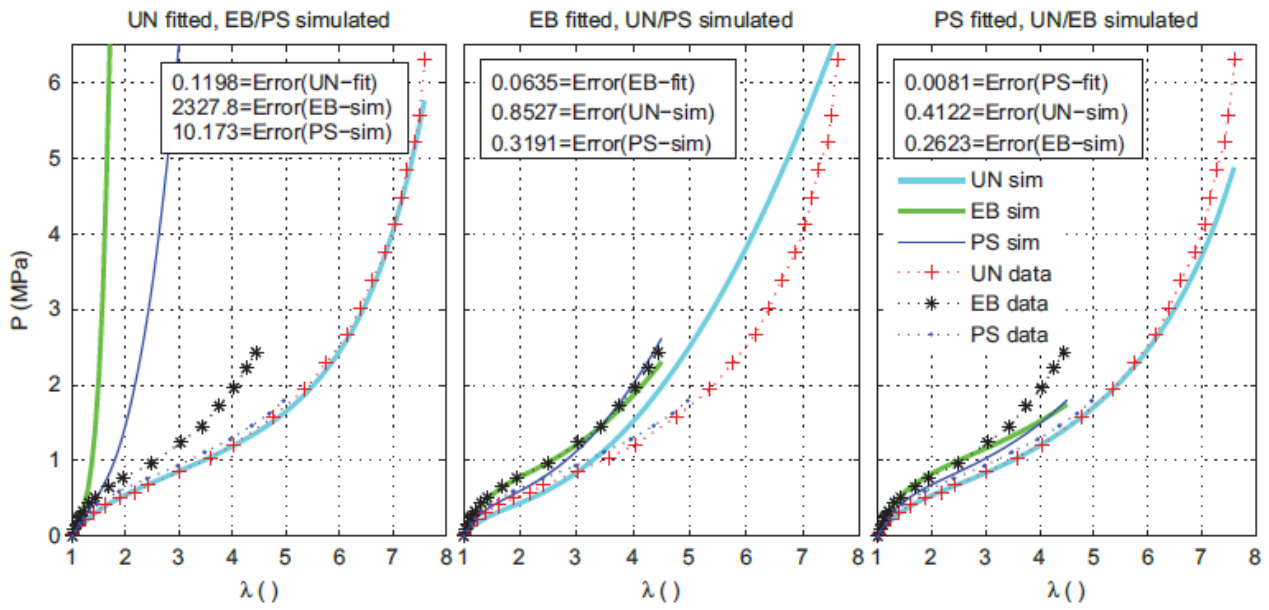


Figure 21: Stress-Strain curve for Shariff model [9]

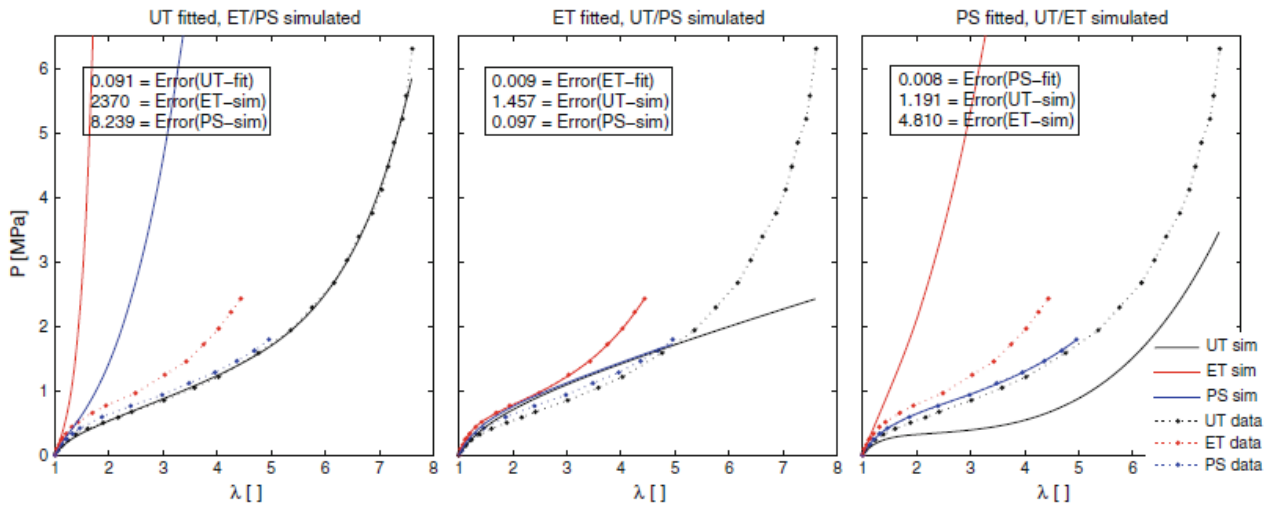


Figure 22: Stress-Strain curve for Swanson model [5]

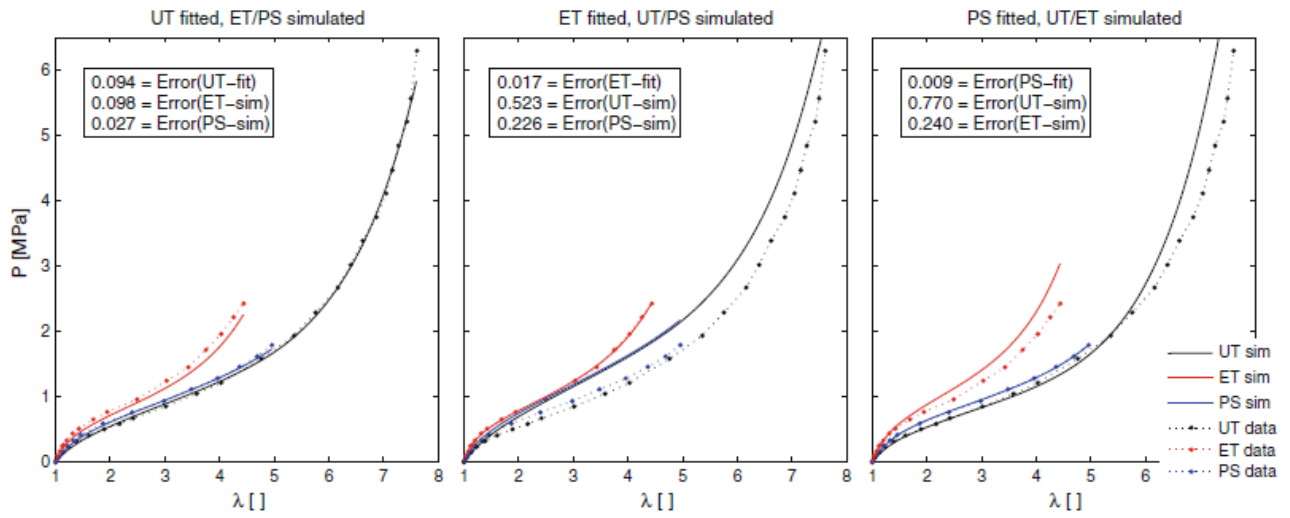


Figure 23: Stress-Strain curve for Carroll model [5]

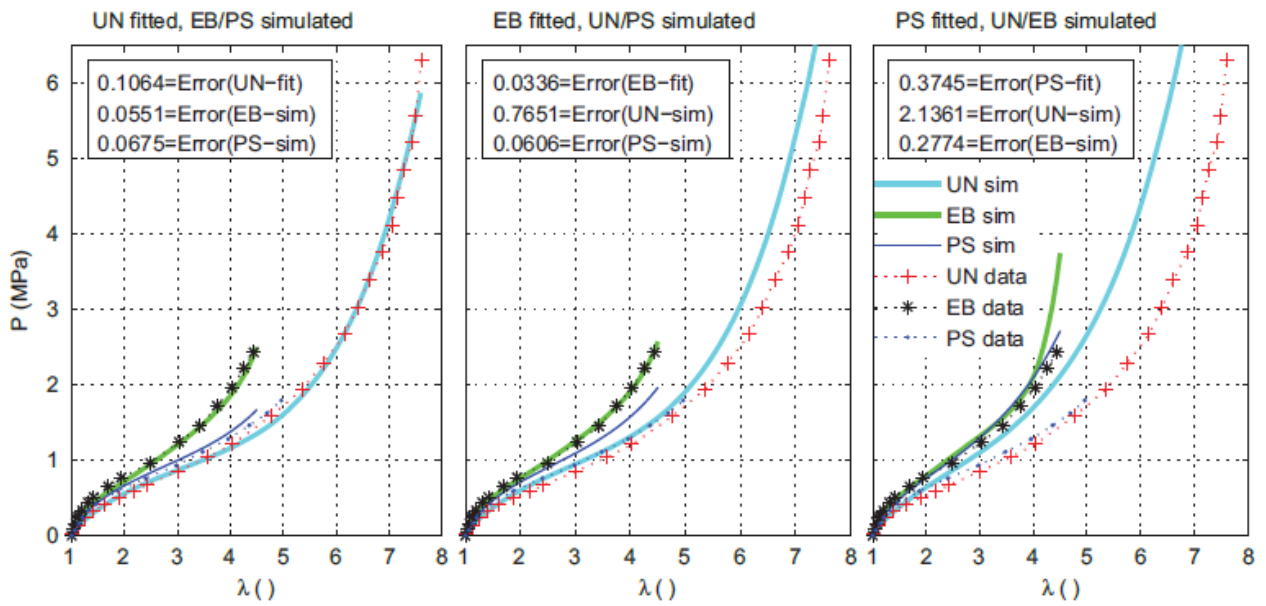


Figure 24: Stress-Strain curve for Attard model [9]

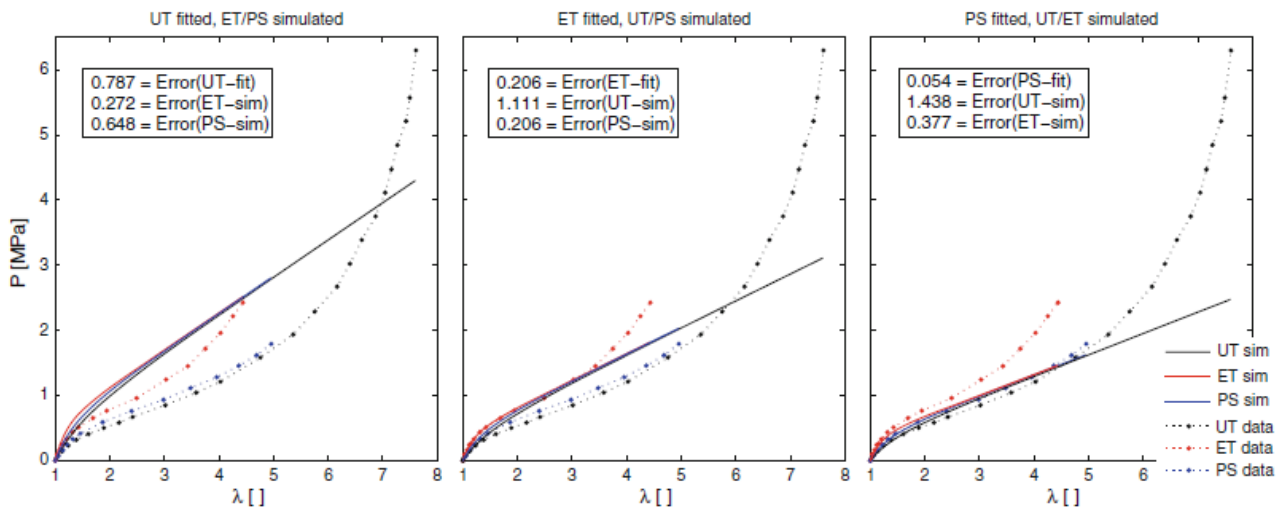


Figure 25: Stress-Strain curve for Gent-Thomas model [5]

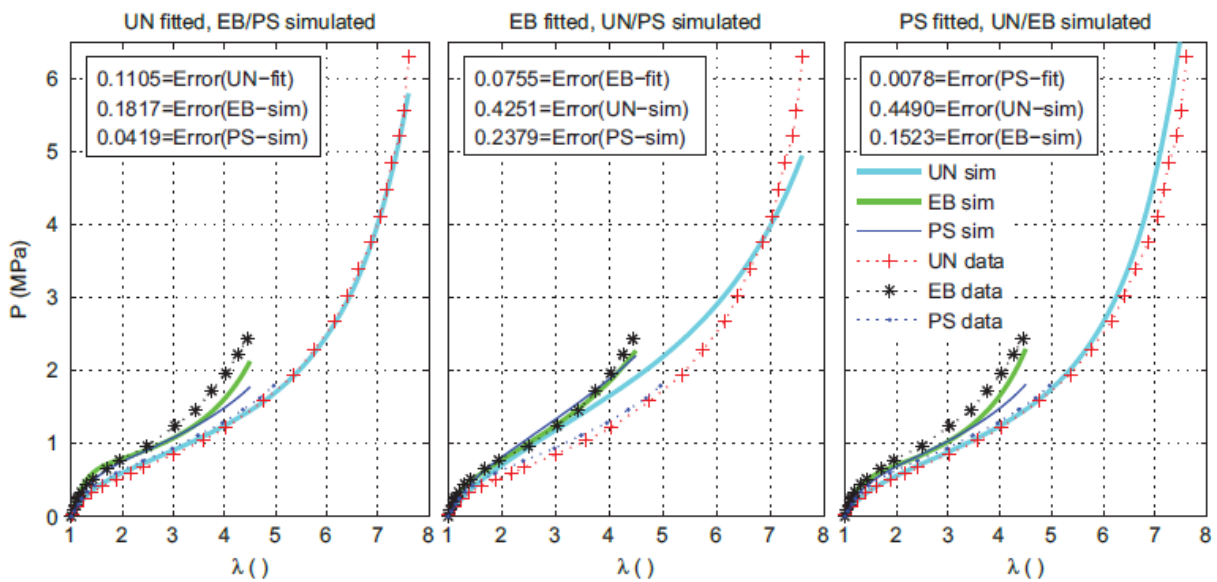


Figure 26: Stress-Strain curve for Hart-Smith model [9]

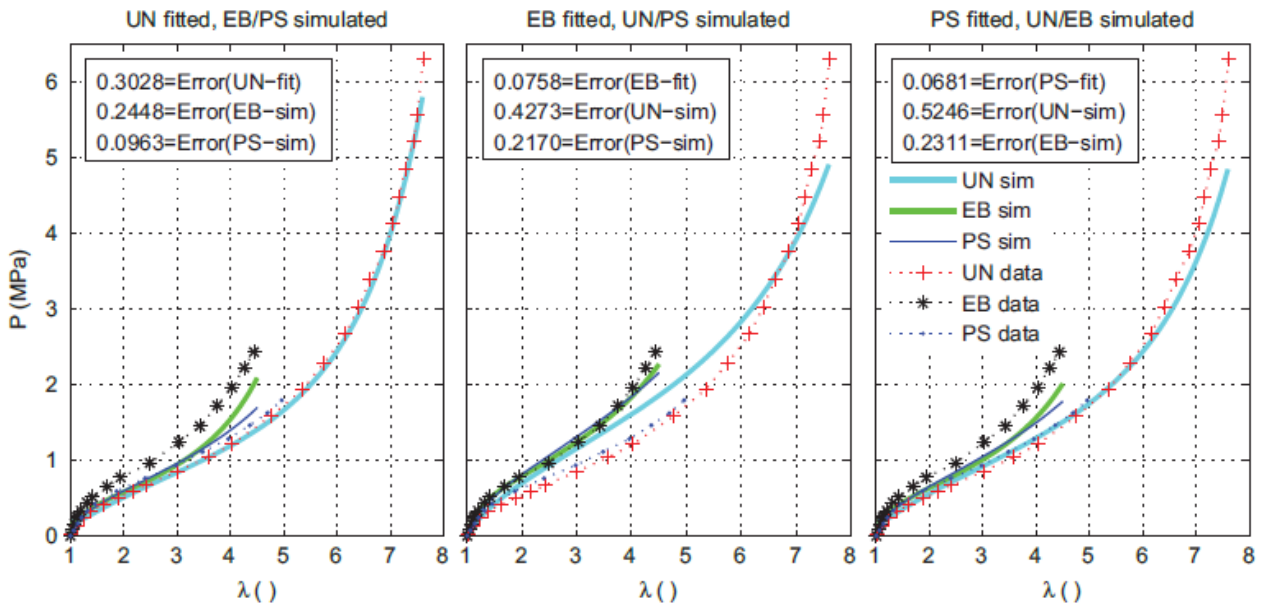


Figure 27: Stress-Strain curve for Alexander model [9]

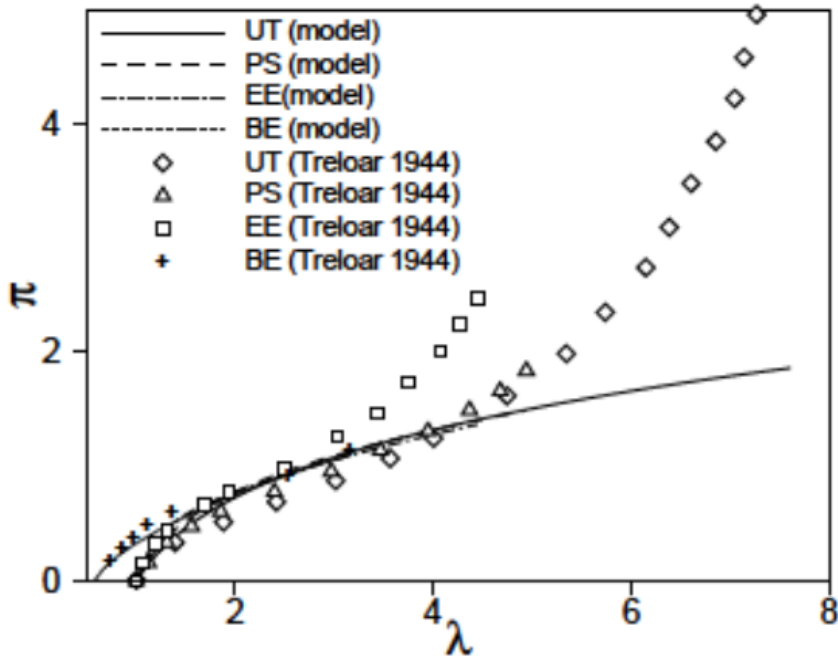


Figure 28: Stress-Strain curve for Valanis-Landel model [1]

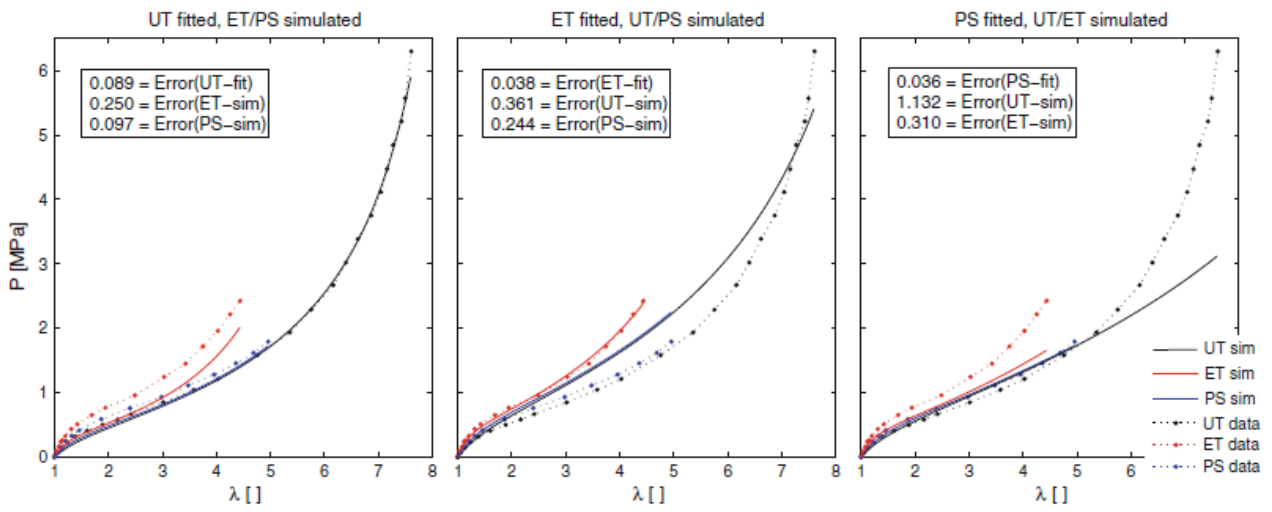


Figure 29: Stress-Strain curve for Gent model [5]

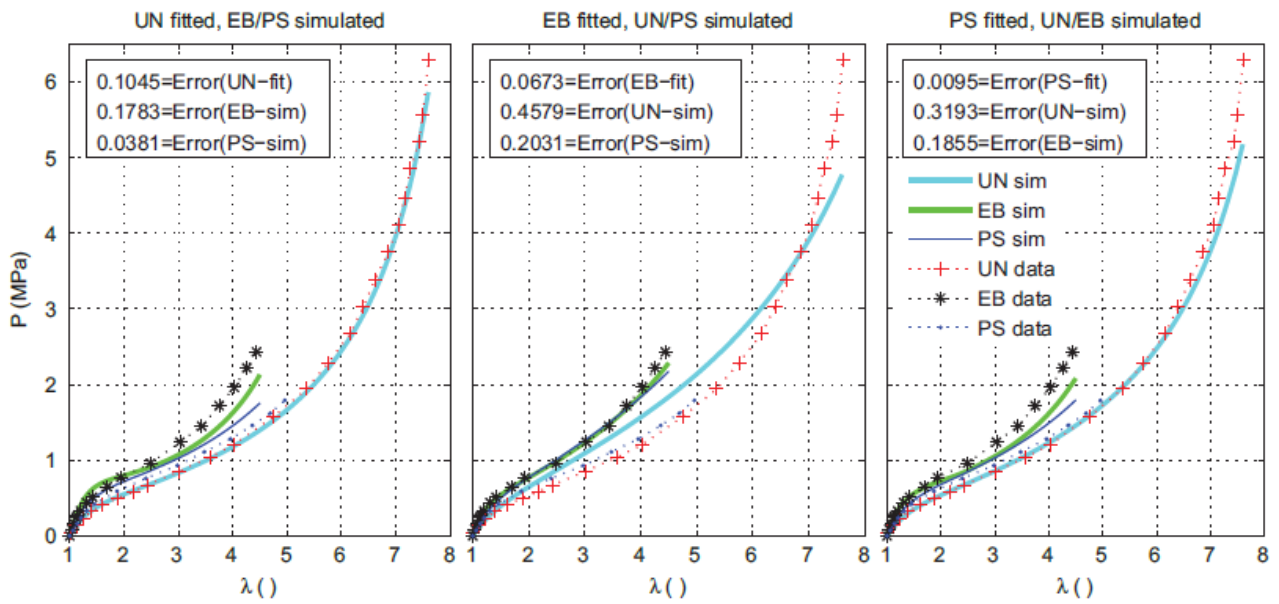


Figure 30: Stress-Strain curve for Pucci-Saccomandi model [9]

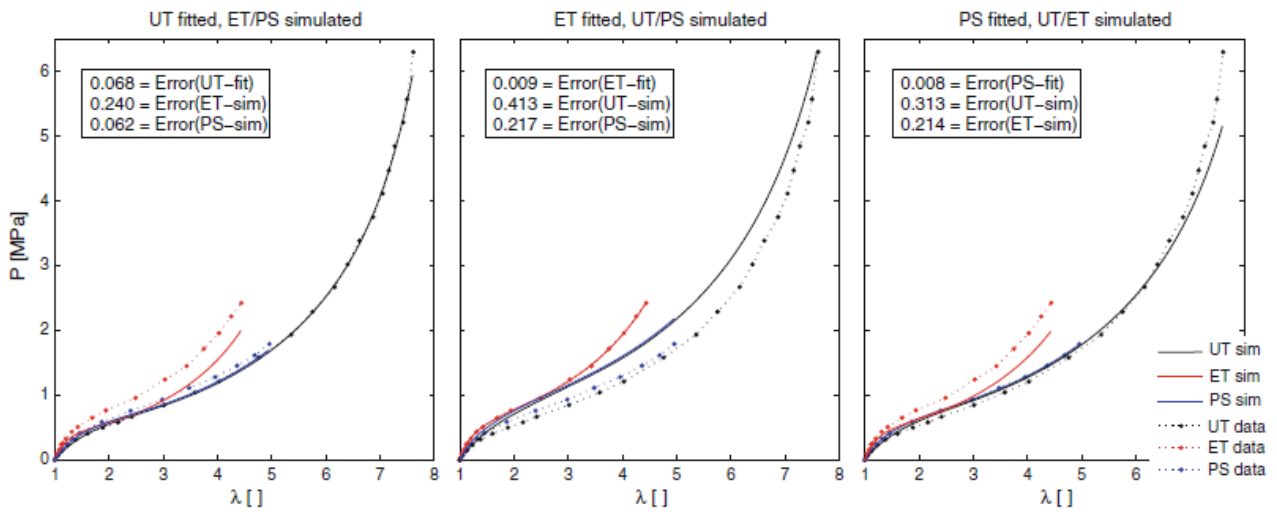


Figure 31: Stress-Strain curve for Yeoh-Fleming model [5]

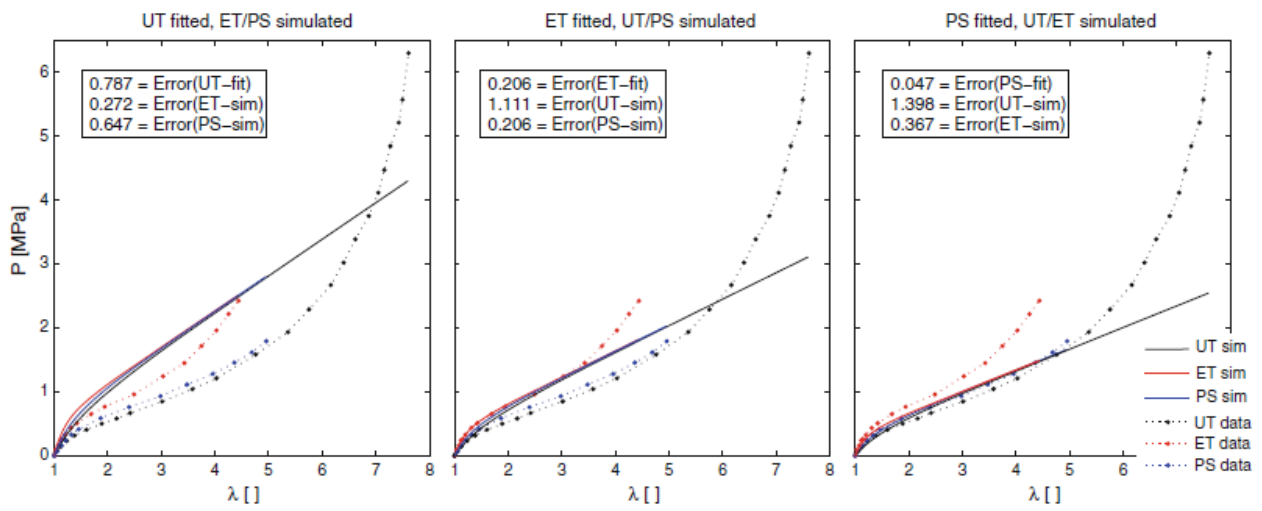


Figure 32: Stress-Strain curve for Neo-Hookean model [5]

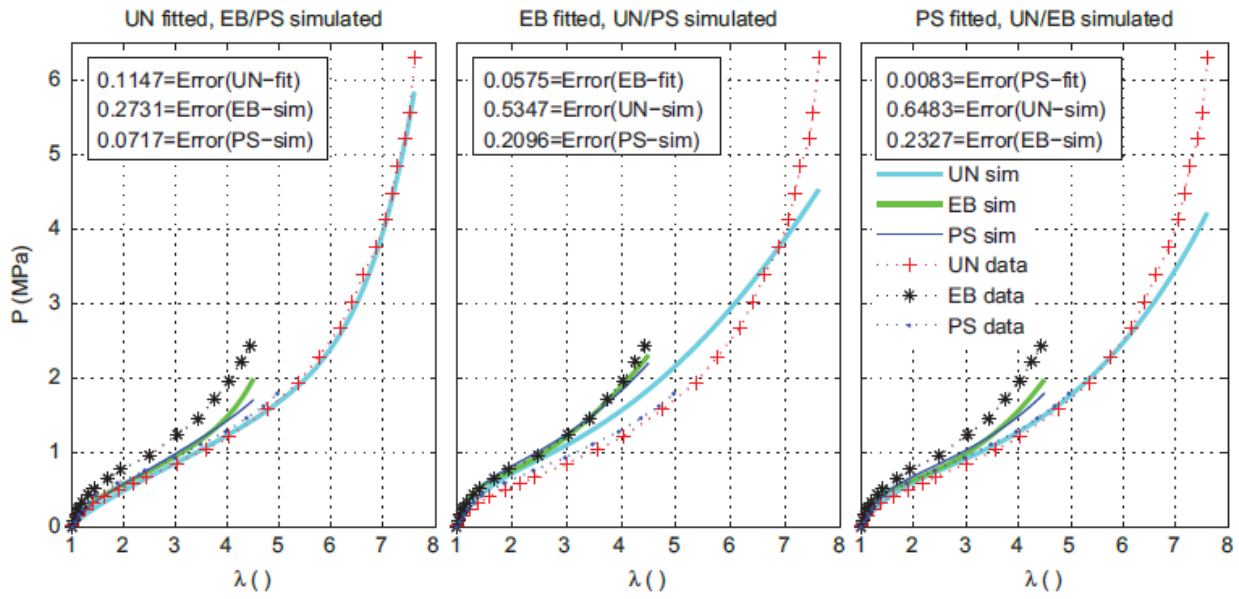


Figure 33: Stress-Strain curve for Lopez-Pamies model [9]

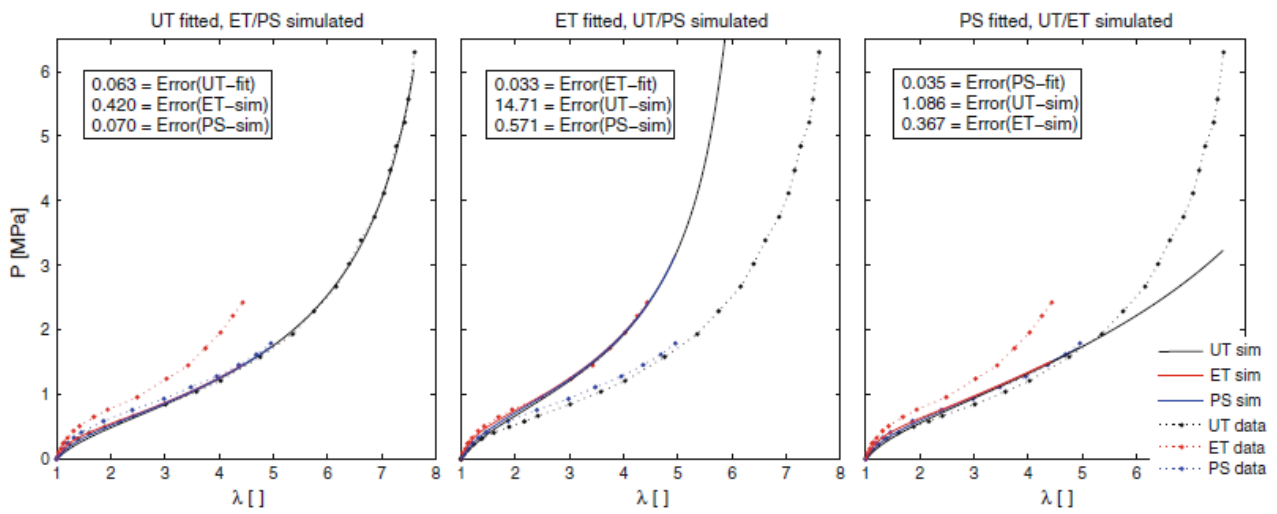


Figure 34: Stress-Strain curve for 3-Chain model [5]

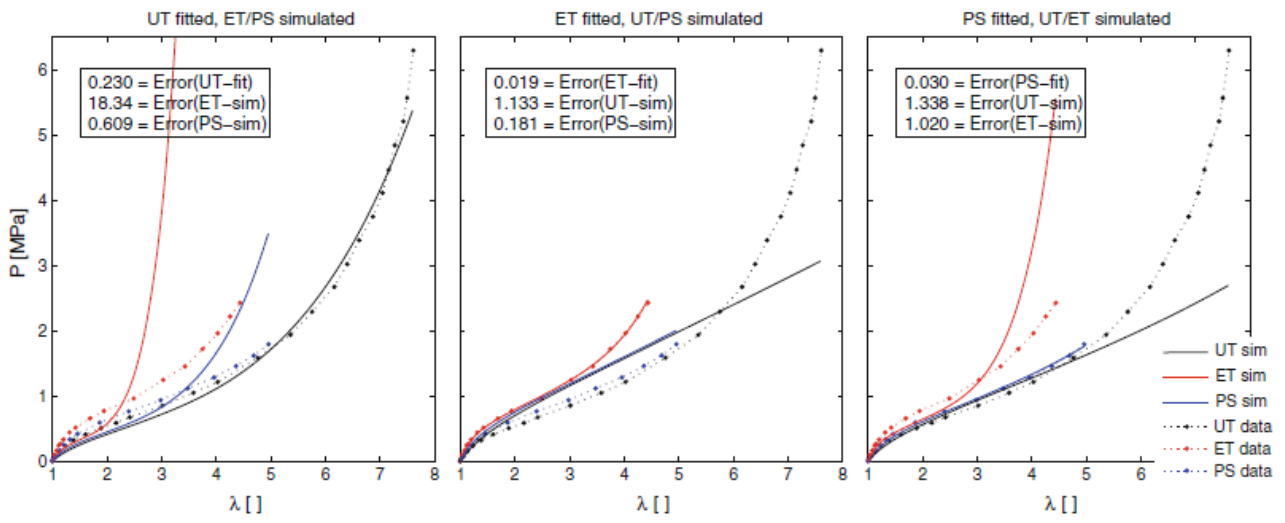


Figure 35: Stress-Strain curve for Isihara model [5]

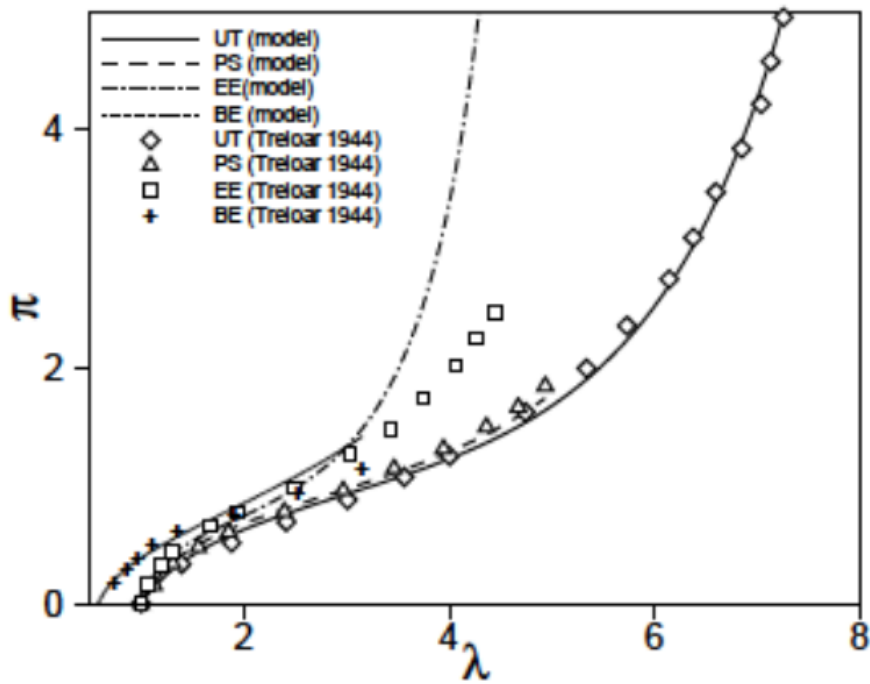


Figure 36: Stress-Strain curve for Van der Waals model [1]

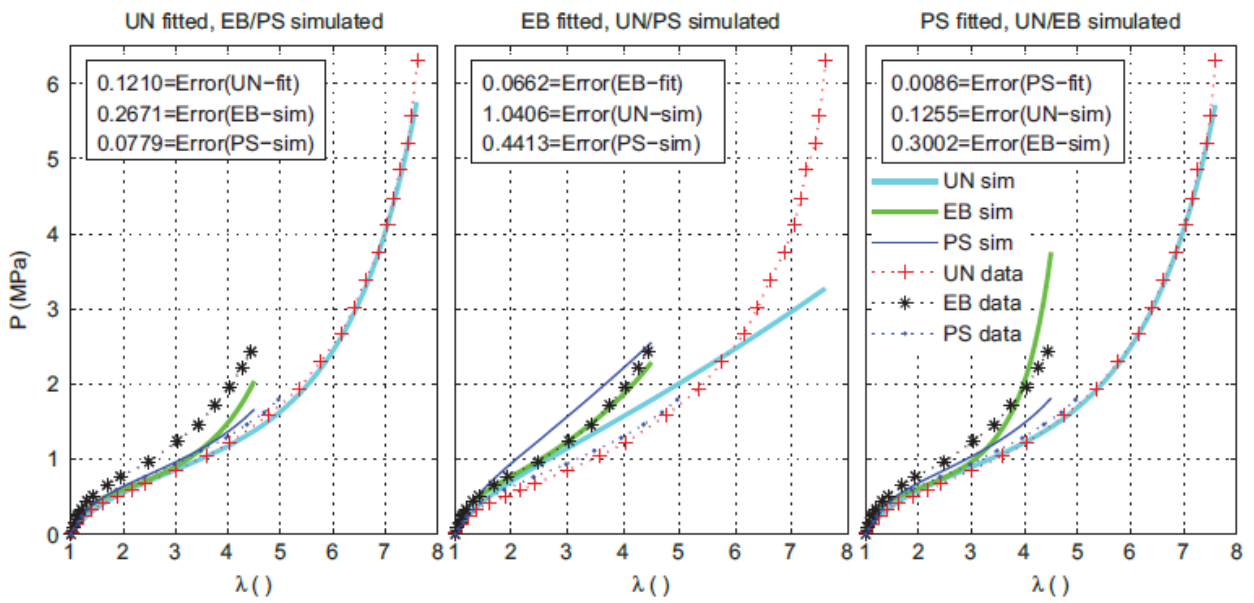


Figure 37: Stress-Strain curve for Van der Waals model [9]

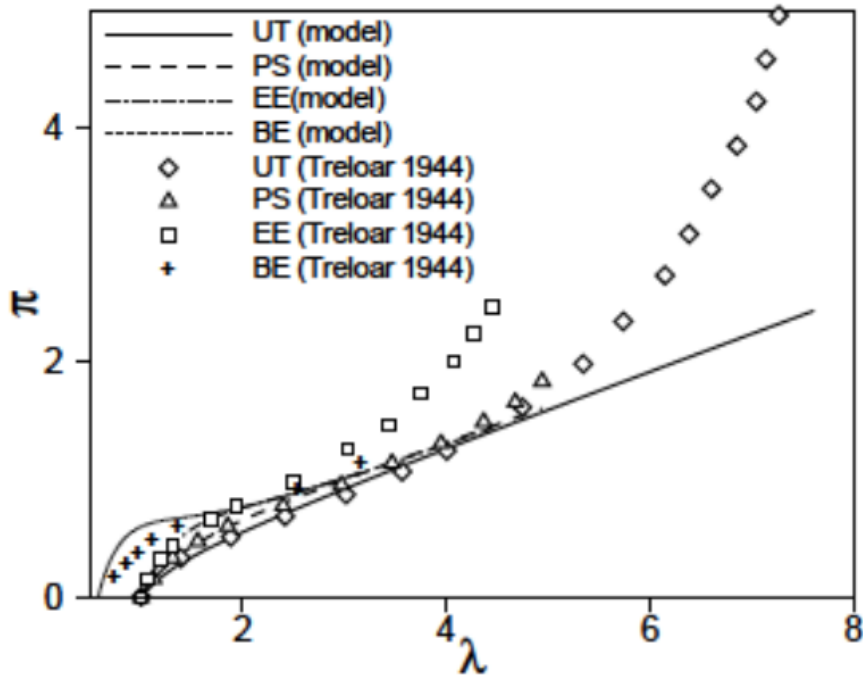


Figure 38: Stress-Strain curve for Flory-Erman model [1]

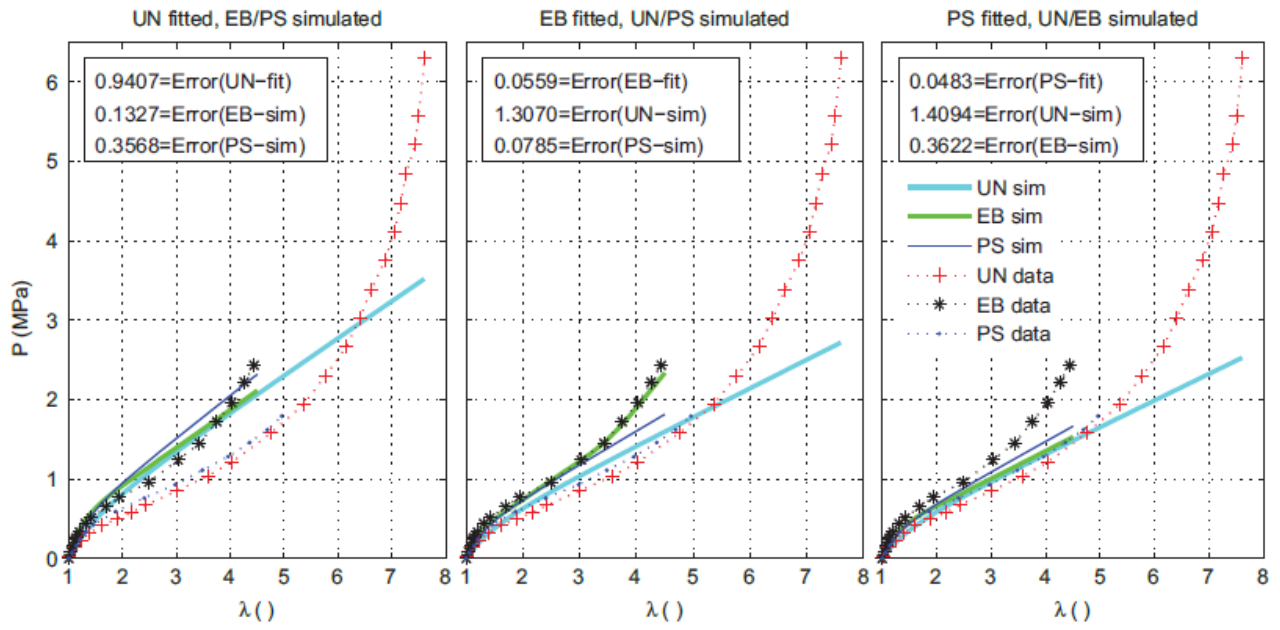


Figure 39: Stress-Strain curve for Flory-Erman model [9]

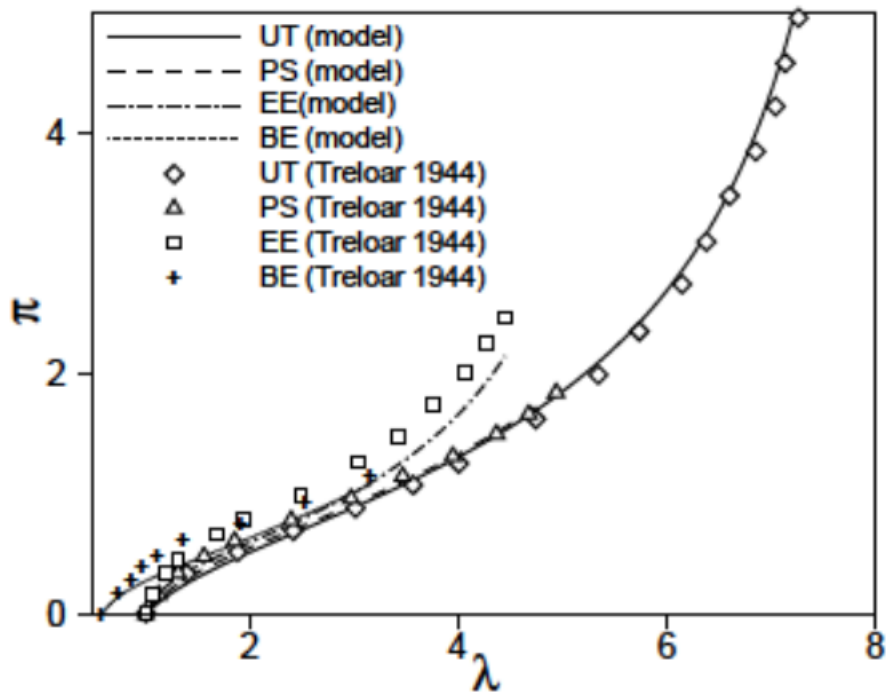


Figure 40: Stress-Strain curve for 8-Chain model [1]

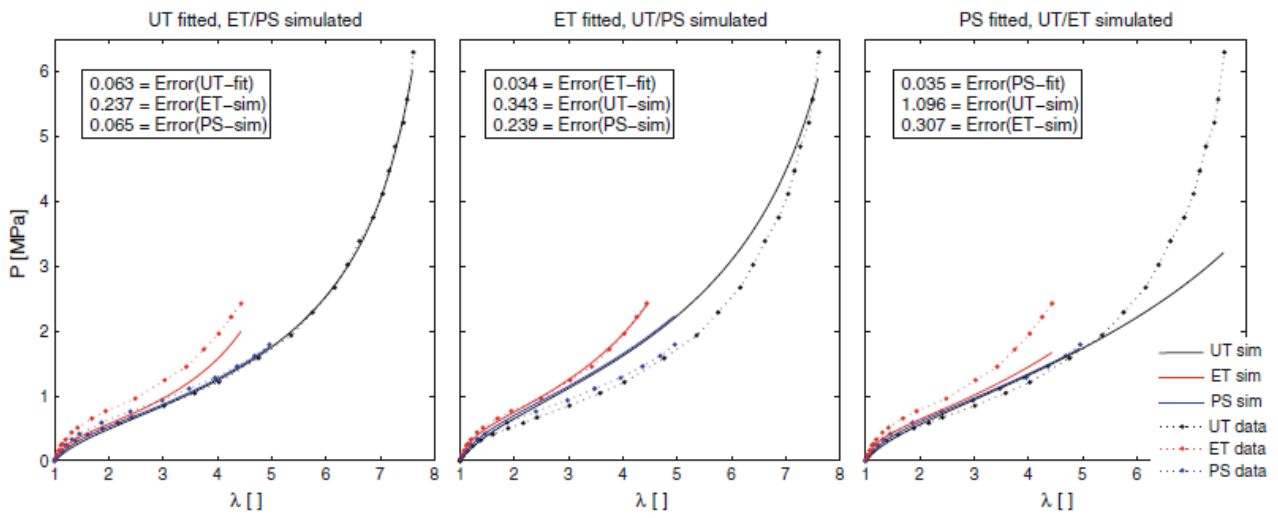


Figure 41: Stress-Strain curve for 8-Chain model [5]

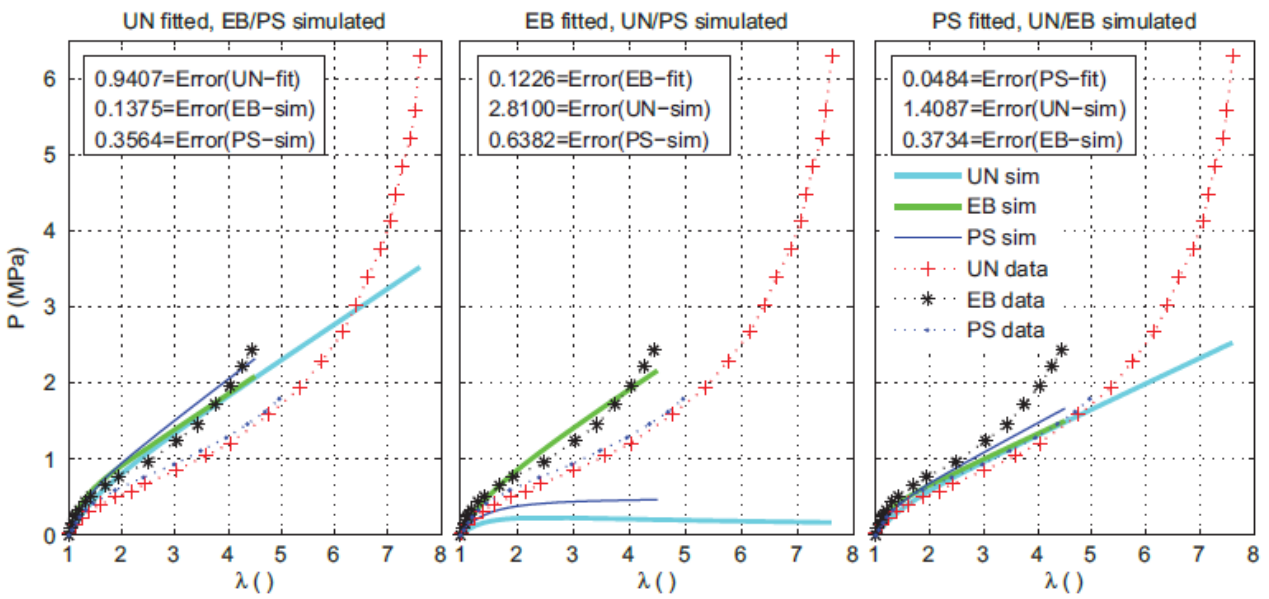


Figure 42: Stress-Strain curve for Tube model [9]

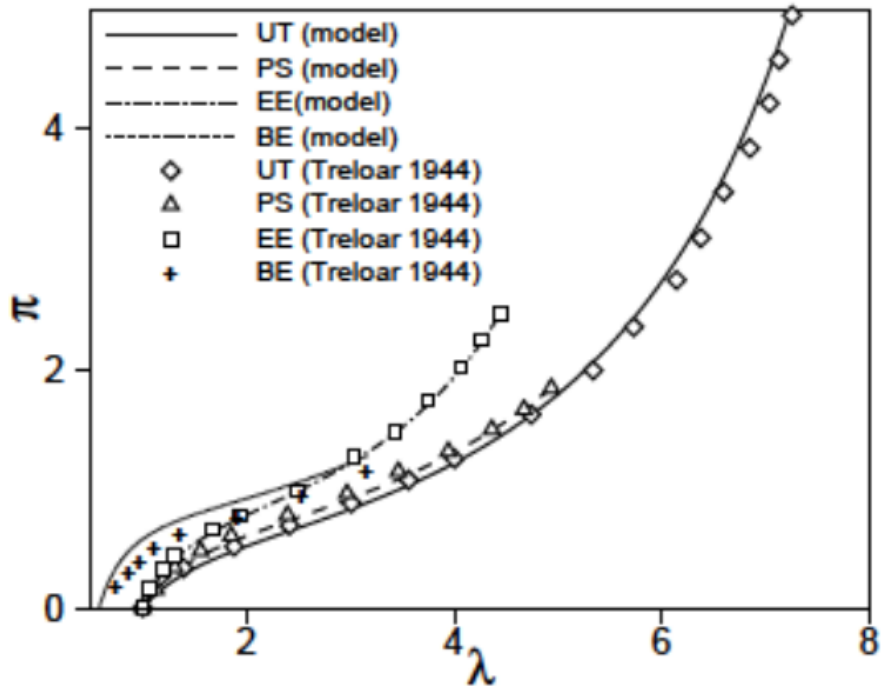


Figure 43: Stress-Strain curve for Extended-Tube model [1]

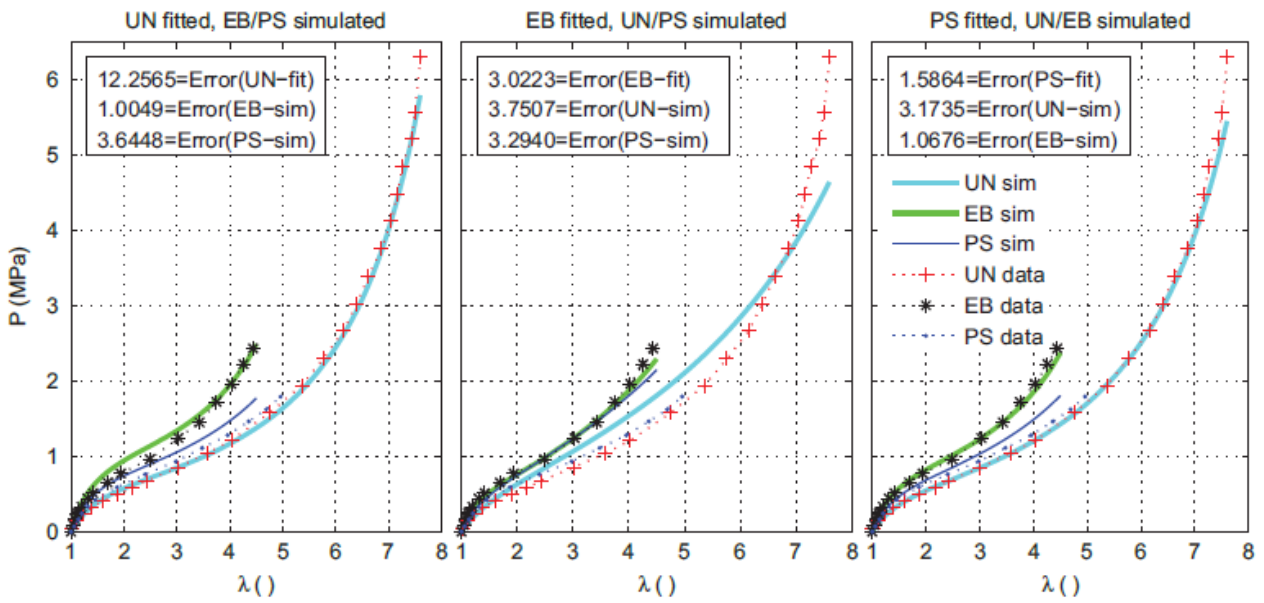


Figure 44: Stress-Strain curve for Extended-Tube model [9]

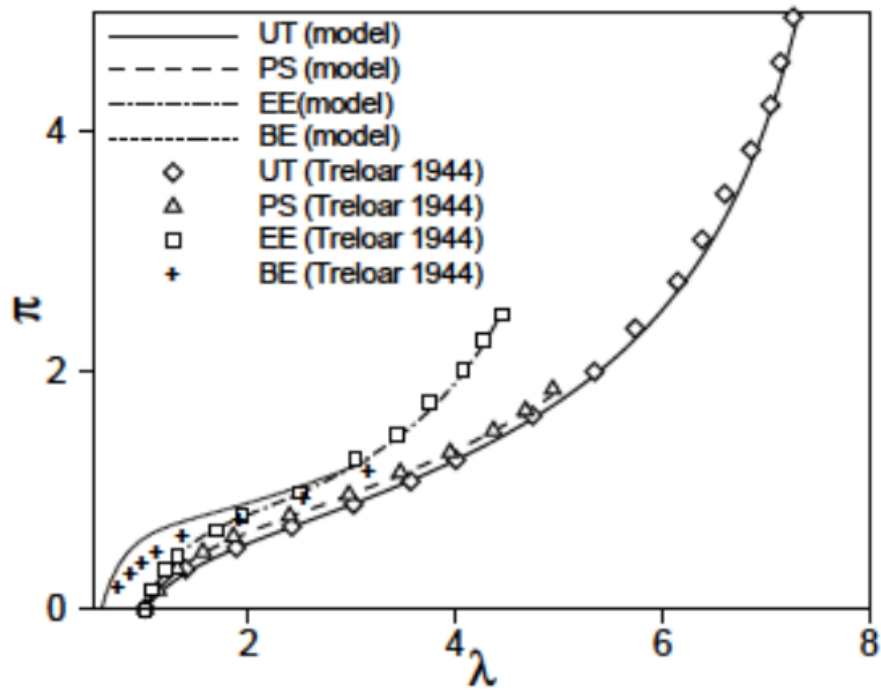


Figure 45: Stress-Strain curve for Unit-Sphere model [1]

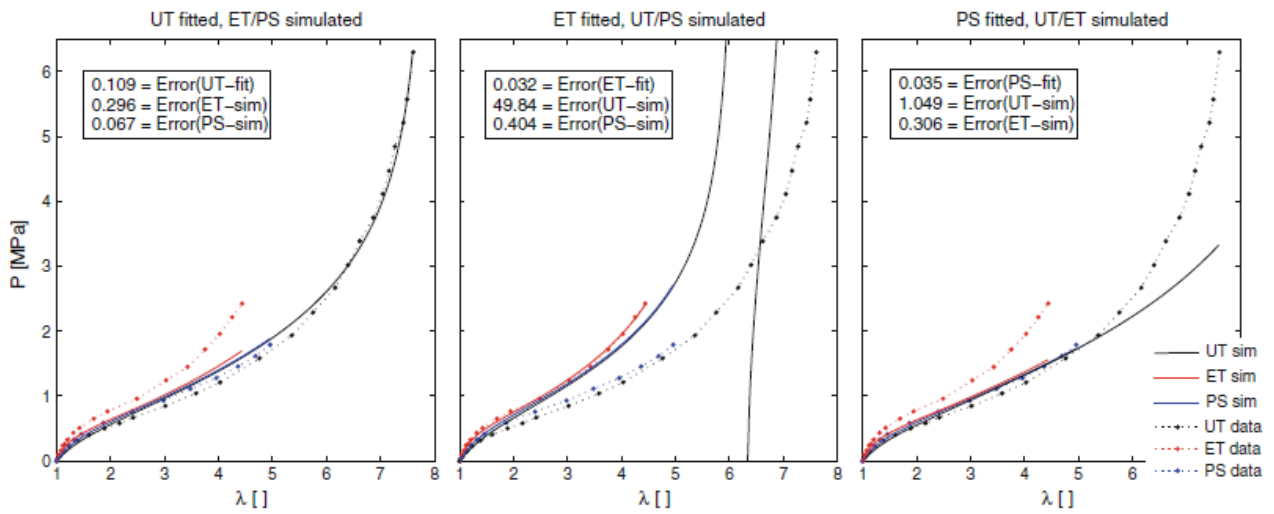


Figure 46: Stress-Strain curve for Unit-Sphere model [5]

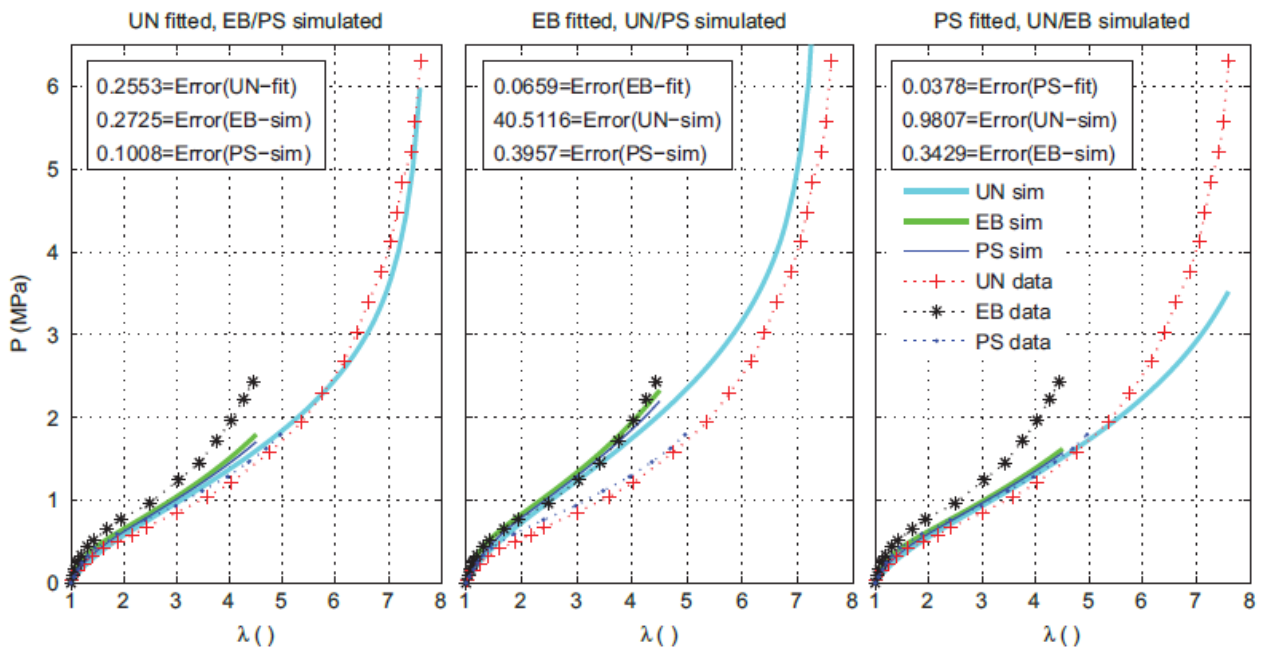


Figure 47: Stress-Strain curve for Full-Network model [9]